INTERROGATION OF THE IMMUNE CONTEXTURE IN BRAIN MALIGNANCY

by

Robert Lyle Bowman

A Dissertation

Presented to the Faculty of the Louis V. Gerstner, Jr.

Graduate School of Biomedical Sciences,

Memorial Sloan Kettering Cancer Center

in Partial Fulfillment of the Requirements for the Degree of

Doctor of Philosophy

New York, NY

March, 2016

_____   _____
Johanna A. Joyce, PhD   Date
Dissertation Mentor

DEDICATION

To my wife Kathryn, for all her love and support.

ABSTRACT

The tumor microenvironment (TME) is composed of an array of non-transformed cell types including endothelial cells, fibroblasts, as well as cells of the innate and adaptive immune system. Amongst these various cell types, tumor-associated macrophages (TAMs) have emerged as a prominent player in multiple roles of tumorigenesis. The brain presents a unique scenario, where TAMs are potentially derived from both tissue-resident microglia and peripherally-derived macrophages, yet the contribution of these cells is unclear. Furthermore, knowledge of the composition of the immune compartment in the brain TME remains incomplete.

Here we utilized genetic lineage tracing models to uncover the ontogenetic heterogeneity of TAMs in glioma. Gene expression profiling revealed that these cells possessed distinct activation states reflective of their different developmental origins. The analyses identified markers capable of distinguishing these cells in both homeostasis and inflammation. We applied these markers in comprehensive flow cytometry panels to characterize the immune contexture in human glioma and brain metastasis, where we identified grade and disease specific immune composition differences.

These studies have provided a comprehensive understanding of the composition and gene expression of the major immune constituents in brain malignancy. We posit that these findings will provide a foundation for development of therapeutic options targeting the brain TME.

BIOGRAPHICAL SKETCH

Robert (Bobby) Bowman was born in Tarzana, California and grew up in Las Vegas, Nevada. From the age of eight throughout the end of high school he was involved in football and wrestling, where countless coaches, especially Hamlet McNeace and Dave Jones, taught him the values of a dedicated work ethic, focus and teamwork. Bobby's interest in science really came to form when he took an AP Chemistry class from Mrs. Stephanie Wiegand at Silverado High School. It was around this same time that he started dating his future wife, Kathryn Ferguson. With the mentorship of Stephanie Wiegand, Eric Drum, and Jose Loya, Bobby reapplied himself to his academic studies and was accepted to Vanderbilt University.

In the summer of 2006, Bobby moved to Nashville, Tennessee to begin his undergraduate studies. Bobby started research studying methods for organic synthesis with Dr. Jeff Johnston. After taking an introductory biology class, Bobby switched to studying the role of sensing amino acid starvation in *Dictyostelium* development with Dr. Charles Singleton. It was in this environment that his passion for scientific research truly emerged. Bobby would spend his remaining semesters and summers in the Singleton lab, graduating in 2010 *cum laude* with a degree in Molecular Cellular Biology. He would receive departmental honors and the undergraduate research award. With the encouragement and mentorship from Dr. Charles Singleton, Dr. Katherine Friedman, Dr. Donna Webb, and Dr. Mark Woelfle, Bobby applied to graduate school with the goal of working on immune system interactions in cancer.

In the summer of 2010, Bobby joined the Gerstner Sloan Kettering graduate program. Captivated by the complexity of the tumor microenvironment, Bobby joined the laboratory of Dr. Johanna Joyce the following summer. In this time, he would be

supported by the Geoffrey Beene Foundation and receive funding through the Ruth L. Kirschstein National Research Service Award. Bobby's passion for scientific research continues, where after graduation he will continue on in post-doctoral studies investigating oncogenic signaling and epigenetics in leukemia.

ACKNOWLEDGMENTS

TABLE OF CONTENTS

LIST OF TABLES

LIST OF FIGURES

CHAPTER 1

INTRODUCTION

Cancer is amongst the leading causes of mortality in the United States and abroad with an estimated 1.6 million new cases, and approximately 600,000 deaths in 2015 alone (Howlader et al., 1975-2011). Efforts in the past century have led to the development of front line therapeutic options that while capable of durable remission in some cancers remain ineffective in others. Towards the end of the 20th century and turn of the current century, fundamental steps forward in targeting cancer specific mutations led to a new paradigm in cancer treatment (Sawyers, 2004). The outlook of personalized cancer therapy has been furthered brightened by focused genomics projects, most prominently led by The Cancer Genome Atlas (TCGA), focused on disease-specific driving mutations that may offer therapeutic targets in combatting the disease (Cancer Genome Atlas Research et al., 2013).

The past century of cancer research has also served as a platform to interrogate many critical aspects of human biology and disease; chief amongst these is the immune system. Indeed, targeting the immune system in efforts to combat disease progression and relapse from standard therapy has emerged as one of the most promising avenues for cancer therapy over the last decade (Couzin-Frankel, 2013). The success of unleashing adaptive immune responses has coincided with renewed interest towards understanding both the composition and function of immune cells in malignancy (Joyce & Fearon, 2015) (Joyce, 2005).

In addition to their roles in inflammation and cancer, immune cells are also critical mediators of development and tissue homeostasis (Pollard, 2009). Tissue-resident macrophages execute a number of different tissue-specific functions, such as surfactant

absorption in the lung, barrier protection in the gut, or synapse guidance in the brain (Y. Okabe & Medzhitov, 2015). Recent efforts have demonstrated that most tissue-resident macrophages are developmentally distinct from their monocyte-derived counterparts, which are abundant under inflammatory circumstances (Gomez Perdiguero, Klapproth, Schulz, Busch, Azzoni, et al., 2015). However, it remains to be seen if the different ontogeny of tissue resident and monocyte-derived macrophages results in different roles in inflammation and malignancy. In my thesis, I have aimed to first uncover the ontogenetic composition of brain-resident macrophages (microglia) and monocyte-derived macrophages in brain malignancy. I have investigated how the different ontogenies of these cells might impact their subsequent functions in cancer progression. Lastly, I sought to evaluate how the composition of the immune contexture as a whole changes with disease progression, with therapeutic intervention, and with different primary tumor types.

Macrophages in the context of the immune system

The mammalian immune system can be organized into innate and adaptive branches each playing critical roles in host defense and homeostasis. Adaptive immune cells, such as B, T and NK cells, play critical roles in mediating antigen-specific immune responses (Parkin & Cohen, 2001). In addition, B cells, T cells and more recently NK cells (Sun, Beilke, & Lanier, 2009), are also responsible for mediating immunological memory to pathogens, resulting in more effective immune responses upon subsequent re-infection. An array of different innate immune cells complements these antigen specific effectors of the immune response, including mast cells, neutrophils, basophils, eosinophils, monocytes, dendritic cells, and macrophages (Iwasaki & Medzhitov, 2010). Each of these cells plays a contributing role in sensing tissue damage, potentiating an inflammatory response, and contributing to the activation of the adaptive immune

response (Newton & Dixit, 2012). Amongst these cells, macrophages act as a critical vertex between the immediate responses of the innate immune system and the epitope-specific adaptive immune system. Macrophages derive their name from their extensive capacity for phagocytosis of extracellular material, including bacterial pathogens, opsonized particles, and apoptotic cells (Aderem & Underhill, 1999). Following internalization, these entities are broken down into constituent nutrients, lipids and peptides. This phagocytic function is not only important for the clearance of debris and pathogens, but also serves as an opportunity to present peptide antigens to T cells through major histocompatibility complex (MHC) class I and II molecules, a process known as antigen presentation (Trombetta & Mellman, 2005). Thus, macrophages are capable of sensing the initiating events of infection, initiate inflammatory responses to eliminate the disease, and engage the adaptive immune system to provide long-term memory against future infections.

In addition to their roles in inflammation and disease, immune cells play critical roles in homeostasis and development. The focus of Chapter 3 of my thesis, the macrophage, then termed phagocyte, was first identified by Ilya Metchnikoff in 1883 for its role in sponge development. While Metchnikoff's initial research motivations were primarily focused on elucidating the trophic role of macrophages in establishing order in multi-cellularity, development, and homeostasis, he has since been more celebrated for the implications of these functions in inflammation and wound healing; work for which he was awarded the Nobel Prize in 1908 with Paul Ehrlich (Tauber, 2003). Since then, substantial research has placed macrophages as a mediator of not only wound healing, but also as a critical link between the innate and adaptive immune response. Over one hundred years later, the field has returned to investigating the role of macrophages in

maintaining tissue homeostasis, and importantly how these tissue-resident macrophages (TRMs) are themselves developmentally regulated.

Macrophage development origins

A previously held view of immune system development suggested that all macrophages differentiated through a series of hematopoietic stem cell progenitors starting with the hematopoietic stem cell (HSC), followed by a common myeloid progenitor (CMP), then through differentiation into a pro-monocyte, and eventually an inflammatory monocyte state (Fogg et al., 2006; Gordon & Taylor, 2005). In addition to their role in generating macrophages during inflammation, it was thought that classical monocytes of the blood system were primarily responsible for homeostatic turnover of TRMs (Gordon & Taylor, 2005). While this canonical view of TRM turnover remains true for some macrophage populations, especially within the intestine (Bain et al., 2014), this theory has been supplanted in recent years through sophisticated genetic lineage tracing approaches demonstrating diverse origins for TRMs (Ginhoux et al., 2010; Gomez Perdiguero, Klapproth, Schulz, Busch, Azzoni, et al., 2015; Hashimoto et al., 2013; Hoeffel et al., 2015; Kierdorf, Erny, et al., 2013; Yona et al., 2013).

Perhaps the most prominent cell type of interest in interrogating TRM development has been microglia, the brain-resident macrophage. Their distinct developmental patterns were first recognized early on due to their seemingly unique capacity for radiation resistance and self-renewal compared to other myeloid cells (Kennedy & Abkowitz, 1997; Sedgwick et al., 1991). Subsequently, Langerhans cells of the skin have also been identified to share a similar radiation resistance capacity (Merad et al., 2002; Price et al., 2015), befitting their constant bombardment by UV rays and exposure to other potential genotoxic stressors. In 2010, Ginhoux and colleagues utilized a combination of

genetic knockouts and fate mapping tools in mouse to demonstrate that microglia entered the brain at embryonic day E8.0, before definitive hematopoiesis began in the aorta-gonada-mesenephrons (AGM) region of the early embryo (Ginhoux et al., 2010). They further showed that these cells developed in a colony stimulating factor-1 receptor (CSF-1R)-dependent manner, a factor which is now appreciated to be necessary for the development and maintenance of nearly every macrophage population (Chitu & Stanley, 2006). This first wave of evidence of extra-hematopoietic development of TRMs has been extended in the subsequent years to include TRMs of the brain, skin, lung, liver, and spleen (Gomez Perdiguero, Klapproth, Schulz, Busch, Azzoni, et al., 2015; Hoeffel et al., 2015). Many of these organs, with the key exception of the brain (Ajami, Bennett, Krieger, Tetzlaff, & Rossi, 2007) (Kierdorf, Erny, et al., 2013), show some homeostatic turnover from HSC-derived cells during homeostasis. Meanwhile, the small intestine appears unique in its constant recruitment and turnover of TRMs solely from HSC-derived monocytes (Bain et al., 2014), with no notable or long-standing contribution from early HSC-independent erythro-myeloid progenitor (EMP) cells, unlike other TRMs (Hoeffel et al., 2015). The functional relevance, if any, for why these specific organs show these particular patterns of contribution of EMP- and HSC-derived TRMs remains to be determined. While the fetal origins of most TRMs has been clarified, there remains controversy over the timing of embryonic development and the precursors responsible for TRMs of different tissue types (Gomez Perdiguero, Klapproth, Schulz, Busch, de Bruijn, et al., 2015) (Schneider & Kopf, 2015).

Despite similar developmental origins, different TRMs possess distinct, tissue-specific functions and transcriptional profiles (Gautier et al., 2012). For instance, microglia are poised to perform brain-specific functions such as synaptic pruning (Paolicelli et al., 2011) and axon guidance (Y. Li, Du, Liu, Wen, & Du, 2012). Osteoclasts, macrophages

of the bone, are necessary for bone resorption and remodeling (Teitelbaum, 2000). Red pulp macrophages (RPM) of the spleen are responsible for the processing of heme and iron from dying red blood cells (Bennett & Kay, 1981). How these TRMs acquire their tissue-specific auxiliary functions is still under investigation, though one well-supported hypothesis centers around the concept of "functional demand" (Y. Okabe & Medzhitov, 2015). This hypothesis refers to the idea that tissue-specific signals mediate TRM differentiation after seeding of either monocytes, fetal liver progenitors, or yolk-sac progenitors. This appears to be the case for RPM, where local heme availability drives Bach1 degradation and de-repression of *Spic (Haldar et al., 2014)*, a transcription factor necessary for red pulp macrophage development and function (Kohyama et al., 2009). In the case of hemolysis, excess heme can drive differentiation of monocytes into RPMs (Haldar et al., 2014), demonstrating the capacity for "functional demand" to facilitate TRM differentiation under pathophysiologic conditions. Similar faculties seem to be at play for alveolar macrophages, microglia and peritoneal macrophages (Schneider et al., 2014) (Gosselin et al., 2014). While this concept certainly has experimental support, it remains unclear how ontogenetic differences may influence tissue-specific transcriptional signals, i.e. do monocyte-derived alveolar macrophages differ from fetal liver-derived alveolar macrophages? Chapter 3 of my thesis will aim to address this question with regard to ontogenetically distinct brain macrophage populations in brain tumors.

Macrophage lineage specification

Despite differing developmental origins, TRMs and peripherally-derived macrophages possess many unifying factors necessary for their differentiation and growth (Gordon & Taylor, 2005). As previously mentioned for microglia, all macrophages require signaling through the receptor tyrosine kinase (RTK) CSF-1R for differentiation, and survival (Dai

et al., 2002) (Pixley & Stanley, 2004). CSF-1R activation leads to canonical mitogen signaling (Kato, Roussel, Ashmun, & Sherr, 1989), which is responsible for macrophage proliferation and survival. While GM-CSF (*Csf2*) can functionally compensate for loss of CSF-1 signaling *in vitro* (Pyonteck et al., 2013)*,* such compensation is limited *in vivo* as the *Csf1r* knockout mouse has lethal phenotype with the longest surviving pups reaching only post-natal day 7 (Dai et al., 2002).   This lethality is associated with deficiencies in microglia and other macrophage development (Dai et al., 2002). While the canonical CSF-1R ligand, CSF-1, is the necessary ligand for the majority of receptor function (Cecchini et al., 1994), a second ligand, IL-34, has shown to play a prominent role in the development and maintenance of microglia and Langerhans cells, the TRMs of the epidermis (Greter et al., 2012; Y. Wang et al., 2012).   Indeed, *Csf1*-deficient mice are viable; though with deficiencies in bone morphogenesis and osteoclast development, yet show normal levels of Langerhans cells and microglia (Cecchini et al., 1994). Meanwhile, *Il34* knockout mice, while also viable, show a decrease in microglia and Langerhans cell numbers with no alterations in osteoclasts (Greter et al., 2012; Y. Wang et al., 2012). Collectively, these genetic experiments highlight the tissue specificity of CSF-1R ligands and importantly demonstrate the necessity of CSF-1R, and macrophage function, *in vivo.*

In addition to this lineage-specific receptor, macrophage development is critically dependent upon the lineage determining transcription factor (LDTF), PU.1 (*Sfpi1)* (Scott, Simon, Anastasi, & Singh, 1994)*.* Like *Csf1r* knockout mice, PU.1 knockout mice also have a lethal phenotype. PU.1 plays an important role as a LDTF not only in myeloid development, but also in B cell development (DeKoter & Singh, 2000). As a member of the ETS family of transcription factors, PU.1 itself has a limited DNA recognition motif (Kodandapani et al., 1996), and its specificity for macrophage or B cell enhancers is

driven by co-binding with cofactors such as CEBPα in macrophages and E2A in B cells (Heinz et al., 2010; Spooner, Cheng, Pujadas, Laslo, & Singh, 2009). Binding of these partners is sufficient to drive the opening of heterochromatin, and recruitment of histone methyltransferases, leading to the deposition of the poised enhancer marker H3K4me1 (Choukrallah & Matthias, 2014). Subsequent TF binding can lead to the deposition of H3K27Ac mark denoting active enhancer elements (Heinz et al., 2010).

In addition to co-factor expression, PU.1 expression itself is also tightly regulated (Mak, Funnell, Pearson, & Crossley, 2011). Reductions in expression by even 30% lead to the development of a pre-leukemic state that, when combined with mismatch repair deficiency, manifests in fully penetrant AML (Will et al., 2015). As such, fine regulatory controls are in place to maintain precise PU.1 levels. The upstream responsive element (URE) of PU.1 is the framework for mediating an autoregulatory loop whereby macrophage-specific TFs are capable of binding enhancer elements along with Ikaros (*Ikzf1*) leading to stable *PU.1* transcription. In B cells, Ikaros combines with B cell specific factors to act as a transcriptional repressor to temper PU.1 expression (Zarnegar & Rothenberg, 2012). Interestingly, overexpression of PU.1 and CEBP can lead to transdifferentiation of fibroblasts and B cells into macrophages, demonstrating the necessity of rigid transcriptional regulation of PU.1, as well as the lineage-determining capacity of this master regulator (Bussmann et al., 2009; Feng et al., 2008).

While PU.1 and CEBPα are responsible for directing macrophage-specific enhancer selection, further specification is necessary for TRM differentiation. Recent studies have demonstrated that TRMs indeed posses not only distinct transcriptional profiles, but also distinct enhancer selection (Gautier et al., 2012; Lavin et al., 2014). Motif enrichment at these enhancers revealed tissue-specific transcription factors, such as Mef2c for

microglia and Gata3 for peritoneal macrophages; which are specifically expressed by these TRM subtypes (Lavin et al., 2014). This suggests that, like CEBPα, TRM-specific cofactors influence PU.1 binding and enhancer selection to further drive tissue-specific differentiation. Indeed, ChIP-sequencing studies demonstrate that PU.1 peaks are enriched for MEF and SMAD motifs in microglia (Gosselin et al., 2014). SMAD motif enrichment is of particular interest, as TGF-β signaling in the brain has been shown to be necessary for microglia development and maintenance (Butovsky et al., 2014), suggesting that environmental cues drive TRM specification through enhancer selection. This concept is supported by transplantation studies where peritoneal macrophages injected intranasally into the lung acquire the transcriptional and epigenetic signatures of alveolar macrophages (Lavin et al., 2014). Collectively, these experiments provide further mechanistic insight into the specialization through "functional demand", where tissue-dependent cofactor expression/ activation can influence further specialization.

Macrophage activation and polarization

Enhancer selection is not only important for establishing tissue-specific identity, but also lays the molecular foundation for the selectivity of stimulus-regulated transcription factors (SRTFs) such as STAT6, STAT1, PPARγ, and NFκB, amongst others (Glass & Natoli, 2015) (Lawrence & Natoli, 2011). In most cases, these SRTFs are insufficient to induce changes in heterochromatin, and rather bind open chromatin as specified by PU.1 and other cofactors (Link, Gosselin, & Glass, 2015). This generates a hierarchical view of macrophage transcriptional regulation whereby PU.1 and CEBPα establish the general macrophage enhancer landscape that is skewed by tissue-specific transcriptional programs. This establishes regions where SRTFs can potentially bind, and skews a macrophage to a set of subsequent responses (Glass & Natoli, 2015).

Critically, SRTFs link macrophage tissue residency and ontogeny to sensing of the exterior environment, and serve as executors of transcriptional response to external stimulation. It is through induction of these pathways that macrophages show their greatest plasticity, and adopt phenotypes associated with distinct activation states (Mosser & Edwards, 2008).

This plasticity to tissue residency extends beyond homeostasis and into inflammatory conditions. As potentiators of immune and inflammatory responses, macrophages must respond to and parse signals of various tissue disruptions including wounding, but also non-self infections from bacteria, viruses and parasites (Pollard, 2009). Each of these disturbances to homeostasis requires appropriate inflammatory responses, as inappropriate responses may manifest in autoimmunity (Hamilton, 2008). These situations generate a diverse array of cytokines capable of stimulating TRMs and peripherally-derived macrophages, including members of the interleukin family, interferons, CXCL cytokines, CCL cytokines, bacterial glycolipids, fatty acids, TLR ligands and metabolic intermediates (Mosser & Edwards, 2008). Careful parsing and integration of these signals are necessary to maintain homeostasis, generate the appropriate host defense response, and eventually resolve inflammation. The integrated input, combined with tissue-specific gene expression programs, defines the macrophage activation, or polarization, state.

Nomenclature

To unambiguously discuss macrophage activation states, it is important to understand the historical perspective leading to the most commonly used nomenclature. "Alternative activation", describing IL-4 activated macrophages, was first coined in juxtaposition to "classically activated" macrophages treated with interferon (IFN)-γ or LPS (Stein,

Keshav, Harris, & Gordon, 1992). The term "macrophage polarization" was originally introduced as a framework for understanding macrophage arginine metabolism, where M1 macrophages (stimulated by IFN-γ or LPS) processed arginine to produce nitric oxide species, and M2 macrophages (stimulated by IL-4) engaged in metabolic processes converting arginine to polyamines (Mills, Kincaid, Alt, Heilman, & Hill, 2000). This paradigm of M1/M2 polarization quickly expanded to encompass inflammatory initiation and wound healing, whereby M1 macrophages were thought to be potentiators of a pro-inflammatory response, while M2 macrophages were thought to mediate an anti-inflammatory, wound-healing, responses (Mills, 2012). The similarity in nomenclature with T cell driven Th1 and Th2 immune responses is no coincidence, as in addition to their roles in inflammatory initiation and resolution, these macrophages were thought to promote Th1 (M1) and Th2 (M2) inflammatory conditions (Mills et al., 2000). Since then, this terminology has been broadly adopted and dominates the field of macrophage biology. This dichotomy can be experimentally supported *in vitro,* where transcriptional networks regulating M2 polarization (STAT6) have been shown to directly antagonize M1 polarization (STAT1) (Ohmori & Hamilton, 1997). Further subdivisions, particularly within the M2 phenotype, have been suggested in efforts to account for the diversity of macrophage marker expression (Biswas & Mantovani, 2010). Despite the widespread adoption of this nomenclature, it remains insufficient to explain the breadth of responses that a macrophage is capable of eliciting.

Recently, a community of macrophage researchers has worked to refine the macrophage polarization nomenclature (Murray et al., 2014). While they still acknowledge the seemingly opposed nature of M1 and M2 macrophages, they preferred to shelf the idea of sub-classifications of M1, M2, M2a, M2b, and M2c for a distinction regarding specific cytokine activation states such as M[IL-4]. Recent efforts describing

in vitro macrophage transcriptional responses to over 25 different stimuli have made this a feasible method to codify macrophage activation (Xue et al., 2014). While this offers a description for *in vitro* stimulated macrophages, such nomenclature remains insufficient in the *in vivo* scenario where macrophages possess tissue-specific gene expression programs and are exposed to many different cytokines at varying contributions and time scales. Despite this shortcoming, the critical message of this nomenclature suggestion is that macrophage do not fall within a single dichotomous classification schema, but rather fall along a spectrum of activity, as Mosser and Edwards proposed in 2008 (Mosser & Edwards, 2008). In this way, macrophage activation can be described as a landscape with many potential steady states. Where a given macrophage falls along this landscape might depend on combinations of cell intrinsic and extrinsic factors such as cytokine availability, tissue residency, and ontogeny. This landscape may predispose TRMs and infiltrating macrophages to adopting a distinct phenotype under homeostasis versus inflammatory conditions, a concept that is explored in Chapter 3 of this thesis.

Transcriptional profiling of macrophage activation

Like many other facets of immunology, the relatively recent technological advances in gene expression profiling, with first microarrays and then with high-throughput RNA-sequencing, has led to a transcription-centric view of macrophage activation (Glass & Natoli, 2015). A recent report catalogued transcriptional responses of 27 different stimuli on human macrophages, creating a near-complete transcriptomic landscape of *in vitro* macrophage activation (Xue et al., 2014). The authors identified stimuli-specific gene signatures, as well as modules of genes that were activated by a series of related cytokines. More importantly, the authors identified the core transcriptional regulatory factors underlying these activation states. Analyses such as these transform what was at first a gene expression screening approach into a programmatic survey of pathways

activated under various stimuli. In my thesis I employ transcriptional profiling and machine learning methodology (Setty et al., 2012) to infer transcription factor activity in macrophages (and other immune cells) to identify pathways regulating tumor-mediated macrophage "education". In the following sections I will discuss cytokine family members with well-established roles in regulating macrophage activation states in inflammation and cancer, with a focus on the transcriptional programs that are manifest following stimulation.

Toll-Like Receptors (TLR) and ligands

Host defense against bacteria and parasitic pathogens is one of the major functions of macrophages in innate immunity. One family of receptors that mediate the response to non-self pathogen is the Toll-like receptor (TLR) family of ligand receptors, which is composed of at least 11 family members (Takeda & Akira, 2005). TLR1-9 appear to be evolutionary conserved in both mouse and human. These proteins are a single pass transmembrane receptor, with a well-conserved cytosolic domain resembling the IL-1 receptor. As in IL-1 signaling, dimerization of TLR receptors leads to MYD88-dependent IRAK4 recruitment and eventual activation of IRAK1 and TRAF6 (Takeuchi et al., 2000). This signaling cascade impinges upon two downstream transcriptional pathways: NF-KB and AP-1 (Takeda & Akira, 2005), where these effectors have been found to be responsible for induction of the inflammatory cytokines TNF, IL-12, and IL-6. In addition to immediate NF-KB activation, TLR dimerization also activates TRIF- and TBK1-dependent IRF3 signaling, which can mediate a late response to ligand identification through the transcriptional activation of effectors like IFN-β (Jiang, Mak, Sen, & Li, 2004). This staged activation of early and late responses is a recurring theme in macrophage activation, providing a way for immune cells to provide immediate, rapid responses to external stimuli without generating uncontrollable inflammatory conditions

that cannot be suppressed by negative feedback mechanisms.   Given the nature of the ligands, and the downstream inflammatory cytokines produced, TLR agonists have typically been considered potentiators of the M1 macrophage activation; indeed LPS stimulation is the canonical ligand for classical macrophage activation (Mosser & Edwards, 2008).

While the TLR intracellular domains are highly conserved across family members, the extracellular domains are quite distinct, composed of divergent leucine-rich repeats (Bell et al., 2003). These repeat structures vary across TLR family membrane and, along with co-binding factors, influence the ligand specificity for each family member. The first identified mammalian TLR family member was TLR4, the lipopolysaccharide (LPS) receptor (Poltorak et al., 1998). Distinct family members are capable of recognizing other bacterial ligands including flagellin (TLR5) (Hayashi et al., 2001), unmethylated CpG DNA motifs (TLR9) (Hemmi et al., 2000), and diverse lipoprotein species (TLR1, TLR2, TLR6) (Takeda & Akira, 2005).   In addition to their capacity to recognize these specific ligands, some members of the TLR family such as TLR2 have been shown to heterodimerize with other family members, increasing the repertoire of ligands towards which they are capable of mounting a response (Takeda & Akira, 2005). In addition to plasma membrane recognition of pathogen, some TLR family members signal through the endosome (TLR3, TLR7, TLR8, TLR9), where similar effectors such as MYD88, TRAF6 and IRF7 execute an anti-viral responsive (Hacker et al., 1998).

Interferon stimulation

First named for their capacity to interfere with viral production, the interferon (IFN) family is a set of secreted cytokines that confer responsiveness to viral infection (Isaacs & Lindenmann, 1957). The IFN family can be divided into type I and type II interferons

(Platanias, 2005). Type I interferons include several homologs of IFN-α, in addition to IFN-β, IFN-ω and IFN-τ (Schroder, Hertzog, Ravasi, & Hume, 2004). These IFN family members possess high similarity by both sequence and structure, and are closely located in a cluster of IFN genes on chromosome 4 in mouse and chromosome 9 in human (Diaz et al., 1994; Kelley & Pitha, 1985). While IFN-α expression is restricted to hematopoietic cells, IFN-β is more broadly expressed. Meanwhile IFN-γ is the sole family member of the type II interferon family with distinct structural features and is located outside of the interferon cluster. In addition, IFN-γ shows more restrictive tissue expression than the type I family, with expression restricted to CD8+ T cells, NK cells, and antigen presenting cells. While type I interferons signal through heterodimeric IFNAR1 and IFNAR2 receptors, IFN-γ has a dedicated receptor composed of IFNGR1 and the tightly regulated IFNGR2 (Platanias, 2005). Both families engage in JAK-STAT signaling, however type I interferons induce a STAT1-homodimer whereas IFN-γ predominantly engages a STAT1-STAT2-IRF9 complex referred to as ISGF3 (Platanias, 2005). These differences in complex formation, as well as the enhancer landscape in their respective cell types, lead to differential transcriptional outputs, and responses to cytokine stimulation.

In macrophages, type I and type II interferon stimulation leads to the transcriptional activation of a variety of chemotactic molecules including IL-12, IL-18, CXCL10, CCL2, CXCL9, CCL3, CCL4, and CCL5 (Trinchieri, 2010). Many of these factors act to recruit T cells and NK cells primed to produce IFN-γ, leading to a positive feedback loop that establishes a Th1 immune response (Boehm, Klamp, Groot, & Howard, 1997; Yoshida, Koide, Uchijima, & Yoshida, 1994). In addition to chemokine production, IFN-γ stimulated macrophages upregulate MHC-I antigen presentation machinery, including proteasomal subunits and transport proteins optimized for peptide presentation

(Schroder et al., 2004). IFN-γ signaling also drives expression of *Ciita*, the master transcriptional regulator and platform for MHC-II presentation (Boss, 1997). In addition to their coordination of Th1 immunity, IFN-γ stimulated macrophages are potent producers of nitric oxide (NO), reactive oxygen species (ROS) and reactive nitrogen intermediates (RNI), molecules that are capable of mediating cytolytic activity (MacMicking, Xie, & Nathan, 1997; Schroder et al., 2004). With these diverse activities, IFN-γ is the best-described activator of an M1/ classically activated macrophage, typified by their capacity to potentiate a cytolytic immune response by engaging in Th1 immunity.

However, in contrast to the immune-stimulatory effects of acute type I and type II interferon exposure, prolonged type I interferon signaling, as in the case of chronic infection, can lead to immune suppression through the production of IL-10 and induction of PD-L1 (Teles et al., 2013) (Ivashkiv & Donlin, 2014). Such biphasic responses to cytokine stimulation are a predominant feature in macrophage activation, and are of particular interest in diseases associated with chronic inflammation, such as cancer.

<u>Th2 cytokines</u>

One of the most extensively studied mediators of macrophage activation is the family of Th2 cytokines including IL-4, IL-6, IL-10 and IL-13. IL-4 and IL-13 are largely associated with M2/alternative activation, while IL-10 stimulation is associated with an immunosuppressive phenotype (Biswas & Mantovani, 2010). IL-6 plays a role in mediating alternative activation and suppressing IFN-γ signaling, yet shows broad expression patterns associated with pro-inflammatory states (Scheller, Chalaris, Schmidt-Arras, & Rose-John, 2011). Such discrepancies in function and expression

patterns have led to associations for IL-6 with both M1 and M2 polarization (Biswas & Mantovani, 2010; Mauer et al., 2014).

These cytokines largely funnel into two signaling pathways with IL-4 and IL-13 promoting STAT6 signaling (H. W. Wang & Joyce, 2010). IL-4/IL-13 signal transduction occurs through cytokine binding to IL4R-α and the common γ chain receptor, CD132 (Hebenstreit, Wirnsberger, Horejs-Hoeck, & Duschl, 2006). Following binding and dimerization, JAK1 is recruited and results in STAT6 phosphorylation, homodimerization and translocation to the nucleus (Hebenstreit et al., 2006). Once in the nucleus, STAT6 directly binds DNA at available loci in cooperation with PU.1 and IRF family members (Pauleau et al., 2004) (Lawrence & Natoli, 2011) (Gupta, Jiang, Anthony, & Pernis, 1999). Among a variety of genes, STAT6 activation leads to upregulation of factors associated with endocytosis and protein trafficking (*Cd36*, *Folr2, Mrc1*), chemotaxis (*Ccl17, Ccl22, Ccl2, Ccl9*), and amino acid metabolism (*Arg1, Hspa5, Timp1*) (Martinez et al., 2013) (Ostuni et al., 2013) (H. W. Wang & Joyce, 2010). In addition to induction of antigen presentation factors and co-stimulatory molecules (MHC-II, *Cd74, Cd273*) (Huber, Hoffmann, Muskens, & Voehringer, 2010), these factors function to mediate a Th2 immune environment and also coordinate the resolution of an inflammatory state (Biswas & Mantovani, 2010).

In contrast, IL-6 typically signals through the transmembrane receptors IL6RA and gp130, whereby subsequent activation through JAK1, JAK2, and TYK leads to STAT3 homodimerization and nuclear translocation (Scheller et al., 2011). Additionally, IL-6 can bind soluble IL6RA to activate signaling in a variety of cell types through transactivation of gp130 (Chalaris, Garbers, Rabe, Rose-John, & Scheller, 2011). IL-6 is one of the first cytokines to be released in an inflammatory setting and mediates the switch from

neutrophil recruitment to monocyte and macrophage accumulation through the induction *CCL2*, *CCL8*, and *CXCL16* (Hurst et al., 2001). In addition IL-6 induces the expression of *CSF1R* on monocytes, subsequently promoting their differentiation (Chomarat, Banchereau, Davoust, & Palucka, 2000). This role in early inflammation suggests a pro-inflammatory role for IL-6, however functional analyses indicate that IL-6 directly suppresses Type II IFN signaling through the induction of SOCS3, ultimately skewing infiltrating T cells to adopt a Th2 or Th17 phenotype (Diehl & Rincon, 2002).

In contrast to IL-6, IL-10 displays more restricted cell type-specific production and activation profiles, albeit with similar downstream activation of STAT3 following binding to IL10RA and IL10RB (Lai et al., 1996). Functionally, IL-10 has been associated with an anti-inflammatory program for its capacity to suppress CD8+ T cell activation (Caux et al., 1994) (Ruffell et al., 2014) and blunt LPS-mediated macrophage transcriptional activation (O'Farrell, Liu, Moore, & Mui, 1998) (Murray, 2005). The molecular mediators of this anti-inflammatory response are still being characterized, but it seems to occur in a cell type-specific fashion, where the anti-inflammatory response in macrophages is largely mediated by the suppression of NF-κB target genes (Hutchins, Takahashi, & Miranda-Saavedra, 2015). Thus IL-10 and IL-6 signaling in macrophages leads to what has been termed a "regulatory macrophage" by engaging in immune-modulatory behavior (Biswas & Mantovani, 2010).

These signal transduction pathways are critical in mounting host defense to parasitic pathogens such as helminthes, mediating allergic response, and coordinating wound healing response to injury (Martinez, Helming, & Gordon, 2009). It is this last function that is most reminiscent of a tumor-associated macrophage (TAM) phenotype (Biswas & Mantovani, 2010) (Crowther, Brown, Bishop, & Lewis, 2001). Functionally, we have

found that combined STAT3 and STAT6 signaling in macrophages leads to robust secretion of lysosomal enzymes, namely cathepsin proteases, promoting the invasion of tumor cells in vitro (Yan, Wang, Bowman and Joyce; under review).   We have shown that these two signaling arms can synergize to additively boost transcriptional output, as well as transcriptionally activate targets that neither pathway is capable of regulating alone (Yan, Wang, Bowman and Joyce; under review).   This simple pairwise interaction illustrates the complexity of macrophage activation, an issue that is only further complicated *in vivo* where a complex milieu of cells leads to multiple signaling inputs.

The brain tumor microenvironment and TAMs in disease

While the macrophage activation spectrum has been largely interrogated *in vitro* in monoculture, these cells execute their functions through a diverse milieu of cytokines, metabolic gradients, extracellular matrix proteins, and a variety of cells that give rise to this complex *in vivo* environment (Y. Okabe & Medzhitov, 2015) (Amit, Winter, & Jung, 2015). In the context of cancer, this is referred to as the tumor microenvironment (TME) composed of tumor cells, blood and lymphatic vessels, fibroblasts, lymphocytes, tumor-associated macrophages (TAMs) and other tissue-specific cell types (Quail & Joyce, 2013). Given the unique components of microglia development and homeostasis, the brain lends itself well to investigating the composition and role of tissue-resident macrophages in malignancy. In addition to these unique developmental components, the brain has traditionally been considered an immune-privileged site, with restricted influx of peripheral immune cells (Barker & Billingham, 1977). While initially attributed to the tight adherence junctions of the blood-brain barrier, recent work has challenged the idea of immune privilege in brain inflammation and malignancy (Carson, Doose, Melchior, Schmid, & Ploix, 2006) (Louveau, Harris, & Kipnis, 2015) (Louveau, Smirnov,

et al., 2015). These paradigms make the investigation of the composition and function of immune cells in the brain tumor microenvironment of great interest.

Previous analyses of immune cell infiltrates in GBM patients revealed that tumor-associated macrophages and microglia are the major immune cell constituent (Hussain et al., 2006; Komohara, Ohnishi, Kuratsu, & Takeya, 2008; Parney, Waldron, & Parsa, 2009). Studies from our lab have demonstrated that TAMs are also the major immune cell constituent in brain metastases originating from primary breast tumors (Sevenich et al., 2014). TAMs have been shown to promote tumor cell proliferation and invasion through the production of factors such as MMP2, MMP9, TGF-β, STI1, EGF, IL-6, and IL-1β (Gabrusiewicz et al., 2011) (Ye et al., 2012) (Hambardzumyan, Gutmann, & Kettenmann, 2015). Recent studies have placed TAMs in a paracrine loop supporting the establishment of the perivascular niche, a region critical to the glioma stem cell maintenance (Zhou et al., 2015). Clinical evidence suggests that as glioma grade increases so does the accumulation of macrophages that express the M2/ alternative activation markers CD163 and MSR1 (Komohara et al., 2008). However, further profiling efforts of bulk TAM populations have revealed a mixed M1/M2 phenotype (Szulzewsky et al., 2015), underscoring the current insufficiency of dichotomous M1/M2 polarization characterizations.

Critically, it is likely that there are important contributions from both microglia and peripherally-derived macrophages (Hambardzumyan et al., 2015). This has been investigated in experimental models, where bone marrow transplantation (BMT) can be used to distinguish these two populations (Muller, Brandenburg, Turkowski, Muller, & Vajkoczy, 2015; Pyonteck et al., 2013; Sedgwick et al., 1991). Using BMT in a murine GBM model, it was shown that bone marrow-derived cells were actively recruited to the

tumor in a HIF-1a/ SDF-1-dependent manner (Du et al., 2008; Kioi et al., 2010). Work from our lab has also shown that bone marrow-derived cells constitute ~40% of the total TAM pool in a PDGF-driven Proneural GBM model (Pyonteck et al., 2013). However, these studies have relied upon irradiation-based BMT (IR-BMT), a process known to elicit ectopic recruitment of peripherally-derived macrophages to the brain (Bruttger et al., 2015; Capotondo et al., 2012; Mildner et al., 2007; Muller et al., 2015). In addition to TAMs, the glioma immune infiltrate has been proposed to contain neutrophils and monocytes (Gabrusiewicz et al., 2011; Pyonteck et al., 2013) with multiple reports ascribing these populations to myeloid derived-suppressor cells (Fujita et al., 2011; Raychaudhuri et al., 2015) (Umemura et al., 2008). Despite the breadth of these studies, very few use consistent marker standards, making comparisons across grade or disease type difficult to interpret. In addition, these studies are severely limited by their inability to distinguish brain-resident microglia and peripherally-derived macrophages, a question that is central to Chapter 3 of my thesis.

Beyond the myeloid compartment, much work has focused on understanding the composition of lymphoid cell infiltrates and uncovering means to elicit an anti-tumor immune response. Lymphocyte infiltration into primary brain tumors was first appreciated in the 1970's where histological identification of lymphocytes invading the perivascular space was associated with more favorable outcome (Brooks, Markesbery, Gupta, & Roszman, 1978; Ridley & Cavanagh, 1971). Immunohistochemical analyses have demonstrated that most of these immune cells are CD4+ T helper cells, with very few patients showing extensive CD8+ cytotoxic T cell infiltration (Kmiecik et al., 2013). One flow cytometric study suggested that these CD4+ cells show extensive TCR-α/β rearrangement and express CD56, suggestive of a cytolytic CD4 phenotype (Waziri et al., 2008). Other groups have shown an increase in T regulatory cells with tumor grade

(El Andaloussi & Lesniak, 2006), while peripheral depletion of such cells in murine glioma models led to an increase in overall survival (Maes, Verschuere, Van Hoylandt, Boon, & Van Gool, 2013).

Despite the limited information for which lymphocyte populations are present in brain malignancy, there has been much focus on development of immunotherapies (Preusser, Lim, Hafler, Reardon, & Sampson, 2015). The major avenue of investigation has focused on vaccination strategies either utilizing tumor lysates or targeted to the specific neo-antigen produced by the EGFR-VIII mutation enriched in glioblastoma patients (Jackson, Ruzevick, Brem, & Lim, 2013). The latter is currently under investigation in phase III clinical trials (Clinical trial NCT01480479) (Swartz, Li, & Sampson, 2014). In addition, T cells re-engineered to express a chimeric antigen receptor (CAR-T) against EGFR-VIII have shown efficacy in preclinical models (Johnson et al., 2015) and phase I trials are expected to begin soon. However, intratumoral heterogeneity remains a fundamental roadblock for either of these single antigen targeted therapies (Sottoriva et al., 2013). Immune checkpoint blockade may be a feasible strategy to overcome this roadblock, and has shown efficacy in other genetically heterogeneous tumor types. After some preclinical success (Vom Berg et al., 2013; Wainwright et al., 2014), several trials are underway to assess the efficacy of CTLA-4, PD-1 and PD-L1 blockade in glioma. Meanwhile, some of these therapies have already been approved for metastatic melanoma (Ipilimumab, anti-CTLA4) and non-small cell lung cancer (Nivolumab, anti-PD1) (Borghaei et al., 2015; Larkin et al., 2015). It remains to be seen if the therapeutic benefit will extend to patients with brain metastases (Ahmed et al., 2015).

To date, immune-profiling studies have been performed on small subsets of either lymphoid or myeloid cells, masking potential co-variable changes in leukocyte

composition. Recent efforts have aimed to address this through computational deconvolution of bulk tumor RNA sequencing data (Engler et al., 2012; Gentles et al., 2015). These methods rely upon "gold standard" gene signatures to predict relative signature enrichment across samples, and thus infer immune cell frequencies. Such reports have verified experimental findings that TAMs are indeed an abundant population within glioma, and show a molecular subtype-dependent enrichment (Gentles et al., 2015). While these techniques are useful for capitalizing on the wealth of genomic and transcriptomic data available for primary brain malignancies, these are incapable of identifying new populations of cells for which signatures of genes are not available, or may misidentify populations that change dramatically from the "gold standard" signature upon entry into the tumor for example. Thus, comprehensive immunohistochemical and flow cytometric immune profiling remains an important standard for elucidating the composition of the tumor microenvironment at baseline and following recurrence (Maecker, McCoy, & Nussenblatt, 2012). Such an atlas of the immune cell contexture, as presented in Chapter 4 of this thesis, will provide a foundation for further understanding and therapeutically targeting the immune system in brain malignancy.

Clinical characteristics of primary and metastatic brain malignancy

The World Health Organization (WHO) has classified brain malignancies according to distinct entities, including the neuroepithelium, cranial and paraspinal nerves, meninges, lymphomas, germ cell, sellar region, and metastases (Louis et al., 2007). In my thesis, I focus on oligodendrogliomas and astrocytomas of the neuroepithelium as well as metastases from breast, lung and melanoma primary tumors. Each of these diseases displays distinct epidemiological and genomic characteristics as outlined below.

Glioblastoma multiforme

Glioblastoma multiforme (GBM) is a grade IV primary brain disease that presents with seizures, headache, nausea, vomiting, weakness, or loss of mental focus. While these symptoms are common, they are not unique to brain malignancy and confirmatory imaging studies are necessary. MRI can distinguish contrast-enhancing grade IV lesions from lower grade, non-enhancing, lesions (Hakyemez et al., 2005). Histological findings in GBM patients include extensive regions of necrosis, pseudopalisading necrosis, microvascular proliferation and extensive invasive patterns into the non-malignant brain (Rong, Durden, Van Meir, & Brat, 2006). This invasive patterning makes complete surgical resection difficult, given the biological necessity of the surrounding tissue (Berens & Giese, 1999). As such, GBM remains the most aggressive and fatal of adult primary brain tumors with a median survival of only 15-18 months following initial diagnosis. Standard of care remains surgical resection, with adjuvant temozolomide and fractionated ionizing radiation (IR) (Stupp et al., 2005). Following surgery, additional adjuvant therapy with Bevacizumab and steroids are often utilized for alleviation of cranial edema, though these show limited efficacy in extending overall survival (Gilbert et al., 2014). These therapeutic regimens have been shown to increase median survival, yet GBM remains nearly universally fatal, with a 2-year survival rate of only 26.5% (Stupp et al., 2005).

Given the dismal prognosis associated with this disease, The Cancer Genome Atlas (TCGA) identified GBM as one of the earliest diseases to be targeted for genomic and transcriptomic profiling (Cancer Genome Atlas Research, 2008) (Brennan et al., 2013) (Verhaak et al., 2010). These efforts have led to a nearly exhaustive catalog of mutations and genomic alterations thought to be driving this disease (Ceccarelli et al., 2016). The most common events include loss of chromosome 10q and gain of

chromosome 7p (Cancer Genome Atlas Research, 2008). While *PTEN* deletion on 10q was appreciated early on (S. I. Wang et al., 1997), only recently has *PDGFA* been identified as a putative driver gene on chromosome 7p (Ozawa et al., 2014). In addition to these genes, recurrent mutations and amplifications have been identified in *PIK3R1, PIK3CA, RB1, NF1, EGFR, CDKN2A, TP53, MDM2, ATRX* and *IDH1* (Brennan et al., 2013). Other more infrequent mutations have been identified, but these remain centered around the PI3K pathway and regulators of TP53 signaling. Many of these mutations have been associated with one of four transcriptionally identified subclasses of GBM: Proneural, Mesenchymal, Classical and Neural (Verhaak et al., 2010). For instance, *NF1* mutations are enriched in Mesenchymal tumors, while *EGFR* and *TP53* mutations are found in Classical tumors. In addition to *PDGFRA* amplification, Proneural tumors are most notably enriched for *IDH1* mutations, which are associated with a Glioma-CpG Island Methylator Phenotype (G-CIMP) (Noushmehr et al., 2010). G-CIMP GBM patients have notably increased survival, more reminiscent of low-grade disease.

Whereas other primary diseases have benefited from such extensive genomic profiling, few targeted therapy options have shown efficacy in glioma. In addition to this mutational heterogeneity between patients, there is also substantial cellular heterogeneity within a given tumor (Patel et al., 2014). Regional sampling during surgical resection has revealed that distinct regions can have different molecular subtypes, as well as different mutation statuses (Sottoriva et al., 2013). In addition, *PDGFRA* and *EGFR* amplicons have been shown to exist on extrachromosomal double minutes, leading to heterogeneity in their expression within a given tumor (Sanborn et al., 2013). This, combined with activation through heterodimerization, might explain why targeting of either mutation alone has been an ineffective therapeutic strategy.

Low grade glioma (LGG): Oligodendroglioma and astrocytoma

While less prevalent than grade IV GBM disease, primary brain tumors can also manifest as low grade lesions including grade I pilocytic astrocytomas, diffuse astrocytomas, and oligodendrogliomas (Louis et al., 2007). The latter two can present as grade II and grade III disease, whose histological features include moderate cellularity for grade II tumors, with anaplasia and increased mitotic figures and cellularity for grade III tumors (Louis et al., 2007). Unlike grade IV glioma, low-grade disease shows a large variance in overall survival ranging on the order of months up to greater than 10 years, with median survival around 7.5 years (Cancer Genome Atlas Research et al., 2015). Therapeutic options include surgical resection followed by adjuvant chemotherapy with Temozolomide for *MGMT* methylated patients (Hegi et al., 2005). Despite these interventions, most tumors recur and a subset progress to the more fatal grade IV GBM (Sanai, Chang, & Berger, 2011).

While also being a primary brain tumor, the genetic events underlying LGG are distinct from the grade IV GBM described above. In addition to rarer mutations, the major genetic events underlying LGG development include mutations in *TP53, IDH1, IDH2, TET2,* and ATRX (Cancer Genome Atlas Research et al., 2015). In addition, mutations in the promoter of *TERT,* leading to overexpression, have been broadly identified (Killela et al., 2013). While the prominent copy number alterations in GBM involve chromosome 10 losses and 7p amplifications, low-grade glioma can be subdivided into patients with and without 1p/19q co-deletion (Jenkins et al., 2006). Further subdivision on co-occurrence with *IDH1/IDH2* mutation generates three molecularly distinct groups of patients: 1) *IDH1/2* mutant 1p19q co-deletion, 2) *IDH1/2* wild-type 1p19q co-deletion, and 3) *IDH1/2* wildtype 1p19q intact (Eckel-Passow et al., 2015) (Cancer Genome Atlas

Research et al., 2015). This third group of patients contains enrichment for mutations in *CDKN2A, NF1*, *PTEN*, and *EGFR* making these patients more reminiscent of the high-grade disease described above, and as expected these patients have a less favorable outcome (Ceccarelli et al., 2016). Thus, genomic alterations may offer a better indication of prognosis than histological grade, where some histologically low-grade gliomas may present with unfavorable prognosis given lack of *IDH1* mutations. Conversely, the presence of an *IDH1* mutation, and a hypermethylated phenotype, confers a favorable prognosis even with grade IV histological findings (Ceccarelli et al., 2016).

Brain metastases (BrM):

Compared to the primary brain lesions described above, metastatic brain lesions are much more prevalent with an expected incidence of 7-14 in 100,000 patients (Howlader et al., 1975-2011). It is estimated that 8-10% of cancer patients have brain metastases (BrM) (Brastianos, Curry, & Oh, 2013), a number likely to be under-reported given the presence of seemingly asymptomatic BrMs on autopsy (Gavrilovic & Posner, 2005). In recent decades, this number is on the rise, in part due to improved imaging modalities and earlier detection (Niwinska, Tacikowska, & Murawska, 2010). In addition, increased efficacy of systemic therapy may contribute to the emergence of metastases in the brain; a suggested sanctuary site where standard chemotherapy and targeted antibodies such as Trastuzumab cannot reach disseminated tumor cells (Palmieri, Chambers, Felding-Habermann, Huang, & Steeg, 2007) (Yau et al., 2006). As such, therapeutic options remain limited, and are centered on stereotactic radiosurgery (SRS), whole brain radiotherapy (WBRT), and surgical resection (Brastianos et al., 2013). The decision to operate and/or irradiate is influenced by the size, location and number of lesions (Brastianos et al., 2013). Surgery is suggested when there is either a solitary lesion conducive to resection without damaging critical brain function, or if removal of a lesion

will improve quality of life (Patchell et al., 1990). The choice between SRS and WBRT is also influenced by number of metastases, where it is preferred to use SRS when there is a solitary lesion, and WBRT is reserved for patients who present with greater than 3 lesions (Chang et al., 2009).

Despite the vast genomic characterization of primary brain lesions and primary tumors that give rise to brain metastases, comparatively less is known about the genomic details of BrMs. Recent efforts have aimed to address this paucity of information through whole exon sequencing of trios of normal tissue, primary lesions, and BrMs (Brastianos et al., 2015).   While these analyses did identify some conserved mutations in BrMs compared with their matched primaries, few were recurrent across multiple patients. Mutations included members of the PI3K/mTOR pathway including PTEN, MET and PIK3CA. Other mutations were found in cell cycle regulators such as CDKN2A, MCL1, CCND1 and CDK6. Lastly, mutations were also identified in the MAPK pathway including KRAS, BRAF, HRAS and NRAS. In addition to this mutational heterogeneity between patients, BrMs isolated from the same patient even showed distinct mutations, indicative of branched evolution (Brastianos et al., 2015). Additional efforts to identify copy number alterations and epigenetic modifications in BrM identified a similar lack of recurrent patterns (Salhia et al., 2014). The vast genetic heterogeneity, and lack of recurrent mutations, poses a challenging scenario for the implementation of targeted therapies that have been successful in other contexts.

Thesis Aims

Each of the diseases discussed above pose a unique scenario to interrogate the brain tumor microenvironment. Low-grade glioma and GBM offer venues for dissecting grade dependent changes in TME. In addition, these diseases offer distinct genetic landscapes

that may generate unique effects on the immune cell composition and function. In addition to these primary brain malignancies, brain metastases offer an intriguing setting where there are potentially both brain-derived and primary site-derived tissue-specific signals. It remains to be seen how this combination of diverse environmental signals regulates the metastatic immune contexture. In addition to this inter-tumoral heterogeneity, there remains a fundamental question regarding the ontogenetic composition of the TAM compartment and how the balance between microglia and peripherally-derived macrophages changes between diseases. In my thesis I utilize multiple genetic lineage tracing models in murine glioma and brain metastasis models in combination with flow cytometric and transcriptional profiling of surgical samples to interrogate these questions.

In Chapter 3 of my thesis I aimed to interrogate the ontogeny of TAMs in brain malignancy. I employed multiple models of murine brain malignancy and genetic lineage tracing models to demonstrate that peripherally-derived macrophages are indeed abundant in primary and metastatic brain tumors. Transcriptional profiling of tumor associated, peripherally-derived macrophages and tumor-associated microglia revealed that these cells obtain substantially different gene expression profiles. These data suggest that these transcriptional networks are associated with tumor-mediated signals, yet are heavily influenced by ontogeny specific enhancer selection. I demonstrate here that microglia specifically silence *Itga4* (Cd49d) allowing for its usage as a discriminatory marker between brain-resident microglia and peripherally-derived macrophages in both primary and metastatic disease in mouse and human.

In Chapter 4 of my thesis, I develop an atlas of the immune contexture in human brain malignancy. Using multi-color flow cytometry, we catalogued the abundance of over 15

myeloid and lymphoid cell types across 60 fresh surgical samples encompassing low-grade glioma, high-grade glioma, recurrent glioma, and brain metastases from primary breast, lung and melanoma lesions. These analyses revealed grade specific immune compositions, where microglia were found to be most abundant in low-grade glioma, peripherally-derived macrophages most abundant high-grade glioma, and neutrophils largely abundant in brain metastases. Subsequent RNA-sequencing analyses uncovered cell specific gene expression patterns, with distinct grade-dependent alterations. These analyses identified putative heterotypic signaling cascades underlying the immune composition differences in both glioma and brain metastasis tumors. The findings here provide a complete characterization of the immune microenvironment and advance our understanding of the role of the constituent cells across brain malignancies.

CHAPTER 2

MATERIALS AND METHODS

Mice, cells and tumor models

<u>Mice</u>

Flk2-switch (*Flt3*:Cre, Rosa26:mTmG) mice were kindly provided by Dr. Camilla Forsberg (UCSC) (Benz, Martins, Radtke, & Bleul, 2008; Boyer, Schroeder, Smith-Berdan, & Forsberg, 2011; Muzumdar, Tasic, Miyamichi, Li, & Luo, 2007). Only male mice showed expression or transmittance of Cre, and as such only male mice were used for these experiments. *Cx3cr1*:CreER-IRES-YFP mice were obtained from Jackson Labs and bred to Rosa26:lsl-TdTomato reporter mice (Jackson Labs) (Madisen et al., 2010; Parkhurst et al., 2013). Nestin:Tva (nTva) mice in a mixed background, as described previously, were bred to C57BL/6 background for 10 generations (Holland, Hively, DePinho, & Varmus, 1998; Pyonteck et al., 2013). *Pten^{Flox/Flox}* mice were obtained from Dr. Charles Sawyers and Dr. Brett Carver (MSKCC) (Trotman et al., 2003). *Ccr2*:DTR-CFP mice were kindly provided by Dr. Eric Pamer (MSKCC) (Hohl et al., 2009). LysM:Cre (Clausen, Burkhardt, Reith, Renkawitz, & Forster, 1999) and CAG:GFP (M. Okabe, Ikawa, Kominami, Nakanishi, & Nishimune, 1997) mice were obtained from Jackson labs. Athymic nude mice were obtained from NCI Frederick and maintained at MSKCC. CAG:RFP mice (Long, Lackan, & Hadjantonakis, 2005) were obtained from Jackson labs and crossed to Athymic nude mice for 10 generations. All animal procedures and studies were approved by the MSKCC Institutional Animal Care and Use Committee (protocol 04-08-022).

Cells

DF1 chicken fibroblasts were obtained from the ATCC. RCAS vectors expressing PDGFB-HA, Cre and a short hairpin against mouse T*p53* (shP53) were kindly provided by Dr. Tatsuya Ozawa and Dr. Eric Holland (Ozawa et al., 2014). GL261 murine glioma cells were kindly provided by Dr. Sal Coniglio and Dr. Jeff Segall (Albert Einstein). MDA-MB-231 brain-homing variant cells (MDA-BrM) were kindly provided by Dr. Joan Massague (MSKCC) and labeled with a triple imaging vector (Tk-GFP-Luc) as previously described (Bos et al., 2009; Ponomarev et al., 2004; Sevenich et al., 2014). All cell lines were maintained in DMEM with 10% fetal bovine serum with penicillin and streptomycin.

Tumor models

For the glioma models, intracranial injections were performed on 5-6 week old mice as previously described (Pyonteck et al., 2013) (performed by Dr. Leila Akkari and Dr. Daniela Quail). Briefly, mice were fully anesthetized with ketamine/xylazine and bupivacaine was applied as a local anesthetic. Using a stereotactic apparatus, cells were injected into the right frontal cortex (1 mm caudal, 1.5 mm lateral from bregma, 2-3 mm deep). For the RCAS PDGFB-P53 model, $3x10^5$ DF1 cells (1:1 mixture of DF1: RCAS-PDGFB-HA, and DF1:RCAS:shP53) were injected. Similarly, for the PDGFB-PTEN model, $3x10^5$ cells were injected (1:1 mixture of DF1:RCAS-PDGFB-HA and DF1:RCAS-Cre). For the GL261 model, $2x10^4$ cells were injected. For brain metastasis models, 6-8 week old athymic nude mice were intracardially injected with $1x10^4$ MDA-BrM cells as previously described (performed by Dr. Lisa Sevenich and Dr. Florian Klemm) (Sevenich et al., 2014).

Tamoxifen lineage tracing and bone marrow transplantation:

For the Cx3cr1:CreER-IRES-YFP Rosa26:lsl-TdTomato lineage tracing system, 4 week old mice were injected twice, 48 hours apart, i.p. with 1 mg of tamoxifen citrate dissolved in corn oil. Mice were used for intracranial injection of DF1 cells 3 weeks after tamoxifen administration. For bone marrow transplantation, recipient mice were irradiated (Gammacell-40 Exator) with a split dose scheme of 2x4.5 Gy with a window of 4 hours between doses. Whole bone marrow was isolated from the femurs of a CAG:GFP donor mouse (6-8 weeks old) and $1x10^6$ cells were injected i.v. into previously irradiated recipients. Athymic nude mice were irradiated with a split dosage scheme of 2x4 Gy, and were reconstituted using Athymic CAG:RFP donors. Experimental mice were intracranially injected with DF1 cells 4 weeks after bone marrow transplantation.

Institutional Review Board (IRB) approval and patient information

All human specimens were collected from patients consented to MSKCC IRB protocol #06-107 and under MSKCC IRB protocol #14-230.

Flow cytometry and cell sorting

For blood analysis, mice were bled either retro-orbitally or submandibular under isoflurane anesthesia. For all other tissue analyses, mice were anesthetized with 1.25% Avertin, and transcardially perfused with PBS. Single cell suspensions from spleen and bone marrow were isolated by macrodissection and mechanical tissue dissociation. Liver, kidney, and lung were macrodissected and dissociated using the Mouse Tumor Dissociation Kit (mTDK, Miltenyi) using the OctoMACS disocciator. Mouse brain, mouse brain tumors, and human brain specimens were macrodissected and dissociated using the Brain Tumor Dissociation Kit (BTDK Miltenyi) and a single cell suspension was generated using the OctoMACS dissociator. Human

lung tumors were dissociated with the Human Tumor Dissociation Kit (hTDK Miltenyi.) All tissues were filtered through a 40 μM mesh filter and underwent RBC lysis (PharmLyse BD). Brain and brain tumor tissue underwent myelin removal using the Myelin Removal Beads (Miltenyi). Single cell suspensions were FC blocked (BD cat #553141) for 15 minutes at 4 degrees Celsius. Cells were then incubated with directly conjugated antibody panels for 15 minutes at 4 degrees Celsius. Cell suspensions were washed (PBS +2% fetal bovine serum) and resuspended in a DAPI solution. All flow cytometry analysis was completed on a BD Fortessa device at the Flow Cytometry Core Facility (FCCF) at MSKCC. All cell sorting was completed on an Aria III device at the FCCF at MSKCC. Cells were sorted directly into Trizol LS, and snap frozen in liquid nitrogen following collection. All antibodies for flow cytometry were titrated in a lot-dependent manner and are displayed in Table 2.1.

Immunohistochemistry

For histology tissue collection, mice were anesthetized with 1.25% Avertin, and transcardially perfused with PBS and 4% PFA. Tissues were macrodissected and the brain was post fixed in 4% PFA overnight and then placed in sucrose, while the spleen was immediately placed in 30% sucrose. Tissue was transferred to 30% sucrose for 2 days, embedded in OCT, and 10 μM cryosections were cut. Immunofluorescent staining followed. First slides were rehydrated with two washes of PBS for 5 minutes. Tissue was then permeabilized with 0.2% Triton-X in PBS and washed twice with PBS for 5 minutes. Hydrophobic circles were drawn surrounding tissue followed by 2 more washes with PBS for 5 minutes. Tissue was blocked with 0.5% PNB blocking buffer. Primary antibody was applied in 0.25% PNB blocking buffer overnight at 4 degrees Celsius. Tissues were washed 3 times with PBS for 5 minutes. Secondary antibody was applied (1:500 Molecular Probes) for 1 hour at room temperature followed

by 3 washes of PBS for 5 minutes. Slides were counterstained with DAPI (1:5000 Molecular Probes) for 5 minutes at room temperature, washed 3 times with PBS, and mounted with Dako fluorescent mounting media. Primary antibodies used were: chicken-anti GFP (AbCam 1:500), rat anti-Cd68 (Serotec 1:500), and rabbit anti-Iba1 (Wako, 1:500). Endogenous tomato was visible without immunohistochemical staining from both the Rosa26:mTmG and Rosa26:lsl-TdTomato reporter mice. Microscopy images were taken on a Zeiss Z1 AxioImager equipped with a TissueGnostics stage. Tiling images were acquired at 20x magnification using TissueFAXS (Tissuegnostics) and single images at 20x and 40x were acquired using Axiovision (Zeiss).

Table 2.1: Antibodies used in this study

Antigen	Clone	Target Species	Catalogue Number	Dilution
CD45	30-F11	Mouse	Biolegend 103128	--
CD11B	M/170	Mouse/Human	BD Biosciences 563553	--
Ly6C	HK1.4	Mouse	Biolegend 128026	--
Ly6G	1A8	Mouse	BD Biosciences 563005	--
Cd49d	R1-2	Mouse	Biolegend 103618	--
Cd11a	M17/4	Mouse	Biolegend 101120	--
Cd44	IM7	Mouse/Human	Biolegend 103012	--
CD45	HI30	Human	Biolegend 304042	--
CD66B	G10F5	Human	Biolegend 305106	--
CD14	HCD14	Human	Biolegend 325610	--
CD16	3G8	Human	Biolegend 302026	--
CD49D	9F10	Human	Biolegend 304308	--
CD11A	HI111	Human	BD Biosciences 563935	--
CD11C	3.9	Human	Biolegend 301630	--
HLA-DR	L243	Human	Biolegend 307617	--
CCR2	K036C2	Human	Biolegend 357211	--
CD3	UCHT1	Human	Biolegend 344821	--
CD4	A161A1	Human	Biolegend 357406	--
CD8	HIT8a	Human	Biolegend 300913	--
CD127	A019D5	Human	Biolegend 351316	--
CD25	BC96	Human	Biolegend 302606	--
CD20	2H7	Human	Biolegend 302314	--
CD56	HCD56	Human	Biolegend 316336	--
TCRγδ	B1	Human	Biolegend 331209	--
Iba-1	polyclonal	Rabbit anti-mouse	Wako Chemicals 01-1974	1:500
Cd68	polyclonal	Rat anti-mouse	AbD Serotec MCA1957	1:500
GFP	polyclonal	Chicken anti-GFP	AbCam 13970	1:500

RNA-sequencing and bioinformatics

RNA-sequencing

RNA was isolated using chloroform extraction and isopropanol precipitation with glycogen carrier. RNA-sequencing libraries were generated with the SMART-Seq preparation kit (CloneTech). Single end, 100 base pair, sequencing was performed by GeneWiz (New Jersey, USA) on an Illumina HiSeq 2500. FASTQ files were mapped to the mouse genome (mm10) or the human genome (hg19) using STAR (version 2.5.0e) with default parameters (Dobin et al., 2013). Transcript abundance was quantified using STAR with a GTF file from iGenomes (Illumina). A count matrix was produced in R and differential gene expression was assessed with DESeq2 using a fold change cutoff of +/- 2 and a false discovery rate of 5% (Love, Huber, & Anders, 2014). T-SNE probably distributions were generated in R with the Rtsne package (Maaten & Hinton, 2008) and visualized with ggplot2 (Wickham, 2009). Gene ontology analysis was performed using DAVID with default parameters (Dennis et al., 2003).

External dataset download and analysis:

All TCGA data was analyzed using the web-portal Gliovis (http://gliovis.bioinfo.cnio.es). Normalized gene expression data for the Immunological Genome Project (ImmGen) was obtained from the GEO under accession GSE15907 (Gautier et al., 2012). RNA-seq, ATAC-Seq and ChIP-Seq datasets for tissue resident macrophage transcriptional and epigenetic profiling were downloaded from the SRA using the NCBI SRA-toolkit from the following GEO accession numbers: GSE63338, GSE62826, GSE62826 and GSE63339 (Gosselin et al., 2014) (Lavin et al., 2014). RNA-sequencing data on microglia and macrophages in the non-malignant brain were downloaded under accession number GSE68376 (Bruttger et al., 2015). Each of these datasets was mapped to the mouse

genome mm10 as described above. For ChIP-seq and ATAC-seq datasets the STAR parameter "--alignIntronMax" was set to 1. PU.1 ChIP-Seq peak calling was performed with HOMER (Heinz et al., 2010). Peaks were considered within a promoter if they fell within 2kb upstream of 0.5kb downstream of the nearest transcription start site. Enhancer regions were considered up to 50kb upstream and downstream of the nearest transcription start site, excluding the promoter region. Deeptools was used to assess ChIP-seq and ATAC-seq density over the indicated windows surrounding either transcription start sites, or PU.1 binding sites within enhancers (Ramirez, Dundar, Diehl, Gruning, & Manke, 2014). The findPeaks script with HOMER was used to identify peaks for PU.1 binding with default parameters. The annotatePeaks.pl scripts in the HOMER suite was used to find enriched motifs in ChIP-seq peaks and in gene sets identified through RNA-sequencing. For promoter motif enrichment, only known motifs were considered in regions 300bp and 50bp downstream of the transcription start site.

Transcription factor activity analysis:

Transcription factor (TF) activity analysis was performed as an adaptation of two previously published methods: RegulatorInference (Setty et al., 2012) and ISMARA (Balwierz et al., 2014). Briefly, a set of transcription factor binding sites (TFBS) was screened across the promoters (500 bp upstream and 50 bp downstream of the transcription start site) of each gene present in the mouse genome (mm10). TFBS were predicted from known motifs provided by HOMER. The AnnotatePeaks.pl script in HOMER was used to make presence and absence calls for each TFBS in each promoter region. This was then tabulated into a matrix with TFBS motifs as columns and genes as rows. This tabulated matrix was used in a ridge regression to model log2 gene expression values generated by 'varianceStabilizingTransformation' function in the DESeq2 package in R. The glmnet function in R was used to perform the ridge

regression. Lambda, the regularization parameter, was determined for each sample by 10-fold cross validation (Friedman, Hastie, & Tibshirani, 2010). The model coefficients for each TFBS motif were z-scored. Differentially enriched TFBS motifs were determined by evaluating the z-scored values in limma with a fold change cutoff of +/-2 and a false discovery rate of 5% (Ritchie et al., 2015).

Statistical analysis and graph generation

All statistical analyses were completed using R (version 3.0.1), GraphPad Prism Pro v6, Gliovis (http://gliovis.bioinfo.cnio.es/) or as indicated in the bioinformatics section of the methods. Heatmaps were drawn with the ggplot2, gplots (Warnes et al., 2015) and pheatmap(Kolde, 2015) packages in R. Flow cytometry biplots and histograms were plotted in FlowJo v10.8. ChIP-sequencing tracks were visualized in IGV v2.3.66. Venn diagrams were drawn with the VennDiagram (Chen, 2015) and Vennerable (Swinton) packages in R. All other scatterplots, barplots, and boxplot were plotted with the ggplot2 package in R or with GraphPad Prism Pro v6.

CHAPTER 3

CD49D distinguishes ontogenetically distinct TAMs in brain malignancy

Introduction

In addition to their immense signal-dependent diversity, macrophages possess substantial developmental diversity (Mosser & Edwards, 2008; Y. Okabe & Medzhitov, 2015). Recent work has offered expansive insights into the developmental origins of tissue-resident macrophages as well as uncovered tissue specific gene expression patterns and enhancer landscapes (Lavin et al., 2014) (Gomez Perdiguero, Klapproth, Schulz, Busch, Azzoni, et al., 2015) (Ginhoux et al., 2010) (Gautier et al., 2012; Ginhoux et al., 2010). While it has been shown that the local environment heavily sculpts macrophage transcriptional profiles and epigenetic states, it remains to be seen how differences in ontogeny may influence macrophage function within an inflammatory tissue environment (Gosselin et al., 2014; Lavin et al., 2014). This is of particular interest in malignancy, where TAMs have been shown to be recruited from peripheral monocytes and are also potentially derived from tissue-resident macrophages (Charles, Holland, Gilbertson, Glass, & Kettenmann, 2011; Du et al., 2008; Pyonteck et al., 2013; Solga et al., 2015).

One particularly interesting tissue in which to study the role of tissue-resident macrophages in malignancy is the brain. Brain-resident macrophages, microglia, develop from yolk sac erythro-myeloid progenitor cells before definitive hematopoiesis (Ginhoux et al., 2010; Gomez Perdiguero, Klapproth, Schulz, Busch, Azzoni, et al., 2015). Unlike other tissue-resident macrophages, during homeostasis, microglia undergo self-renewal and their pool not replenished by monocytes (Ajami, Bennett, Krieger, McNagny, & Rossi, 2011; Ajami et al., 2007; Alliot, Godin, & Pessac, 1999;

40

Bruttger et al., 2015). They also exhibit robust resistance to myeloablative levels of irradiation (Kennedy & Abkowitz, 1997). Indeed this has been used extensively in bone marrow transplantation models to distinguish self-renewing, radio resistant microglia from bone marrow-derived macrophages (BMDM) (Sedgwick et al., 1991). Only under conditions of blood-brain barrier preconditioning (irradiation (IR), chemotherapy), does there appear to be a significant contribution of BMDMs to the brain macrophage pool (Bruttger et al., 2015; Capotondo et al., 2012). Studies utilizing IR-BMT have demonstrated BMDM abundance in murine glioma, however it remains mechanistically unclear exactly how the irradiation preconditioning precisely impacts BMDM recruitment in glioma (Huang et al., 2014; Muller et al., 2015; Pyonteck et al., 2013).

Here, we utilize multiple genetic lineage tracing models to demonstrate that BMDM are indeed present in murine glioma. Gene expression profiling revealed that while BMDM and microglia (MG) share some components of tumor education, they also exhibit distinct modes of activation along the canonically defined macrophage activation paradigm. Our data suggest that these faculties are a result of transcriptional networks poised before the onset of tumorigenesis, where ontogeny pre-biases cells to engage in classical and alternatively activated macrophage states. Lastly, we identify markers capable of distinguishing microglia and macrophages under homeostasis, as well as in glioma and brain metastasis in both mice and humans.

Results

<u>TAM BMDMs are present in glioma</u>

To reliably track the ontogeny of myeloid cells in murine gliomas we utilized a pan-hematopoietic lineage tracing system, Flt3:Cre; Rosa26:mTmG (Boyer et al., 2011; Buza-Vidas et al., 2011). This system has been previously used to support the finding

that microglia develop independent of a Flt3+ hematopoietic stem cell (HSC), while most peripheral myeloid cells originate from these precursors (Boyer et al., 2011; Gomez Perdiguero, Klapproth, Schulz, Busch, Azzoni, et al., 2015). We found that while >95% of blood monocytes were GFP+, only <1% of microglia showed recombination for the Rosa26:mTmG switch reporter (Figure 3.1A). Likewise, the spleen was composed of GFP+ germinal centers, surrounded by Tomato+ stromal cells, while the brain did not contain any GFP+ cells (Figure 3.1B). We next bred the Flt3:Cre; Rosa26:mTmG mice to the Nestin:T-va (nTva) allele to utilize the RCAS model of murine gliomagenesis. Tumors were induced in adult mice by intracranial injection of RCAS:PDGFB and RCAS:shP53 DF1 cells as previously described (Figure 3.1C) (Ozawa et al., 2014). This led to robust glioma formation with full penetrance within 6 weeks. Flow cytometry analysis of end-stage tumors demonstrated that all monocytes and neutrophils within the tumor were GFP+ and of HSC origin, as expected (Figure 3.1D,E). However the TAM compartment (Cd45+Cd11b+Ly6C-Ly6G-) revealed the presence of both GFP+ TAM BMDM and GFP- TAM MG in the tumor (Figure 3.1D-F). Meanwhile the contralateral, non-malignant, brain contained only GFP- MG, demonstrating the specificity of abundance of TAM BMDM within the tumor (Figure 3.1F).

We and others have previously utilized irradiation bone marrow transplantation (IR-BMT) to demonstrate that TAM BMDM are recruited to murine gliomas (Huang et al., 2014; Pyonteck et al., 2013). However, several reports have demonstrated that IR can lead to ectopic recruitment of BMDM to the brain and increase their relative contribution (Bruttger et al., 2015; Muller et al., 2015). We verified these findings in the GL261 glioma model, and similarly found that the TAM compartment was composed of both TAM MG and TAM BMDM using both IR-BMT lineage tracing and IR-free Flt3:Cre,mTmG lineage tracing (Figure 3.1G,H).

Figure 3.1

A Normal Brain Microglia

Blood Monocytes

B DAPI GFP TOMATO

Brain

1.5 mm

0.75 mm

Spleen

0.5 mm

0.15 mm

C Flt3: Cre
Rosa26: mTmG

Initiate tumors
RCAS: PDGFB-shP53

~5 weeks

Isolate TAMs
Microglia: Tomato+ GFP-
BMDM: Tomato- GFP+

D

Myeloid 20.0
Tumor Cells 57.6
Lymphocytes 8.19

Granulocytes 13.0
TAMM 33.2
Monocytes 30.5

Microglia 43.9
BMDM 50.9

E Tomato+ / GFP+

Mono Gran MG — Normal
Mono Gran TAM — Tumor

F Tumor — DAPI IBA1 GFP

Adjacent brain — DAPI IBA1 GFP

G Flt3: Cre mTmG
GL261 Tumor

MG 41.8
BMDM 53.3

H p <0.02

Brain Resident / Peripheral

Mono Gran TAM IR TAM

Flt3:Cre: mTmG | IR-BMT

43

Figure 3.1: Flt3:Cre and IR-BMT lineage tracing reveals peripheral macrophage recruitment in murine glioma

(A)   Brian microglia (Cd45+Cd11b+Ly6C-Ly6G-) and blood monocytes (Cd45+Cd11b +Ly6C+Ly6G-) were isolated from Flt3:Cre Rosa26:mTmG mice. GFP and Tomato expression were assessed by flow cytometry. **(B)**Representative immunofluorescent images for DAPI (blue), GFP (green) and tomato (red) shown for the brain (top) and spleen (bottom) from Flt3 lineage tracing mice. The hippocampus and splenic germinal center are shown on the right. **(C)** Flt3:Cre; Rosa26:mTmG; nTva+ mice were injected with RCAS vectors encoding PDGFB and a short hairpin RNA targeting TP53 (shP53). Tumors were isolated from symptomatic mice 5-6 weeks after intracranial injection. **(D)** Gating scheme for identification of TAMs. Bulk myeloid cells are identified as Cd45+Cd11b+, which are further subdivided into Ly6C+Ly6G- monocytes, Ly6Clow Ly6G+ Granulocytes, and Ly6C-Ly6G- macrophages. Macrophages are further subdivided into GFP-Tomato+ microglia (MG) and GFP+Tomato- bone marrow-derived macrophages (BMDM).**(E)** Quantitation of Tomato+ and GFP+ monocytes and granulocytes in peripheral blood, microglia in non-tumor bearing brain, and monocytes, granulocytes and TAMs in RCAS tumors as depicted in (A) and (D). **(F)** Immunofluorescent (IF) staining of Iba1 (white) and GFP (green) in tumor tissue and normal tissue adjacent to tumors as described in (C). Scale bars in bottom right corner indicate 40 μM.**(G)** Flow cytometry of TAMs gated as in (D) from GL261 tumors in the Flt3:Cre Rosa26:mTmG model.**(H)** Composition of Tomato+ and GFP+ monocytes, granulocytes, and TAMs in the GL261 Flt3:Cre; Rosa26:mTmG model. Composition of TAMs in GL261 tumors using an IR-BMT protocol with GFP+ donor cells.

We found that TAM BMDM abundance was significantly increased in the IR-BMT model compared to the Flt3:mTmG lineage tracing model (Figure 3.1H), reinforcing previous findings that IR-BMT can skew the ratio of microglia and macrophages. Critically, we found that BMDM still composed over half of the TAM population in non-irradiated tumors, demonstrating that TAM BMDM recruitment is not solely an artifact of irradiation (Figure 3.1H).

To exclude the possibility that this finding was an artifact of a subset of TAM MG spontaneously up regulating Flt3, we utilized a complementary lineage tracing approach shown to be specific for microglia; Cx3cr1:CreER-IRES YFP; Rosa26:lsl-TdTomato (Parkhurst et al., 2013). We injected ~4 week old mice with 2x tamoxifen to induce recombination of the TdTomato reporter. We found that at 7 days, >99% of microglia and circulating monocytes were TdTomato+ (Figure 3.2A). However after 3 weeks, the blood monocytes no longer retained the TdTomato+ reporter, indicating that the previously labeled cells had turned over and were replaced by new monocytes, naive to tamoxifen treatment and therefore unlabeled (Figure 3.2B). By contrast, >99% of microglia remained TdTomato+, highlighting their robust self-renewal and longevity (Figure 3.2B). We then induced tumors using the GL261 glioma model in the Cx3cr1:CreER-IRES YFP; Rosa26:lsl-TdTomato mice to investigate TAM BMDM recruitment (Figure 3.2C). Here, again, we observed both TdTomato+ TAM MG and TdTomato- TAM BMDM, demonstrating the heterogeneity in ontogeny of the TAM compartment (Figure 3.2D). Meanwhile, all monocytes and neutrophils were TdTomato- in both the tumor and the periphery (Figure 3.2E). Together, these complementary genetic lineage-tracing models confirm that peripherally-derived BMDM contribute to the TAM pool in murine models of gliomagenesis, in the absence of irradiation.

Figure 3.2
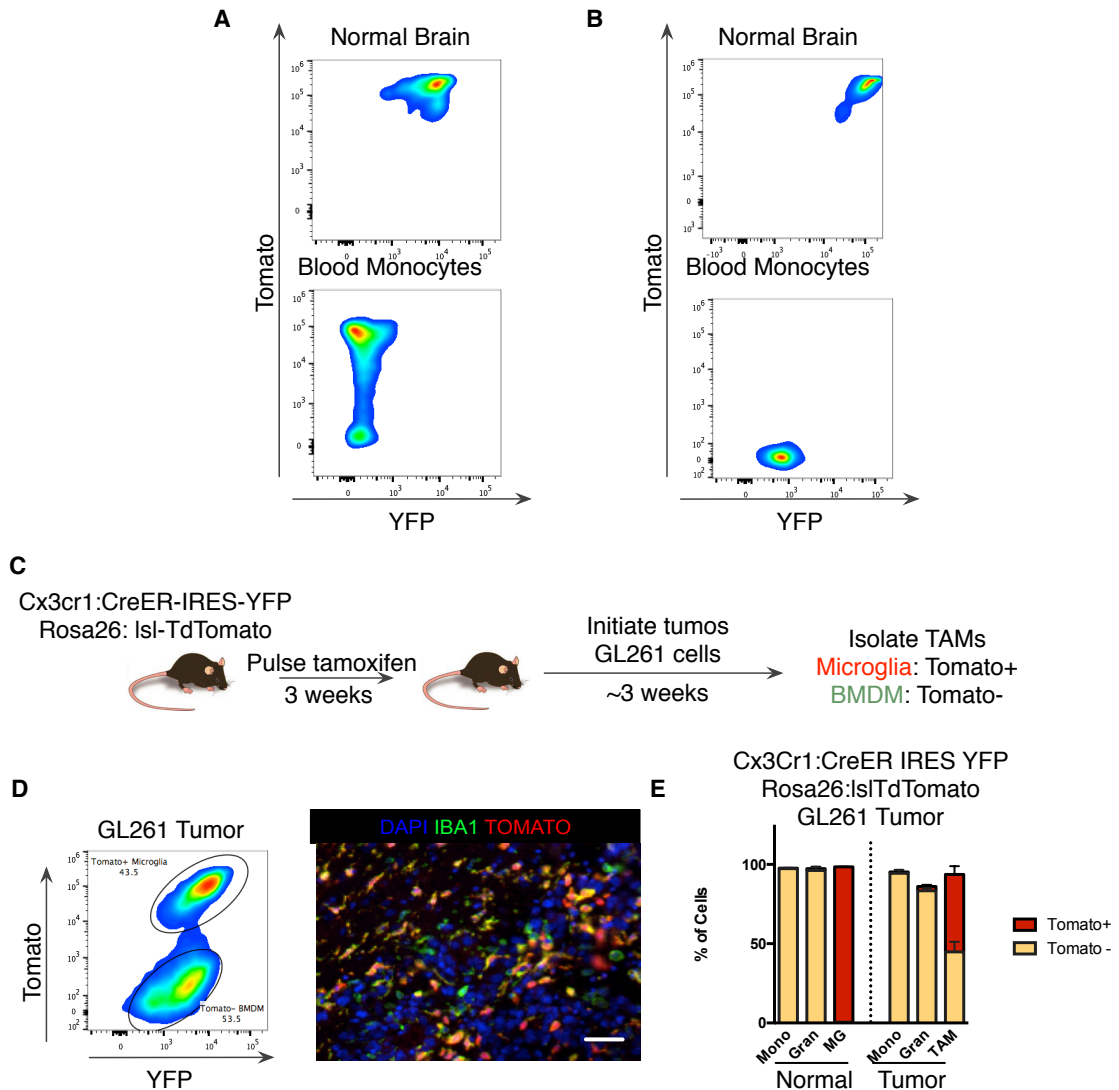
Figure 3.2: Cx3cr1:CreER lineage tracing uncovers heterogeneity in TAM ontogeny in murine glioma

(A) Tomato recombination in monocytes and microglia 7 days after tamoxifen treatment. **(B)** Tomato recombination in monocytes and microglia 28 days after tamoxifen treatment.
(C) Experimental design for Cx3cr1 lineage tracing model. Cx3cr1:CreER Rosa26:lsl-Tomato mice were injected with tamoxifen (2x i.p.) at 4 weeks of age. Mice were intracranially injected with GL261 glioma cells 3 weeks later. Tumors were isolated from symptomatic mice 3-4 weeks after injection. **(D)** TAMs were isolated from tumors as described in (C), and evaluated for Tomato and YFP expression. Representative immunofluorescent staining for Iba1 (green) and Tomato (red) in GL261 tumor. Scale bars in bottom right corner indicate 40 µM. **(E)** Quantitation of Tomato+/- cells using the Cx3cr1:CreER Rosa26:lsl-Tomato lineage tracing model. Normal monocytes and granulocytes were isolated from the blood of non-tumor bearing mice, and microglia were isolated from the brain. Monocytes, granulocytes and TAMs were also isolated from GL261 tumors.

RNA-sequencing reveals conserved patterns of TAM education

We next sought to characterize the transcriptional profiles of TAM MG and TAM BMDM in glioma. We sorted TAM MG and TAM BMDM from the Flt3:Cre; Rosa26:mTmG; RCAS tumors as well as MG and Ly6C-hi peripheral monocytes from non-tumor bearing animals, and performed RNA-sequencing. Principal component analysis revealed clustering of the 4 cell types into distinct clusters with TAM BMDM and TAM MG being most similar (Figure 3.3A). As expected, both TAM MG and TAM BMDM expressed higher levels of macrophage differentiation markers (*Cd14, Mertk,* and *Aif1)*, compared to Ly6C^{high} monocytes (Figure 3.3B,C). Normal MG and TAM MG expressed higher levels of microglia-specific transcripts *(P2ry12*, *Sigelch*, *Cx3cr1*, and *Fcrls)* compared to peripheral monocytes and TAM BMDM (Figure 3.3B). We extended this analysis to a larger panel of MG-specific genes (Gautier et al., 2012) and found consistent enrichment in TAM MG compared to TAM BMDM (Figure 3.3D). Interestingly, several of these transcripts were more highly expressed in TAM BMDM than monocytes (Figure 3.3E). Gene ontology analyses confirmed this finding across a larger panel of genes where TAM BMDM were enriched for terms associated with the brain (benjamini $p <$ 0.0237) and macrophage differentiation (benjamini $p <$ 0.0232) compared to Ly6C^{high} monocytes. Despite this difference, there was still higher expression of MG-related genes in Normal MG and TAM MG than in TAM BMDM. These analyses are consistent with notion that macrophages may acquire tissue-resident gene expression upon migration into a new tissue (Gosselin et al., 2014; Lavin et al., 2014).

Figure 3.3
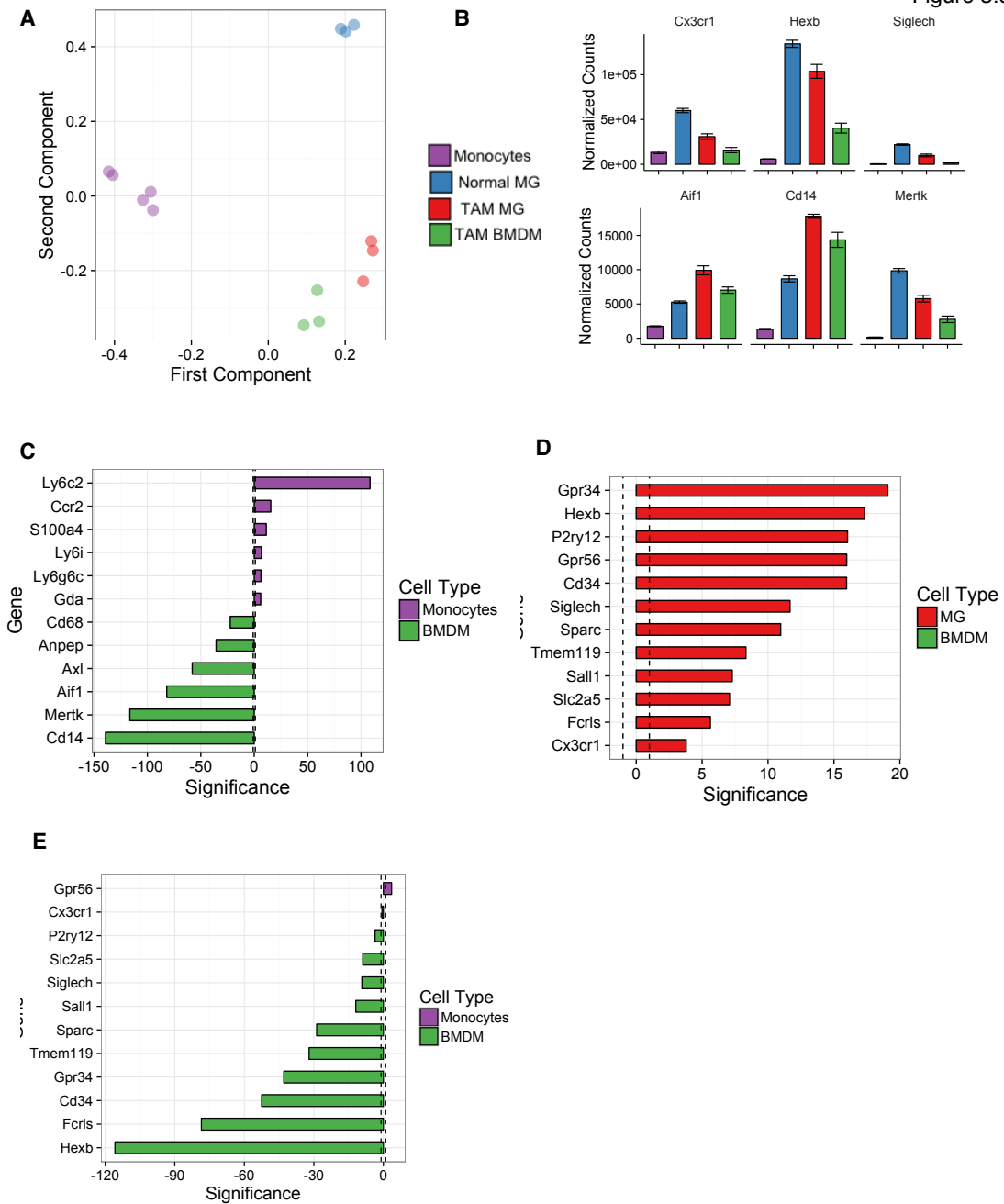
Figure 3.3: RNA-sequencing identifies ontogeny and environment specific gene expression

(A) Principle component analysis of RNA-sequencing performed on microglia and monocytes from non-tumor bearing mice, as well as TAM MG and TAM BMDM from RCAS tumors (as described in Figure 3.1C). **(B)** Normalized counts for the indicated transcripts. **(C)** Barplot depicting the significance (-log10(p value)*sign(fold change)) for macrophage and monocyte specific genes (positive values indicate enrichment in monocytes). **(D)** Barplot depicting significance of microglia-specific genes enriched in TAM MG vs TAM BMDM (positive values indicate enrichment in TAM MG). **(E)** Barplot depicting enrichment of microglia-specific genes enriched in TAM BMDM vs normal monocytes (positive values indicate enrichment in monocytes).

We next sought to identify programs of tumor education that were conserved between TAM MG and TAM BMDM. We identified a set of genes (n=1294) that were upregulated in TAM MG relative to normal MG, and showed no difference between TAM BMDM and TAM MG (Figure 3.4A).

A subset of these genes was found to be upregulated compared to monocytes as well (n=466) (Figure 3.4B). Gene ontology analysis identified a prominent enrichment for terms associated with oxidative phosphorylation, a process known to be upregulated in IL-4 stimulated, alternatively activated, macrophages (Jha et al., 2015). This was corroborated by marked induction of many members of complex I in the electron transport chain (Figure 3.4C). We additionally identified marked upregulation of many cell cycle-related genes, suggestive of increased proliferation in TAMs compared relative to normal MG and monocytes (Figure 3.4D). Conserved upregulation of complement related factors, extracellular matrix components, proteases, lipid metabolism mediators, and clotting factors were also identified (Figure 3.4E). In addition to these programmatic changes, we found upregulation of growth factors (*Igf1, Areg, Osm)*, chemokines and cytokines (*Il1b*, *Cxcl1*, *Spp1*, *Ccl5)*, and other immune modulators including *Cd274/*PD-L1 and MHC class I molecules (*H2-K1*, *H2-D1*, *B2m*) (Figure 3.4F-H).

TAM BMDM and TAM MG show different education patterns

We next investigated the transcriptional differences between TAM BMDM and TAM MG. Differential gene expression analysis revealed 880 genes enriched in TAM MG and 1185 genes enriched in TAM BMDM (Figure 3.5A). These lists were further enriched by filtering for genes enriched against normal MG and monocytes respectively, identifying 148 TAM MG-specific genes, and 311 TAM BMDM-specific genes (Figure 3.5B). Consistent with their tissue-specific function, we found that normal MG and TAM MG

were enriched for *Jam2, Jam3, Ocln,* and *Tjp1* (Figure 3.5C), integral components of the blood-brain barrier (W. Y. Liu, Wang, Zhang, Wei, & Li, 2012). Likewise, TAM MG expressed higher levels of classical complement factors *Ci1q, C1qc C4b, C2,* and *Cfh*, a pathway important for microglia function in synaptic pruning and host defense (Stephan, Barres, & Stevens, 2012).

Figure 3.4
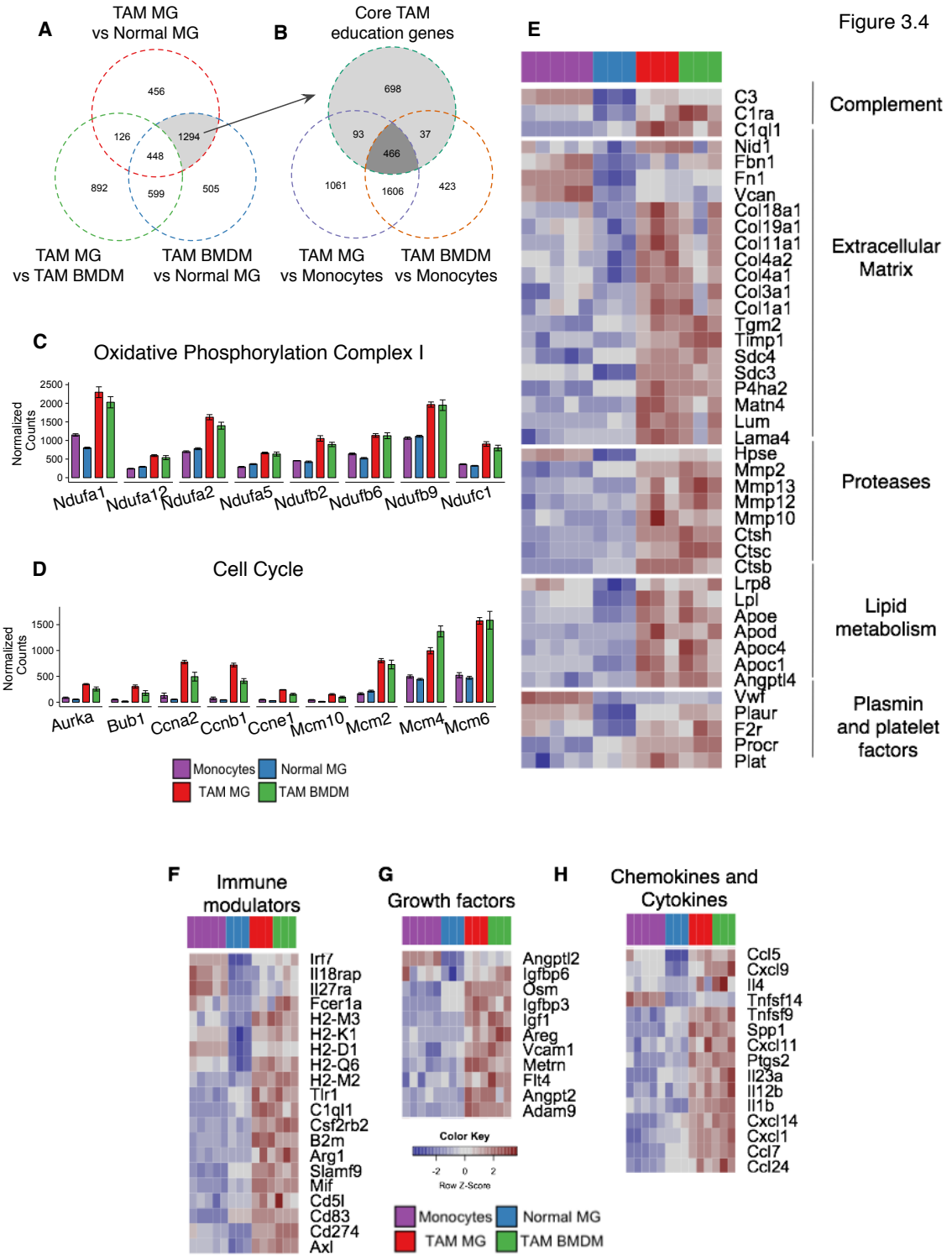
Figure 3.4: TAM BMDM and TAM MG exhibit conserved patterns of tumor education

(A) Venn diagram indicating the number of genes upregulated in TAM MG vs Normal MG and TAM BMDM vs Normal MG. The green circle contains the number genes differentially expressed between TAM MG and TAM BMDM. The grey sector indicates the Core TAM education genes (n=1294). **(B)** A subset of the genes in (A) were also upregulated in TAM MG vs Monocytes and TAM BMDM vs Monocytes (n=466). **(C)** Normalized counts for the indicated subunits of the electron transport chain Complex I/ NADH dehydrogenase demonstrate enriched expression in TAM BMDM and TAM MG. **(D)** Normalized counts for the indicated transcripts associated with cell cycle progression. **(E)** Row normalized heatmap depicting relative expression of select genes associated with complement, extracellular matrix, proteases, lipid metabolism, and platelet factors. **(F-H)** Row normalized heatmap depicting enrichment of select growth factors (F), chemokines and cytokines (G),and immunomodulators (H) across normal monocytes, normal microglia, TAM MG and TAM BMDM.

Meanwhile, TAM BMDM expressed high levels of alternative complement cascade *Cfb*, and *Cfp* (Figure 3.5C). We also identified differential expression of IL-1 pathway ligands, *Il1a* and *Il1b,* which were enriched in TAM MG and TAM BMDM respectively. Interestingly, while *Il1r1* levels did not significantly differ, TAM BMDM expressed higher levels of the IL-1 signaling antagonist *Il1rn*, and the IL-1 decoy receptor *Il1r2* (Figure 3.5C). These findings complement previous reports demonstrating *Il1a* enrichment in microglia compared to peripherally-derived macrophages, where IL-1 signaling played a critical role in microglia repopulation and maintenance in homeostasis (Bruttger et al., 2015). In addition, we identified enrichment of pleiotropic growth factors such as *Vegfa, Thsb1, Thbd* and *Hgf* in TAM BMDM, while TAM MG were enriched for *Adm* and *Thbs2* ((Figure 3.5D).

We were particularly interested in interrogating chemokines, growth factors and immune modulatory factors associated with different macrophage activation states. Indeed, we found that TAM BMDM were enriched for wound healing response chemokines reminiscent of an M[IL-4] stimulated macrophage including: *Ccl22, Ccl17, Cxcl2, Cxcl3,* and *Cxcl16* (Figure 3.5E) (Mosser & Edwards, 2008; Xue et al., 2014). Interestingly, TAM MG were enriched for expression of *Ccl2, Ccl3,* and *Cxcl10*, chemokines associated with an M[IFN-**γ**] driven pro-inflammatory response (Mosser & Edwards, 2008; Xue et al., 2014). In addition, while TAM BMDM were enriched for the anti-inflammatory cytokine *Il10,* microglia expressed higher levels of the pro-inflammatory cytokine *Tnf* (Figure 3.5E).

This difference in activation states was further supported by a programmatic increase in antigen presentation centered around increased expression of the MHC-II master regulator *Clita* (Reith, LeibundGut-Landmann, & Waldburger, 2005), and its

transcriptional targets *H2-DMb2, H2-DMa, H2-DMb1, Cd74, Ifi30, H2-Ab-1, H2-Eb2, H2-Eb1, H2-Oa, and H2-Aa* in TAM BMDM (Figure 3.5F).   In addition to this program, we found increased expression of costimulatory molecules such as *Cd80*, *Cd40, Cd40lg, Cd200* and *Cd200r4,* while TAM MG were enriched for *Cd276/*B7-H3 (Figure 3.5C). Combined with increased expression of *Il10* in TAM BMDM compared to TAM MG, these findings suggest that TAM BMDM engage in a wound healing response with a tolerogenic immunosuppressive program (Locatelli et al., 2012), reminiscent of an alternatively activated macrophage (Mosser & Edwards, 2008).

These findings were further supported by TAM BMDM-enriched expression of the Aryl-hydrocarbon receptor (*Ahr*), a transcription factor shown to mediate immune suppression (Murray et al., 2014) (Figure 3.5C). Previous efforts identified Kyneurine, a downstream product of Tryptophan metabolism, as an *in vivo* ligand for Ahr in glioma (Opitz et al., 2011). While we did not observe any differential expression of indoleamine or tryptophan processing enzymes *Ido1*, *Ido2,* or *Tdo,* we did observe TAM BMDM enrichment of the downstream enzymes *Kynu* and *Kmo*, which are responsible for quinolonic acid production, a molecule capable of relieving oxidative stress in glioma cells (Adams et al., 2012; Adams et al., 2014; Sahm et al., 2013) (Figure 3.5C).
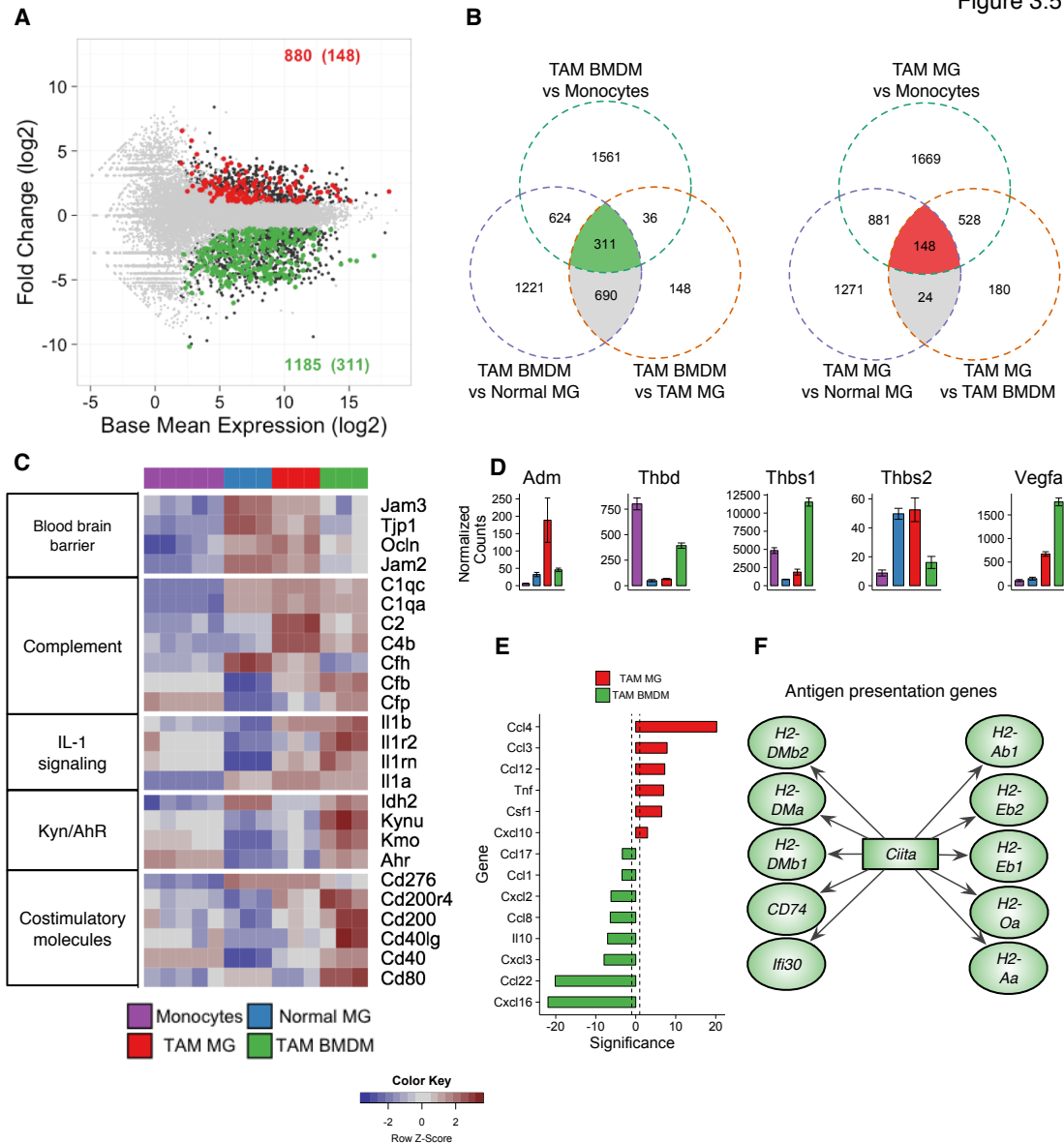
Figure 3.5: TAM BMDM are enriched for wound healing genes compared to TAM MG
(A) MA-plot depicting log2 mean expression (x axis) against log2 fold change (y axis) between TAM MG and TAM BMDM (positive values indicate enrichment in TAM BMDM). Black dots indicate differential expression between TAM MG (n=880) and TAM BMDM (n=1185). Green dots indicate TAM BMDM-specific genes compared to monocytes, normal MG and TAM MG (n=311, Figure 3.5B). Red dots indicate TAM MG-specific genes compared to monocytes, normal MG and TAM BMDM (n=148, see Figure 3.5B). Grey dots indicate genes that are not differentially expressed. **(B)** Venn diagram demonstrating selection of TAM BMDM and TAM MG specific genes. **(C)** Row normalized heatmap indicating expression of select genes related to the blood-brain barrier, Kyneurine/Aryl hydrocarbon signaling, IL-1 signaling, complement, and costimulatory molecules. **(D)** Normalized gene counts across monocytes, normal MG, TAM MG and TAM BMDM angiogenesis-related genes. **(E)** Barplot indicating significance of select cytokine gene expression enrichment in TAM BMDM and TAM MG, positive values indicate enrichment in TAM MG. **(F)** Network indicating gene expression enrichment of antigen presentation genes as controlled by the MHC-II master regulator Ciita, which mediates expression of the other family members listed.

55

Identification of transcription factor networks underlying TAM activation

We next utilized a ridge regression-based linear model to interrogate transcriptional networks underlying the differential activation profiles in TAM BMDM and TAM MG compared to both each other and to normal MG. Similar approaches have been utilized to investigate networks underlying monocyte to macrophage differentiation (Consortium et al., 2009) and global gene expression networks in different molecular subtypes of GBM patients (Setty et al., 2012). Here we identified transcription factor (TF) motifs that were enriched specifically in TAM BMDM and TAM MG compared to normal MG and blood monocytes (Figure 3.6A). These analyses revealed increased TF activity for NF-KB, E2F1, RXR and HIF1A among others, exclusively in TAM BMDM and TAM MG (Figure 3.6A,B). We also identified a set of TF motifs that were upregulated in blood monocytes, TAM BMDM, and TAM MG relative to normal MG. Strikingly, among this group was a set of ISRE/IRF-1 and IRfF-2 motifs indicative of typ1 I or type II interferon signaling (Figure 3.6B), supporting similar findings in bulk TAMs isolated from gliomas and other tumor types (Biswas et al., 2006; Gabrusiewicz et al., 2011).

When comparing TAM BMDM to TAM MG directly, we found MEF2C and SMAD3 enriched in TAM MG. These are two TFs known to be enriched in microglia, whose activity has been shown to be directly related to their tissue identity (Gosselin et al., 2014; Lavin et al., 2014) (Figure 3.6C). In TAM BMDM we found enrichment for TF motifs involved in monocyte to macrophage differentiation including VDR, KLF4, and PU.1 (Figure 3.6C) (Alder et al., 2008; Kreutz et al., 1993). In addition, we also found enrichment for STAT3, NF-kappaB and IRF4, all of which have been associated with differential functions in macrophage activation (Mosser & Edwards, 2008; Ostuni & Natoli, 2011). In addition to being differentially expressed between TAM BMDM and TAM MG, *Klf4* and *Irf4* were of particular interest given their role in mediating IL-4

mediated alternative macrophage activation (Liao et al., 2011; Satoh et al., 2010) (Figure 3.6D). To complement these genome-wide TF activity analyses, we also performed motif enrichment analysis on the promoters of TAM BMDM-specific and TAM MG-specific genes using HOMER (Heinz et al., 2010) (Figure 3.6E).

These analyses again revealed an enrichment of MEF2 motifs in TAM MG, demonstrating the consistent role of tissue-specific transcriptional programs in TAM MG education. Meanwhile, TAM BMDM-specific genes were again enriched in PU.1 and STAT3 binding sites, in addition to STAT6 binding sites, the canonical mediator of IL-4 signaling. Both TAM MG and TAM BMDM-specific gene lists were enriched for NF-κB binding sites, mirroring the global transcription factor activity analysis juxtaposing Normal MG to both TAM BMDM and TAM MG (Figure 3.6A,E). In addition to these transcriptional programs we identified enrichment of *Hdac7* and *Hdac9* in TAM BMDM while *Hdac11* was enriched in TAM MG (Figure 3.6F), and interestingly has been shown to repress *Il10* activation in macrophages (Villagra et al., 2009). Collectively, these analyses demonstrate that transcriptional programs enriched in TAM MG and TAM BMDM are reflective of their differential activation profiles, and are potentially linked to their distinct developmental ontogenies.

Figure 3.6
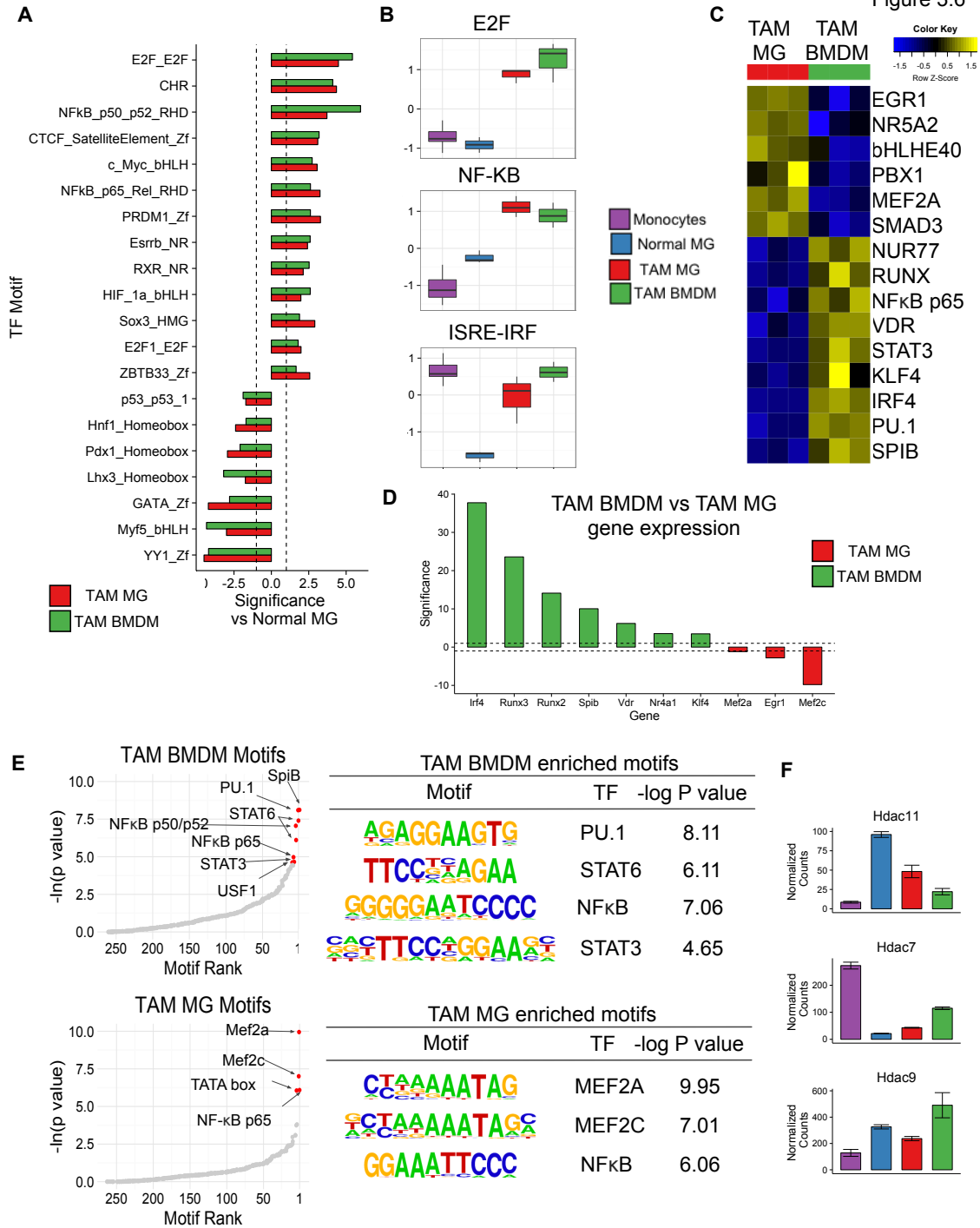
Figure 3.6: Transcription factor activity analysis reveals pathways underpinning TAM activation

(A) Barplot indicating significance of indicated transcription factor (TF) motif for TAM BMDM vs normal MG (green bars) or TAM MG vs normal MG (red bars). Positive values indicate activity enrichment in TAM BMDM/TAM MG vs normal MG. **(B)** Boxplots demonstrating the TF activity for the indicated motif family across normal monocytes, normal MG, TAM MG and TAM BMDM. **(C)** Row normalized heatmap indicating relative transcription factor activation scores between TAM MG and TAM BMDM in global transcription factor activity enrichment. **(D)** Barplot indicating significance of select transcription factor gene expression between TAM BMDM and TAM MG (positive values indicate enrichment in TAM BMDM). **(E)** Ranked transcription factor motifs enrichment in promoters from TAM BMDM-specific genes (n=311) and TAM MG-specific genes (n=148). Red dots indicate significant hits as reported by HOMER, select motifs are shown to the right. **(F)** Normalized gene counts across monocytes, normal MG, TAM MG and TAM BMDM for the indicated Hdac family members.

Ontogeny-specific transcriptional programs influence TAM gene expression

Given the developmental differences in these cells, we hypothesized that transcriptional landscapes established before they encounter a tumor may play a role in regulating their differential activation patterns in late-stage tumorigenesis. Previous studies by Bruttger and colleagues have supported the well-accepted finding that microglia typically self-renew without contribution from the periphery, however, when the brain is preconditioned with irradiation, and in addition microglia are depleted, peripherally-derived macrophages can seed the brain and contribute significantly to the brain macrophage pool (Bruttger et al., 2015). We used this data in comparison with our TAM BMDM and TAM MG RNA-seq data to dissect tumor education differences from ontogenetic, non-tumor associated, differences. This juxtaposition allowed us to identify genes that were enriched in TAM BMDM (n=886) specifically in the context of a tumor, including *Irf4, Il10, Vegfa, Cxcl2, Cxcl3, Ccl17,* and *Cc22* (Figure 3.7A-C). Meanwhile, *Hdac11, Cd276, Ccl2* and *Ccl12* were only enriched in TAM MG, with no differential expression at baseline (Figure 3.7A-C). In contrast, cytokines such as *Ccl3*, *Ccl4*, *Csf1, Cxcl10,* and *Tnf* were already enriched in normal MG compared to brain-resident BMDM, even in the absence of a tumor. We termed genes such as these "MG Core" genes, also including *Jam2, Siglech* and *P2ry12* (Figure 3.7A-C, n=410). Conversely, "BMDM Core" genes were enriched in BMDM compared to MG in the presence and absence of a tumor including *Mrc1, Ciita, Ahr* and *Vdr* (Figure 3.7A-C).

We again utilized TF motif enrichment at the promoters of these genes to determine which transcriptional networks might underlie education and ontogenetic-specific gene expression changes. In "Core BMDM" genes we identified enrichment of PU.1, SpiB and KLF4 TF motifs (Figure 3.7D), of which PU.1 and KLF4 have been shown to play a critical role in macrophage differentiation (Feinberg et al., 2007) (Henkel et al., 1996). As

expected, IRF4 and STAT3 enrichment were restricted to "TAM BMDM" specific genes. We identified enrichment of MEF2C motifs in "Core MG" genes, while SMAD activity was enriched in "TAM MG" genes (Figure 3.7D). These results confirm that while TAM BMDM expression of wound healing genes is directly associated with tumor-mediated education, aspects of TAM MG and TAM BMDM differential expression occur in the absence of a tumor and are thus likely linked to their differential ontogeny.

While the "Core MG" genes were clearly enriched for factors and transcriptional programs known to be enriched in microglia, we sought to further explore what contributed to "Core BMDM" gene specificity. We examined these gene sets across multiple macrophage and monocyte subsets in the immunological genome project (ImmGen) (Gautier et al., 2012). As expected, we found that "Core MG" genes were enriched in microglia compared to all other macrophage and monocyte subsets analyzed (Figure 3.8A). Surprisingly, we found that "Core BMDM" genes were not enriched in any one given macrophage population, but rather were specifically repressed in microglia compared to the other macrophage populations and even monocytes (Figure 3.8A). We corroborated this in our own dataset, where "Core BMDM" genes were enriched even in monocytes compared to normal MG (Figure 3.8B). These results suggest that "Core BMDM" genes are not macrophage-specific *per se*, but instead represent a set of microglia-repressed genes. Recent work has highlighted extensive epigenetic diversity amongst tissue-resident macrophages (Gosselin et al., 2014; Lavin et al., 2014), thus we hypothesized that these microglia-repressed, "Core BMDM" genes may be epigenetically repressed in microglia compared to even the distantly related monocytes.

Figure 3.7
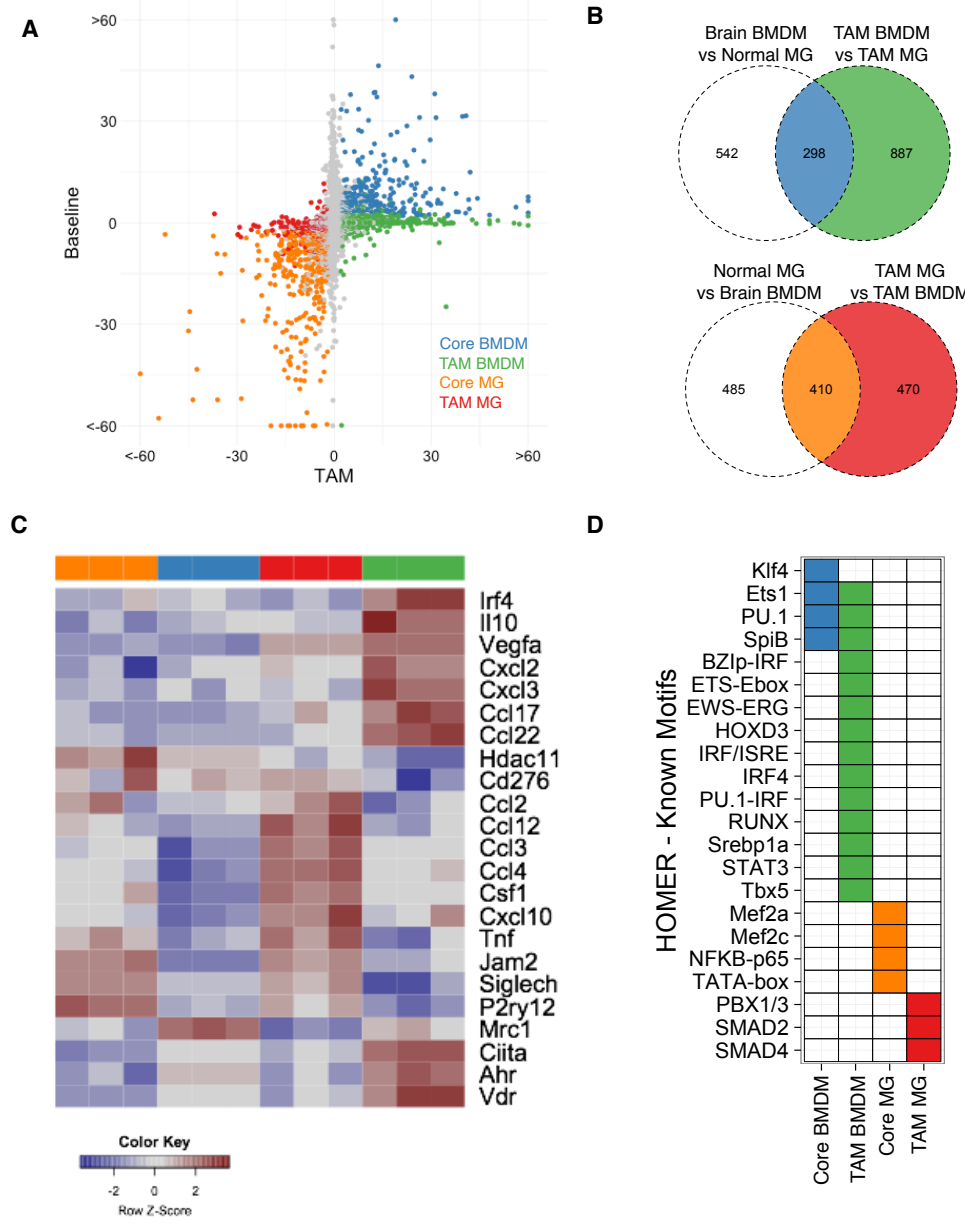
Figure 3.7: Ontogeny underlies differential gene expression between TAM BMDM and TAM MG

(A) Scatterplot indicating significance of differential expression between TAM BMDM and TAM MG (x axis) and Normal MG and Brain resident BMDM (y axis, GSE68376). TAM MG-enriched genes (n=470) are shown in red, TAM BMDM genes (n=887) are shown in green, Core BMDM genes (n-298) are in blue, and Core MG genes (n=470) are in orange (see Figure 3.7B for gene selection). **(B)** Venn diagram demonstrating gene selection for the groups indicated in (A). **(C)** Heatmap of gene expression across normal MG, brain BMDM, TAM MG and TAM BMDM. **(D)** Plot indicating transcription factor motif enrichment at the promoter of the indicated gene sets. Transcription motif enrichment and significance cutoff was performed with HOMER.

Indeed, when we analyzed these published datasets, we observed increased H3K27-Acetylation in the promoters of monocytes compared to microglia for the "BMDM Core" genes (Figure 3.8C). Likewise, we identified increased H3K27-Acetylation in the promoters of the "MG Core" genes in microglia compared to monocytes (Figure 3.8C). Further interrogation of ATAC-seq data (Lavin et al., 2014) demonstrated less open chromatin in the promoters of "BMDM Core" genes in microglia compared to monocytes. Similar trends were seen for "MG Core" genes, where microglia had more open chromatin than monocytes (Figure 3.8C).

Enhancer specification and epigenetic states in microglia and other macrophage populations in experimental models has been shown to be largely associated with differential PU.1 occupancy. Interrogating previously published data (Gosselin et al., 2014), we found that Thyoglycolate-elicited macrophages (TGEM), large peritoneal macrophages (LPM), small peritoneal macrophages (SPM), and BMDM all showed increased PU.1 binding at the promoters of "Core BMDM" genes compared to microglia (Figure 3.8D). Meanwhile, limited differential PU.1 occupancy was evident at the promoters of "Core MG" genes (Figure 3.8D). Similar binding dynamics were at play in enhancer elements, where PU.1 occupancy in enhancer regions of "Core BMDM" genes was higher in BMDM than MG, with less robust differences present in "Core MG" genes (Figure 3.8E).

PU.1 is a critical lineage-determining factor in macrophage development and it typically acts in concert with other transcription factors to specify genomic occupancy (Heinz et al., 2010). To identify putative coactivators, we used HOMER to identify motifs that co-occurred with PU.1 binding in "Core BMDM" genes, where PU.1 was bound in either all macrophage subsets, or in all subsets besides microglia (Figure 3.8F,G). As expected,

for promoters where PU.1 was bound in all macrophage subsets, including microglia, we identified enrichment of the PU.1 motif and the highly related SpiB motif (Figure 3.8G). Interestingly, in the PU.1 peaks where specifically the microglia subset did not show binding, we identified enrichment of PU.1, SpiB, ETS1, HOXA2, AR-halfsite, ERG, KLF4, and HOXB4. KLF4 was of particular interest given its role in mediating monocyte to macrophage differentiation (Feinberg et al., 2007), a process in which microglia do not engage (Gomez Perdiguero, Klapproth, Schulz, Busch, Azzoni, et al., 2015; Kierdorf, Erny, et al., 2013; Shepard & Zon, 2000). In addition, KLF4 acts cooperatively with STAT6 to mediate alternative macrophage polarization (Liao et al., 2011).

Collectively, these data complement the tissue-specific enhancer selection paradigm (Link et al., 2015) with ontogenetically defined enhancer selection mediating downstream stimulus responsiveness, and eventually differential function of tissue-resident and peripherally-derived macrophages in malignancy (Figure 3.9).

Figure 3.8

65
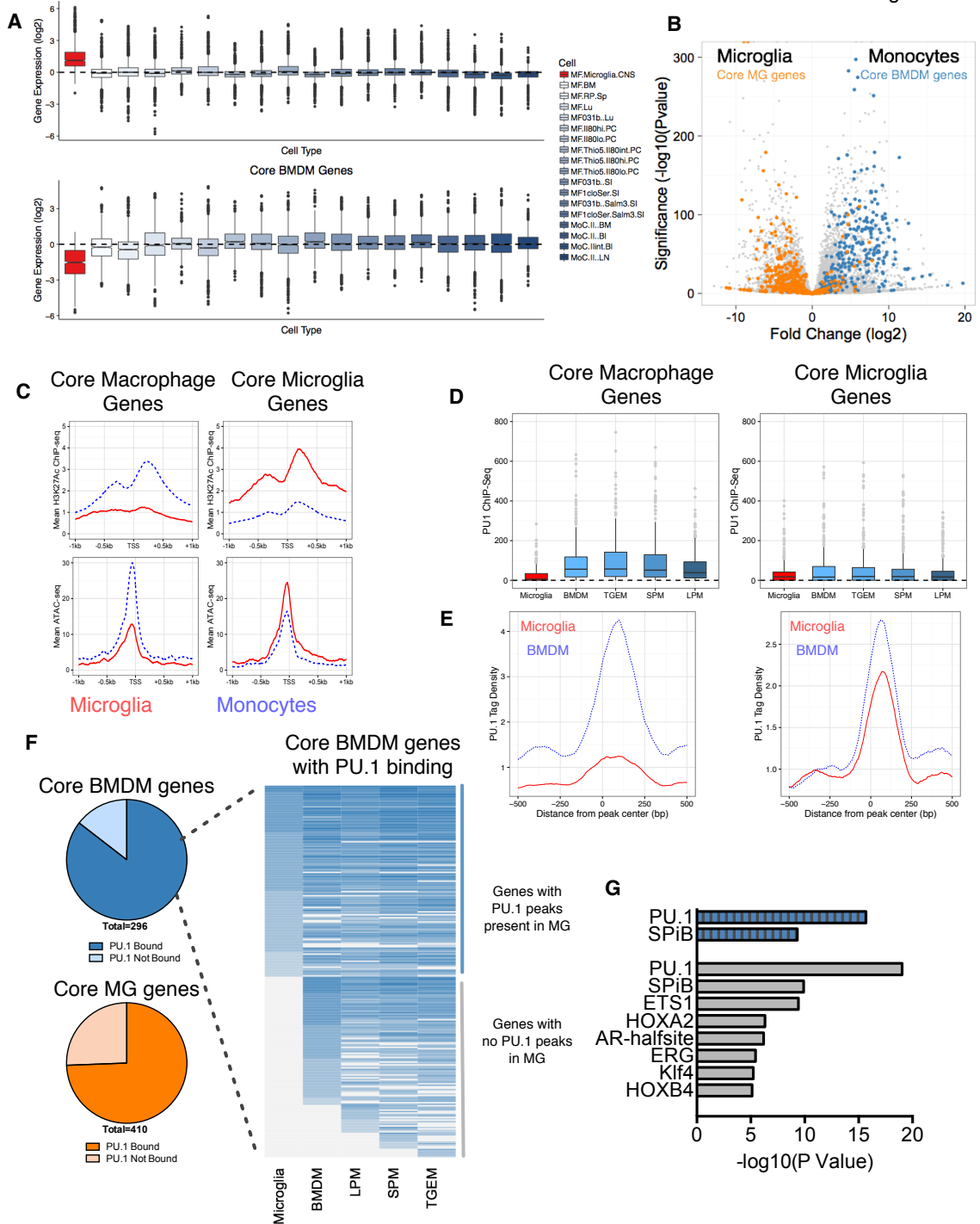
Figure 3.8: Core BMDM genes are epigenetically repressed in microglia
(**A**)   Expression of Core BMDM genes (top) and Core MG genes (bottom) across microglia (red) and monocytes/macrophages (GSE15907). **(B)** Volcano plot with –log10(p value) on the y-axis and fold change between normal MG and blood monocytes on the x axis. Core MG genes are shown in orange, and Core BMDM genes are shown in blue. **(C)** Mean H3K27-Acetylation signal (top) and ATAC-seq signal (bottom) centered around the transcription start site (+/- 1 Kb) in Core BMDM genes (left) and Core MG genes (right). Monocytes are shown in blue and microglia are shown in red. ChIP-Seq from GSE63338 and ATAC-Seq from GSE63339. **(D)** PU.1 binding intensity at the promoters of Core BMDM and Core MG genes in microglia, BMDM, TGEM, SPM and LPM. Genes were subsetted for those that showed binding of PU.1 in at least one of the macrophage subsets (see Figure 3.8F). **(E)** Average PU.1 binding distribution in enhancers of Core BMDM and Core MG genes for microglia and BMDM. Enhancers were defined +/- 50 kb from the transcription start site (excluding the promoter). These plots depict the average PU.1 binding signal around peaks found in either cell type, demonstrating that PU.1 binding is more abundant in BMDM than MG for Core BMDM genes. **(F)** Pie-chart (left) indicating the ratio of Core BMDM genes and Core MG genes where PU.1 binding was observed in at least one macrophage subtype (BMDM, Microglia, or peritoneal macrophage). Heatmap (right) indicating intensity of PU.1 binding at the promoter of Core BMDM genes in microglia, BMDM, TGEM, LPM and SPM. A subset of these genes shows binding in microglia and at least one other macrophage subtype (top), and another subset (bottom) shows absence of PU.1 binding in microglia. **(G)**   Motif enrichment scores from HOMER for the indicated motifs in Core BMDM genes where PU.1 is bound in microglia (top, blue) and genes where PU.1 is not bound in microglia (bottom, grey).

Figure 3.9
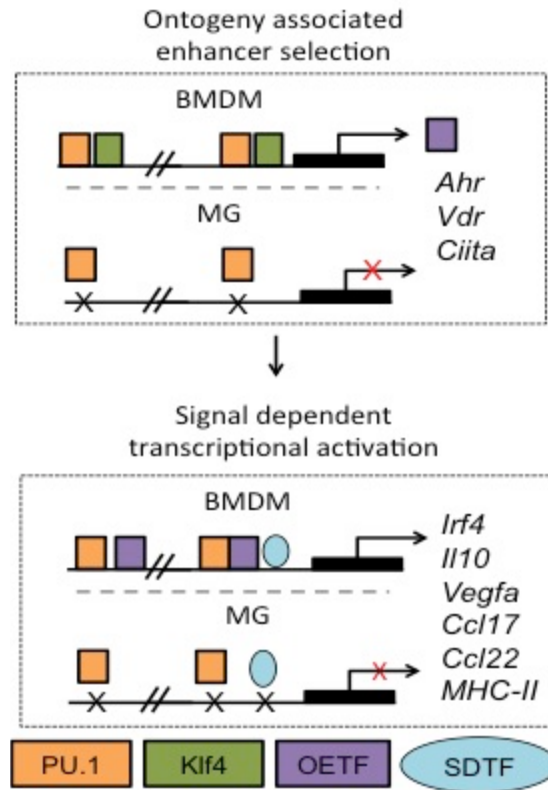
Figure 3.9: Ontogeny-enriched transcription factors stage TAM transcriptional hierarchy
Model depicting the hierarchical transcriptional cascade contributing to differences in activation between TAM BMDM and TAM MG. Differential PU.1 binding between BMDM and MG, influenced by co-factors such as Klf4, dictates expression of ontogeny-enriched transcription factors (OETFs). These OETFs then cooperate with signal-dependent transcription factors (SDTFs) to generate differential responsiveness to cytokine, and eventually differential macrophage activation between TAM BMDM and TAM MG.

<u>*ITGA4/*CD49D distinguishes microglia and macrophages in murine models of brain malignancy</u>

With the understanding that 1) these cell types are both present in murine gliomas, and 2) that they engage in distinct transcriptional programs, we sought to extend these findings to disease states other than glioma. In doing so, we aimed to identify a marker compatible with flow cytometry that could substitute for the complex genetic lineage tracing system employed above. We identified a list of transmembrane proteins from both the "Core MG" and "Core BMDM" genes, and screened these gene lists across gene expression data on tissue macrophages and monocytes from the Immunological genome project (ImmGen) (Gautier et al., 2012). From this list, we identified *Itga4* (Cd49d), *Itgal* (Cd11a) and *Cd44* as promising candidates to be enriched in BMDMs compared to microglia (Figure 3.10A).

In addition to *Itga4, Itgal*, and *Cd44* being enriched in brain-infiltrating BMDM compared to microglia (Figure 3.10B), they also showed lower expressed in microglia compared to other experimental macrophage models (Figure 3.10C). Previous epigenetic profiling (Gosselin et al., 2014; Lavin et al., 2014) prompted us to focus on those genes where there was reduced open chromatin and PU.1 binding in microglia compared to other macrophage and monocyte subsets. We rationalized identifying a stable marker of BMDM might be more reliable than a microglia marker that is conceivably upregulated by signals specific to the brain (as has been shown with *F11r* for example (Pong et al., 2013)). Indeed, for *Itga4*, *Itgal*, and *Cd44,* we found reduced ATAC-Seq signal in microglia compared to monocytes, as well as reduced PU.1 binding in microglia compared to BMDMs (Figure 3.10D-F).
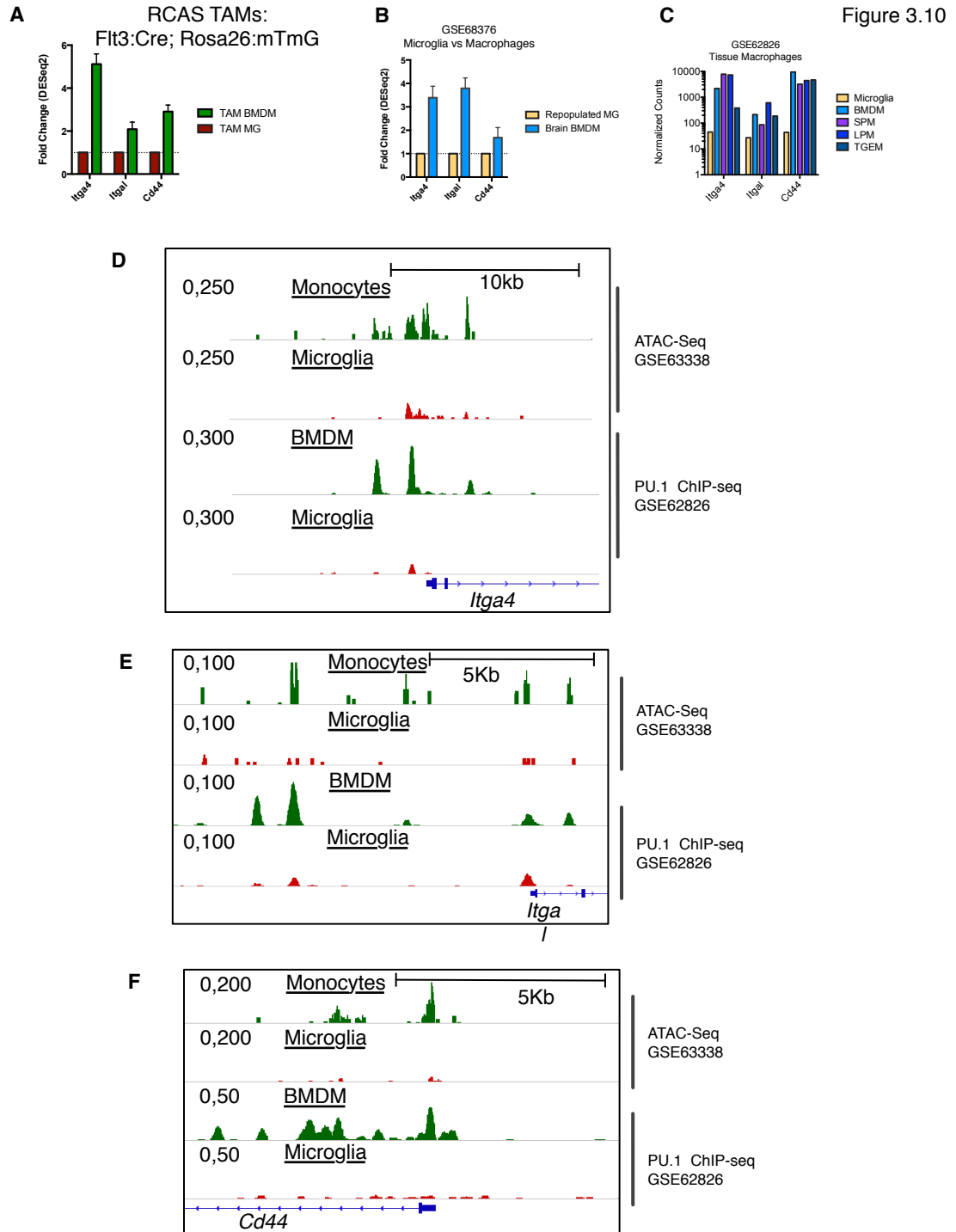
Figure 3.10: Itga4, Itgal and Cd44 are epigenetically silenced and show reduced PU.1 binding in microglia.
(A) Fold change relative to TAM MG of Itga4, Itgal, and Cd44 in Flt3:Cre Rosa26:mTmG RCAS tumors. **(B)** Fold change of Itga4, Itgal, and Cd44 in Brain resident BMDM relative to microglia for (GSE68376). **(C)** Log-10 expression of Itga4, Itgal, and Cd44 in Microglia, BMDM, TGEM, LPM and SPM. **(D-F)**. ATAC-Seq tracks for microglia and monocytes and PU.1 ChIP-Seq tracks for microglia and BMDM surrounding the Itga4 (D), Itgal (E), and Cd44 (F) transcription start sites. Data was replotted from the source as indicated.

We focused on *Itga4* (Cd49d), and experimentally determined by flow cytometry that microglia expressed lower levels of Cd49d compared to macrophages of the spleen, liver, lung, bone marrow and peripheral Ly6C+ monocytes (Figure 3.11A). Interestingly, we also found that Ly6G+ neutrophils were also negative for Cd49d, which served as a useful gating control in subsequent experiments (Figure 3.11A).

Previous reports have suggested that *Cd44* could serve as a useful marker for distinguishing microglia and peripherally-derived macrophages in experimental autoimmune encephalitis (EAE) models (Lewis, Hill, Juchem, Stefanopoulos, & Modis, 2014). Therefore we focused our analyses on the other two markers we identified and assessed the fidelity of Cd49d and Cd11a as markers differentiating TAM BMDM and TAM MG using the Flt3:Cre Rosa26: mTmG lineage tracing model in the RCAS:PDGFB shP53 murine glioma model. After gating on CD45+CD11b+Ly6C-Ly6G- cells, we found that the normal brain only contained Cd45^{low} Cd49d negative cells, while all peripheral monocytes were Cd45high Cd49d+ (Figure 3.11B). In the tumor we found two populations of cells; a set of CD45low Cd49d- microglia and a set of Cd45high Cd49d+ macrophages. Gating on these populations demonstrated that the Cd45high Cd49d positive gate contained GFP+ tomato- peripherally-derived BMDM, while the Cd45low Cd49d- gate contained GFP- tomato+ microglia (Figure 3.11B). Similar results were found for Cd11a (Figure 3.11B). These findings were also replicated in the GL261 glioma model using the same Flt3:Cre lineage tracing approach, as well as in the Cx3cr1:CreER-IRES-YFP Rosa26:lslTdTomato lineage tracing strategy (Figure 3.11C,D). Lastly, we evaluated Cd49d expression in a PTEN-PDGFB driven glioma model with IR-BMT to demonstrate that Cd49d was capable of distinguishing donor and host-derived cells even in glioma models with extended latency (~12 weeks) (Figure 3.11E).
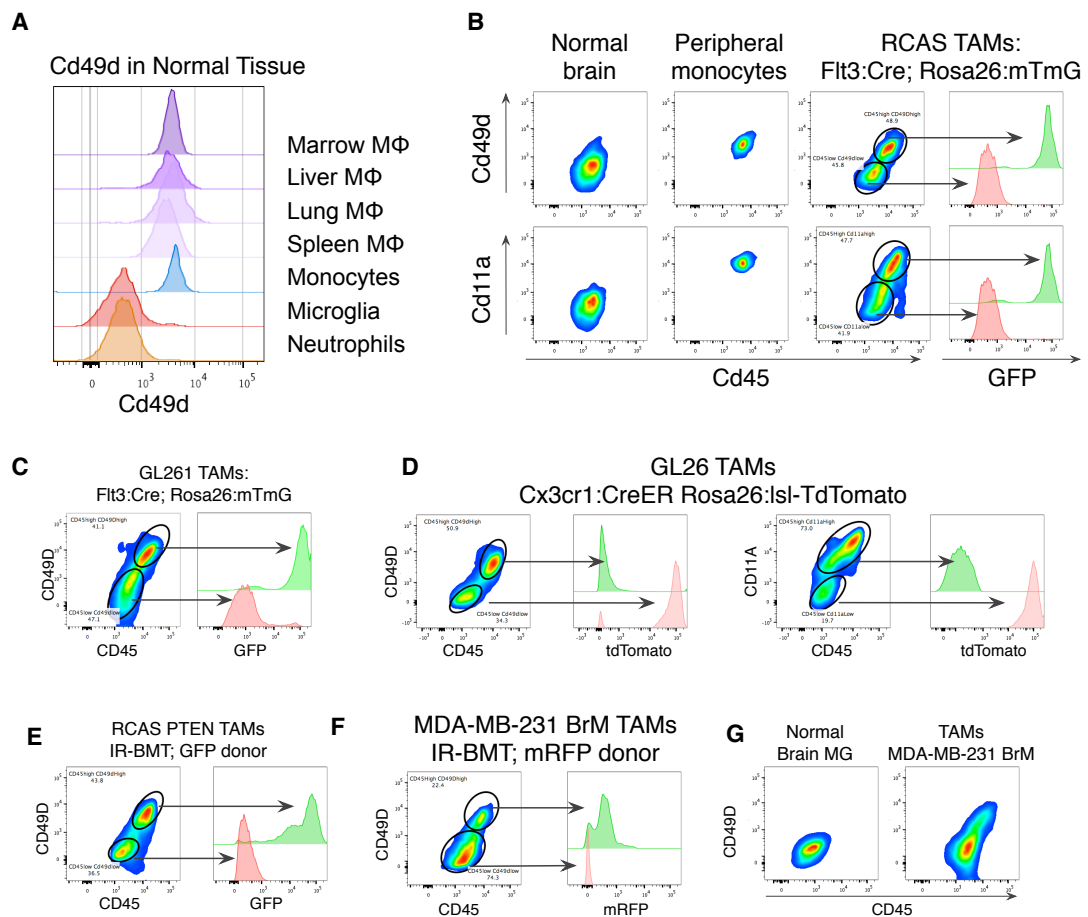
Figure 3.11

Figure 3.11: Microglia do not express Cd49d in murine models of brain malignancy
(A) Histogram of Cd49d expression by flow cytometry in monocytes, neutrophils, and macrophages from the bone marrow, liver, lung, spleen and brain (microglia). **(B)** Flow cytometry for Cd45 and Cd49d (top) or Cd11a (bottom) in normal blood monocytes, normal MG, or TAMs isolated from Flt3:Cre mTmG mice with RCAS tumors. The adjacent histograms indicate GFP expression in the indicated populations. **(C)** Flow cytometry for Cd45 and Cd49d on TAMs isolated from GL261 tumors in Flt3:Cre mTmG mice. The adjacent histogram depicts GFP expression in the indicated populations. **(D)** Flow cytometry for Cd45 and Cd49d (left) or Cd11a (right) on TAMs isolated from GL261 tumors in Cx3cr1:CreER Rosa26:lslTdTomato mice. The adjacent histogram depicts Tomato expression in the indicated populations. **(E)** Flow cytometry for Cd45 and Cd49d on TAMs isolated from a PTEN-RCAS tumor in a mouse that underwent IR-BMT reconstituted with GFP donor cells. The adjacent histogram shows GFP expression of the indicated populations. **(F)** Flow cytometry on Cd45 and Cd49d on TAMs isolated from an MDA-MD-231 xenograft brain metastasis in a IR-BMT mouse reconstituted with mRFP donor cells. The adjacent histogram depicts mRFP expression in the indicated populations. **(G)** Flow cytometry for Cd45 and Cd49d on microglia in the normal brain of an athymic mouse (left) or TAMs isolated from an MDA-MD-231 metastasis from an athymic mouse (right). The panel on the right indicates that Cd49d+ TAMs are present in brain malignancy without pre-treatment with irradiation, or intracranial injection.

To exclude any potential artifact associated with intra-cranial injection, we utilized an intra-cardiac injection model of brain metastasis colonization using brain homing MDA-MB-231 cells (Bos et al., 2009). Using this model, we identified two populations of cells, Cd45low Cd49d- microglia and Cd45^{high} Cd49d+ macrophages. In the IR-BMT setting, the mRFP+ donor cells were exclusively found within the Cd45^{high} Cd49+ macrophage gate (Figure 3.11F). Meanwhile in athymic mice that had not undergone IR-BMT, we still identified an increase in Cd49d+ expressing cells (Figure 3.11G) highlighting that TAM BMDM accumulation does not depend upon IR or intracranial injection preconditioning. These findings thoroughly establish Cd49d as a novel and efficient marker distinguishing resident microglia and peripherally-derived macrophages in homeostasis as well as in primary and metastatic brain malignancies.

CD49D identifies microglia and macrophages in human brain malignancies

We next sought to determine if CD49D could be used to discriminate microglia and macrophages in human brain malignancies. We assessed CD49D expression by flow cytometry across a panel of surgical samples composed of PBMCs, lung adenocarcinomas, non-malignant normal brain, low-grade glioma, high-grade glioma, and brain metastases. Consistent with our findings in mice, neutrophils (CD45+CD11B+CD66B+CD14^{low}CD16+) did not express CD49D, allowing for their use as a scale while gating CD49D+ and CD49D- TAMs (Figure 3.12A). Importantly, we never identified CD49D- TAMs in primary lung malignancy or CD49D- monocytes in healthy donor peripheral blood (Figure 3.12B). In contrast, the CD45+CD11B+CD66B-CD14+CD16- compartment in non-malignant brain samples was predominantly composed of CD49D- microglia (Figure 3.12B). In each glioma and brain metastasis sample we identified both CD49D+ and CD49D- TAMs, presumably representing peripherally-derived macrophages and brain-resident microglia respectively (Figure

3.12B). These findings demonstrate that CD49D-negative macrophages are restricted to brain-resident microglia. Interestingly, we found no difference in CD45 expression between CD49D- and CD49D+ in TAMs, a marker previously suggested to be informative for distinguishing macrophages and microglia in brain malignancy (Hussain et al., 2006; Parney et al., 2009; Sedgwick et al., 1991) (Figure 3.12C). Indeed, we found that CD45 expression differed most prominently between neutrophils and TAMs, as opposed to microglia and macrophages (Figure 3.12C). However, this difference in CD45 expression is not the case in mouse, where CD45 seemed to be an adequate differentiating marker between MG and BMDM in the model systems we tested (Figure 3.12C). These data demonstrate the necessity for thorough and extensive flow cytometry panels when interrogating the myeloid compartment of brain tumors in patient samples and experimental models.

Figure 3.12
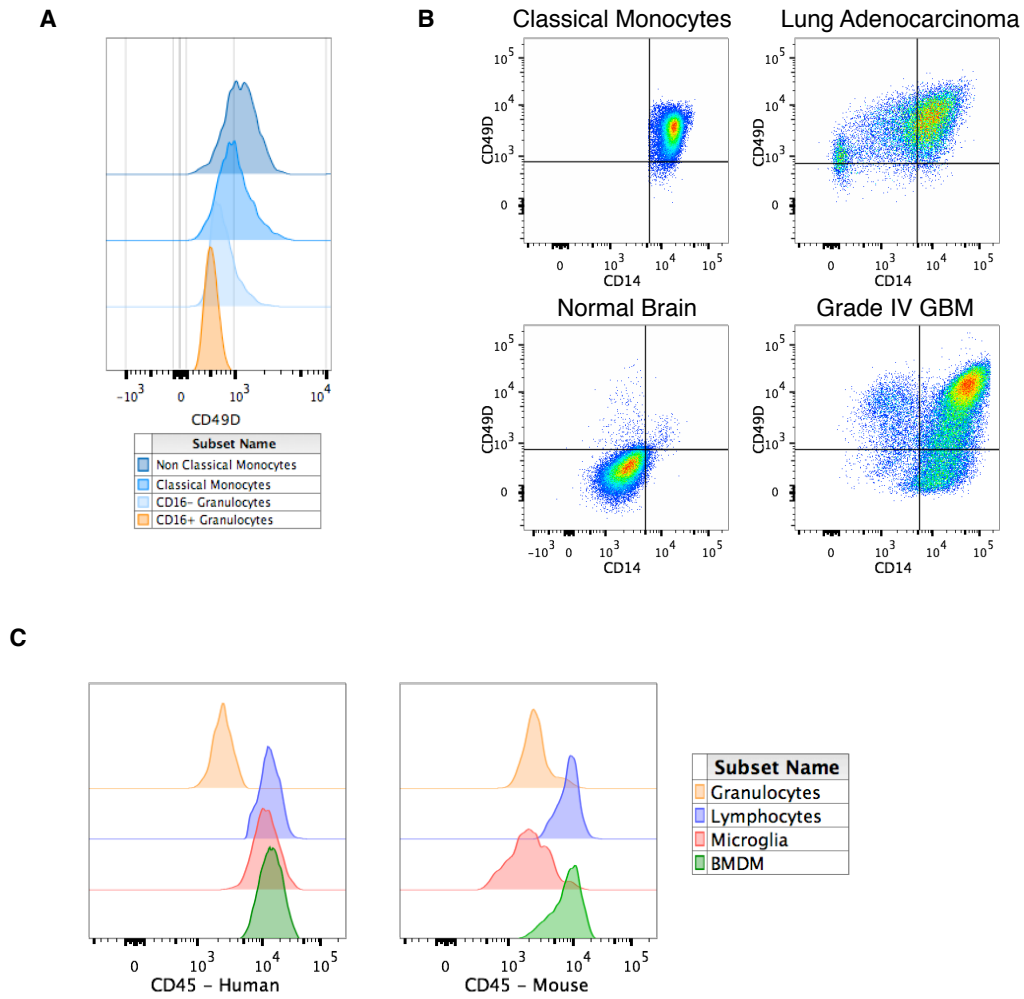
Figure 3.12: CD49D reveals TAM heterogeneity in human brain malignancy
(A) CD49D expression across blood monocytes, granulocytes, and T cells. **(B)** Classical monocytes, microglia, and TAMs were defined as CD45+CD11b+CD66b-CD14+CD16-. Gated cells are then shown for CD14 and CD49D in human classical monocytes from peripheral blood, TAMs from a lung adenocarcinoma patient, non-malignant brain, and a Grade IV GBM patient. **(C)** Histogram of CD45 expression by flow cytometry in mouse (left) and human (right) samples. In the mouse, Cd45+Cd11b+ cells were subdivided into: monocytes (Ly6c+Ly6g-), neutrophils (Ly6clow +Ly6g+), TAM MG in a Flt3:mTmG tumor from RCAS mouse (Ly6c-,Ly6g-Tomato+GFP-), and TAM BMDM from the same model (Ly6c-,Ly6g-Tomato-GFP+). In human samples, CD45+CD11B+ cells were subdivided into blood granulocytes (CD66B+CD16+CD14low), blood monocytes (CD66B-CD16-CD14+), TAM MG from a grade IV glioma (CD66B-CD16-CD14+CD49D-) and TAM BMDM from the same tumor (CD66B-CD16-CD14+CD49D+).

Discussion

Irradiation-based bone marrow transplantation (IR-BMT) has been widely used in experimental models to discriminate the origins of TAMs in brain malignancy, albeit with known concerns regarding potential artifacts due to the irradiation (Huang et al., 2014; Pyonteck et al., 2013) (Ajami et al., 2007) (Mildner et al., 2007) (Muller et al., 2015). Alternative chemical bone marrow transplant approaches have been suggested, though similar effects on the blood-brain barrier cannot be ignored(Kierdorf, Katzmarski, Haas, & Prinz, 2013) scheme (Alder et al., 2008). Here, we demonstrate that IR-BMT leads to increased TAM BMDM content in the GL261 model of glioma, a finding that has been previously reported juxtaposing IR-BMT with and without head-shielding (Muller et al., 2015). Recent reports have also utilized *Cx3cr1*:GFP and *Ccr2*:RFP mice to distinguish microglia and macrophage populations (Szulzewsky et al., 2015; Zhou et al., 2015). Our data here in both primary and metastatic tumors, supported by similar data in normal brain (Bruttger et al., 2015) demonstrates that peripheral macrophages upregulate *Cx3cr1* upon entry into the brain, and downregulate *Ccr2* compared to their monocyte precursors. These changes may lead to mislabeling of the cell types in a *Cx3cr1/Ccr2* reporter system. This further emphasizes the utility of the Cx3cr1:CreER lineage tracing approach employed here, and the necessity of extensive flow cytometry panels with Ly6C and Ly6G to exclude CCR2+ monocytes from a purified TAM population.

Outside of IR-BMT, the most widely employed approach to discriminate microglia and macrophages relies upon CD45 expression, whereupon CD45-high cells are considered macrophages and CD45-low cells are considered microglia (Sedgwick et al., 1991) (Gabrusiewicz et al., 2011). While this marker seems adequate in the murine models we have employed here, cell type-specific CD45 expression appears to be different between

mouse and human, again demonstrating the need for extensive flow cytometry panels to accurately distinguish these cells in both species. Instead, we present *Itga4* (CD49D) as an effective, consistent marker that works in both mice and humans to distinguish microglia and macrophages in multiple brain malignancies. This marker therefore serves as an effective complement to genetic lineage tracing models when such Lox-Cre technology is being used to trace or perturb other cellular compartments. Lastly, given that microglia show closed chromatin and diminished PU.1 binding at the *Itga4* locus, we posit that CD49D may be less malleable to expression fluctuation as compared to CD45.

Recent work has demonstrated extensive epigenetic patterning in tissue-resident macrophages. Our data here is consistent with the notion that such epigenetic states influence stimuli dependent transcriptional induction (Glass & Natoli, 2015; Gosselin et al., 2014; Lavin et al., 2014), thus leading to differential TAM education between microglia and macrophages. Previous work has demonstrated that differential genomic occupancy of PU.1 between microglia and other macrophage populations may dictate this differential enhancer selection (Gosselin et al., 2014). Indeed, here we find that TAM BMDM are enriched for a number of genes where microglia show no PU.1 binding. These data suggest that TAM BMDM are poised to engage in different transcriptional networks based on this initial enhancer selection. It seems most likely that differential expression of binding partners (either signal dependent or not) influences PU.1 genomic occupation. Cooperative binding is evident between PU.1 and CEBPβ to promote macrophage differentiation, and in B cell development where PU.1 occupancy is influenced by E2A expression (Heinz et al., 2010). Such a hypothesis has also been shown to account for microglia specific PU.1 binding in cooperation with TGFβ induced SMAD activity (Mullen et al., 2011). It is likely that similar dynamics are engaged here, where binding partners that are absent in microglia and expressed in macrophages are

sculpting genomic PU.1 occupancy. One possible candidate is *Klf4*, which is more highly expressed in TAM BMDM than TAM MG and shows motif enrichment in promoters where PU.1 binds in BMDM, but not in microglia. While *Klf4* is dispensable for microglia development, it is necessary for monocyte to macrophage differentiation (Feinberg et al., 2007), further implicating its ontogenetic functions and likely role as a PU.1 cofactor influencing genomic occupancy here. Differential DNA methylation and expression levels of PU.1 itself may also contribute to the difference in enhancer selection and downstream transcriptional output.

Current TAM re-education and depletion strategies have largely focused on CSF-1R blockade (Coniglio et al., 2012; Pyonteck et al., 2013), which likely affects both TAM BMDM and TAM MG, albeit through potentially different mechanisms. Further approaches aimed at targeting these cells in glioma should account for the differences in abundance of TAM BMDM and TAM MG, as well as their potentially distinct contributions to tumorigenesis. Understanding the transcriptional networks underpinning the differences between these cells should lead to therapeutic avenues that are capable of ameliorating the potentially pro-tumorigenic immunosuppressive functions of TAM BMDM, while preserving the pro-inflammatory functions of TAM MG. These data collectively demonstrate that peripherally-derived macrophages are indeed present in brain malignancy, and that ontogenetic differences between these cells and microglia is manifest via distinct transcriptional states.

CHAPTER 4

An atlas of the immune contexture in brain malignancy

Introduction

While glioblastoma multiforme (GBM) is the most common form of adult primary brain cancer, secondary disease metastasizing to the brain has a much greater incidence with even fewer treatment options (Brastianos et al., 2013). Extensive genomic and transcriptional profiling has been performed on low-grade glioma (LGG, grade II + grade III) and grade IV glioblastoma (Brennan et al., 2013; Cancer Genome Atlas Research et al., 2015; Ceccarelli et al., 2016; Verhaak et al., 2010), with comparatively less known about the genetic and transcriptional networks underlying metastatic lesions. These studies have motivated the development and clinical testing of tumor cell targeted therapy, however success has been limited (H. Wang et al., 2015). The tumor microenvironment offers an alternative to traditional tumor cell targeting (Quail & Joyce, 2013). Indeed studies in our lab have demonstrated preclinical efficacy for macrophage-targeted therapy through CSF-1R blockade (Pyonteck et al., 2013). Other studies have focused on unleashing T cell responses and dendritic cell vaccines to enact an adaptive immune response (Jackson et al., 2013; Vom Berg et al., 2013). Meanwhile, targeting of the tumor vasculature through VEGFA inhibition with Bevacizumab has led to quality of life improvements, yet no effect on overall survival (Gilbert et al., 2014). As the potential for these therapies grow, so does the need to understand the complete immune contexture of brain malignancy.

While the characterization of the immune infiltrate in the brain tumor microenvironments remains incomplete, there is consistent evidence that tumor-associated macrophages are an abundant cell type with multifaceted roles in disease progression

(Hambardzumyan et al., 2015). Studies in our lab have demonstrated that TAMs compose the majority of non-cancerous cells within brain metastases (BrM) originating from breast cancer primary tumors (Sevenich et al., 2014). In addition, previous reports have suggested that CD163+ /alternatively activated macrophages accumulate with glioma grade (Komohara et al., 2008), and represent the predominant immune population in glioma patients (Parney et al., 2009). However the relative abundance of microglia (MG) and bone marrow-derived macrophages (BMDM) within these compartments remains unclear. While previous reports have characterized the infiltration of subsets of T cells in glioma, a comprehensive analysis of the immune infiltrate in brain malignancy is lacking (El Andaloussi & Lesniak, 2006; Waziri et al., 2008).

We posit that a thorough understanding of the immune cell composition will be critical to unraveling the function of the various cells within the TME. Additionally these studies will facilitate the development of TME-targeted therapy, and inform how tumor cell-targeted therapy that interacts with the TME. Utilizing comprehensive flow cytometry panels we enumerate the abundance of myeloid and lymphoid cells across a panel of fresh surgical specimens. These studies identify glioma grade specific immune cell abundances, as well as distinct abundance patterns in brain metastases. Subsequent RNA-sequencing demonstrated grade- and disease-specific gene expression patterns revealing heterotypic signaling cascades, underlying differential immune cell recruitment across disease grade.

Results

<u>Patient cohort characterization</u>

To gain insight into the brain TME, we acquired fresh surgical samples from consented patients operated on by the MSKCC Neurosurgical department between November 2014 and February 2016 (in collaboration with Dr. Florian Klemm in the Joyce lab). In addition to these samples, we partnered with the Pathology Department at MSKCC to acquire post-mortem cerebral tissue from patients with or without brain malignancy. During this time, we established a bank of tissue specimens from 44 glioma patients, 16 patients with brain metastases, and 7 non-malignant cortex tissues from either autopsy specimens or surgical specimens distal from the malignant site (Figure 4.1A). For each tumor specimen we acquired tissue for frozen histology, snap frozen tissue for further molecular characterization, and performed immune cell profiling by flow cytometry. In addition, for a subset of these patients we were able to establish standard tumor cell lines and neurosphere lines. The remainder of the analyses will focus on samples from which we were able to obtain sufficient tissue quantity and quality to perform immune cell profiling by flow cytometry. Within this set, the majority of the glioma patients presented with grade IV glioma, in addition to the less common grade II and grade III disease (Figure 4.1B). While the tumor specimens arose from distinct grades, for simplicity, we will collectively abbreviate these samples as "glioma" when comparing to brain metastasis (BrM) samples, unless otherwise denoted. The BrM samples were acquired from patients with breast, melanoma or lung primary tumors, with the latter being the most abundant (Figure 4.1C). While we were able to collect tissue specimens from both initial diagnosis and recurrence (Figure 4.1D), no patients were sampled at both initial diagnosis and recurrence during this ~1 year collection window in order to have directly matched samples.

Figure 4.1

Disease	Total Patients	Immune profiling	RNA-sequencing
Glioma	44	29	13
BrM	16	15	7
Non-malignant brain	7	3	1
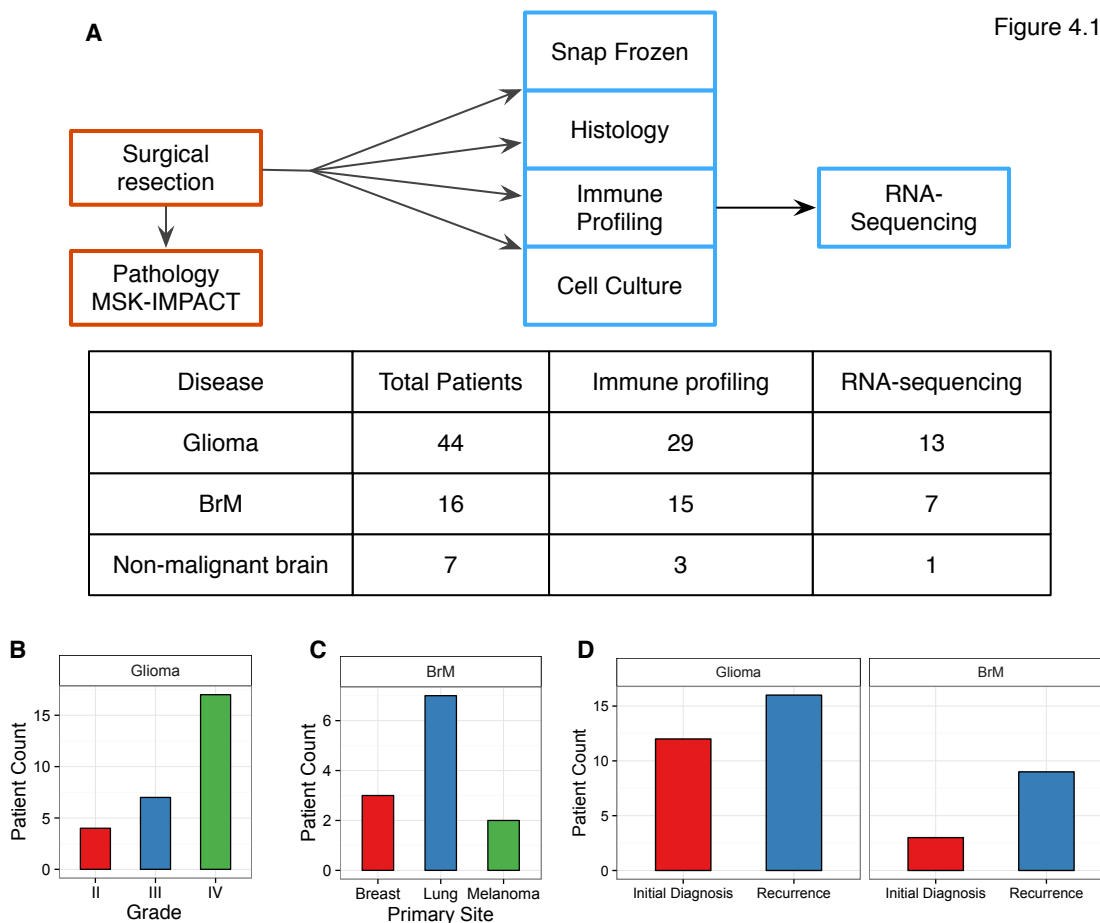
Figure 4.1 Tumor specimen numbers and characteristics
(A) Workflow of sample acquisition from Department of Neurosurgery. For each surgical specimen (tissue abundance permitting), samples were taken for snap freezing, frozen histology, immune profiling, and cell culture. A subset of patient samples were sorted by flow cytometry and specific cell populations were submitted for RNA-sequencing. **(B)** Barchart depicting the number of tumor samples collected with histological grading of grade II, grade III or grade IV glioma. Only samples that underwent immune cell profiling are tallied here. **(C)** As in (B), this barchart depicts the number of brain metastasis (BrM) samples collected from patients with the indicated primary tumor type of breast, lung or melanoma. **(D)** Barchart indicating the number of glioma (left) and BrM (right) tumor specimens that were from primary diagnosis samples (red) or had undergone previous treatment (blue).

Immune cell profiling of patient populations identifies stage- and disease-specific

immune abundances

To interrogate the immune cell infiltration of brain tumors, we implemented two multi-color flow cytometry panels focused on dissecting the myeloid and lymphoid cell compartments of the immune contexture. In the lymphoid cell panel we utilized CD45, CD11B, CD20, CD3, CD56, CD4, CD8, CD127 and CD25. This allowed us to identify B cells, NK cells, and an array of T cells including CD4+ T cells, CD8+ T cells, T regulatory cells, and double negative T cells (CD4- CD8-; DNT). In the myeloid panel we utilized CD45, CD11B, CD66B, CD16, CD14, CD11C, HLA-DR, and CD49D. This allowed us to unambiguously identify granulocytes, dendritic cells, classical monocytes, non-classical monocytes, intermediate monocytes, macrophages, and microglia. The cell surface marker definitions for these cell types are shown in Table 4.1. We verified these panels in buffy coat samples from healthy donors, where the hierarchical gating is shown in Figure 4.2A-B. In tumor samples, microglia and macrophage discrimination was performed using CD49D (Figure 3.12, Figure 4.2C). In addition, since CD16+ granulocytes were CD49D-, we used their expression as an internal gating control to demarcate CD49D- microglia and CD49D+ macrophages (Figure 4.2C).

We first assessed the total immune cell infiltrate (CD45+ cells) and found that it did not vary across glioma grade, nor was it significantly different in BrM samples compared to gliomas (data not shown). We next assessed the relative abundance of the lymphoid (CD45+CD11B-) and myeloid (CD45+CD11B+) cell compartments across glioma grade. Myeloid cells often composed between 25-75% of total cells within the tumor and out-numbered lymphocytes in grade II, grade III and grade IV glioma (Figure 4.3A). Meanwhile, there was no significant difference between myeloid and lymphoid cell numbers in BrM specimens.

Table 4.1: Flow cytometry markers and immune cell definitions

Lymphoid Panel	Cell type	Markers
	CD4+ T cells	$CD45^+CD11B^-CD20^-CD3^+CD4^+CD8^-$ $CD127^+CD25^-$
	T regulatory cells	$CD45^+CD11B^-CD20^-$ $CD3^+CD4^+CD8^-CD127^-CD25^+$
	CD8+ T cells	$CD45^+CD11B^-CD20^-CD3^+CD4^-CD8^+$
	Double negative T cells (DNT)	$CD45^+CD11B^-CD20^-CD3^+CD4^-CD8^-$
	B Cells	$CD45^+CD11B^-CD20^+CD3^-$
	NK Cells	$CD45^+CD11B^-CD20^-CD3^-CD56^+$

Myeloid Panel	Cell type	Markers
	Granulocytes	$CD45^+CD11B^+CD66B^+CD16^+CD14^{low}$
	CD16- Granulocytes	$CD45^+CD11B^+CD66B^+CD16^-CD14^{low}$
	Dendritic cells	$CD45^+CD11B^+CD66B^-CD16^-CD14^{low}$ $HLA-DR^+CD11C^+$
	Microglia	$CD45^+CD11B^+CD66B^-CD16^-CD14^{int}$ $CD49D^-$
	Macrophage	$CD45^+CD11B^+CD66B^-CD16^-CD14^{int}$ $CD49D^+$
	Non-classical monocytes	$CD45^+CD11B^+CD66B^-CD16^+CD14^{low}$
	Intermediate monocytes	$CD45^+CD11B^+CD66B^-CD16^+CD14^+$
	Classical Monocytes	$CD45^+CD11B^+CD66B^-CD16^-CD14^+$
	Immature Myeloid Cells	$CD45^+CD11B^+CD66B^-CD16^-CD14^-$ $HLADR^-CD11C^-$

Table of markers used to define the indicated cell populations by multi-color flow cytometry. All events were first gated for single live cells based on forward and side scatter, then DAPI exclusion for dead cells.

Figure 4.2
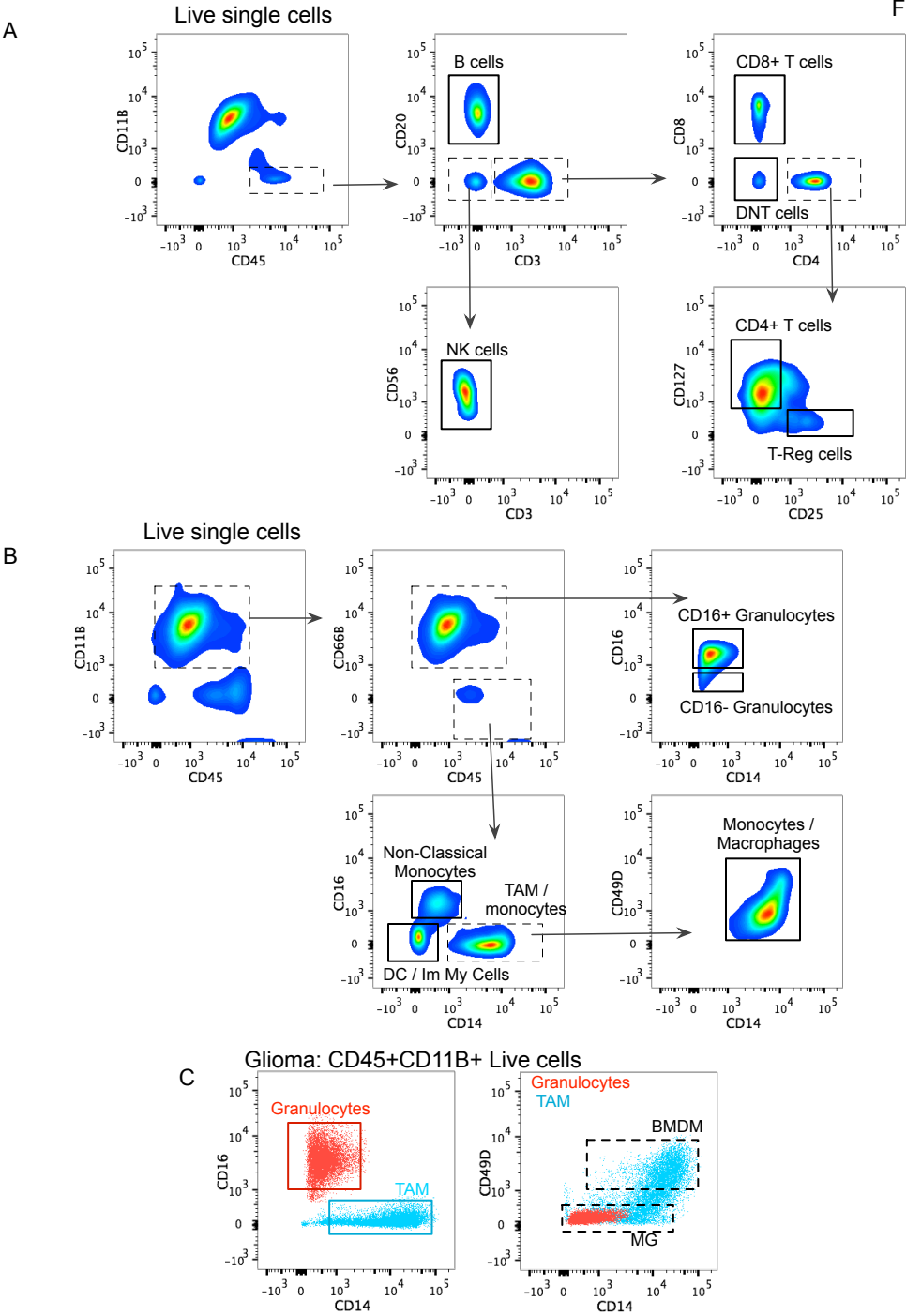
Figure 4.2

Figure 4.2 Hierarchical gating strategies for identification of lymphoid and myeloid cell types.
(A) Lymphoid cell gating strategy on whole blood sample. Single cells were first selected on forward and side scatter with DAPI+ exclusion. CD45+CD11B- cells were considered bulk lymphocytes and further subdivided into CD20+ B cells, CD3+ T cells, or DNT cells. NK cells were identified within the double negative gate based on CD56 positivity. The T cell gate was further subdivided into CD8+ T cells, double negative T cells (DNTs), and CD4+ T cells. The latter was divided split into a CD127highCD25low bulk CD4 T cell fraction, and CD127lowCD25high T-regulatory cell enriched fraction. **(B)** Myeloid cell gating strategy on whole blood samples; single cells were selected as in (A), and the bulk myeloid population was considered CD45+CD11B+. This was subdivided into CD66B+CD45low Granulocytes, and CD66B-CD45High cells. Granulocytes were then split into two groups based on CD16 expression, with CD16+ cells being the more abundant population. CD66B- cells were split into 3 distinct monocyte populations based on the expression of CD14 and CD16, where CD14+CD16- cells are classical monocytes (and bulk tumor-associated macrophages and microglia (TAM in tumor samples), CD14HighCD16+ cells are intermediate monocytes, and CD14lowCD16+ cells are non-classical monocytes. CD14-CD16- cells were enriched for HLA-DR+ CD11C+ dendritic cells, as well as a population of cells that were negative for both of these markers that we refer to as immature myeloid cells. **(C)** Gating strategy in a representative tumor sample for the separation of microglia and macrophages. CD16+ granulocytes (red) and TAMs (blue) were identified as described in (B). Granulocytes expression of CD49D is used as a gating control to determine a cutoff for CD49D staining. Microglia (MG) are TAMs with low CD49D expression while macrophages (BMDM) are TAMs with high CD49D expression.

Interestingly, grade III gliomas contained significantly more myeloid cells than grade IV glioma and BrM samples, with no significant difference compared to grade II glioma (Figure 4.3A). Meanwhile, despite a trend for increased lymphocyte content with advanced glioma grade, there was no significant difference between any of the disease categories (Figure 4.3A).

We next assessed the relative abundance of specific immune cell types within the myeloid cell compartments. Across all patient samples, the most abundant myeloid cells were microglia, macrophages, and CD16+ granulocytes (Figure 4.3B). Few tumor specimens contained non-classical monocytes, intermediate monocytes, dendritic cells, immature myeloid cells or CD16- granulocytes (Figure 4.3B). As expected in glioma, we found that TAMs (microglia and macrophages combined) made up >75% of the myeloid cells in most tumors. Strikingly, the ratio of microglia to BMDM was significantly different with tumor grade, where grade II and grade III gliomas were largely composed of microglia, and grade IV gliomas were more enriched for BMDM (Figure 4.3C). BrM samples showed a similar enrichment of BMDM over microglia. While the granulocyte content did not significantly change across glioma grade, BrM samples were significantly enriched for granulocytes compared to all glioma and normal brain subtypes (Figure 4.3C).

The lymphoid cell compartment was largely composed of T lymphocytes with few NK cells and B cells (Figure 4.3B). CD4+ T cells composed half of the lymphoid compartment in grade II and grade III glioma, with a significant proportional decrease in grade IV glioma (Figure 4.3D). Meanwhile there was no similar or compensatory trend for CD8+ T cells. Interestingly, double negative T (DNT, CD4- CD8-) cells made up a large proportion of the lymphoid compartment in gliomas (Figure 4.3D), with

comparatively less DNT cells in BrM samples. No significant differences were identified

in B cell or NK cell abundance across disease category. When controlled for grade, no

differences in any immune compartment were identified when patients were stratified by

recurrence and initial diagnosis (Figure 4.3B).

Figure 4.3
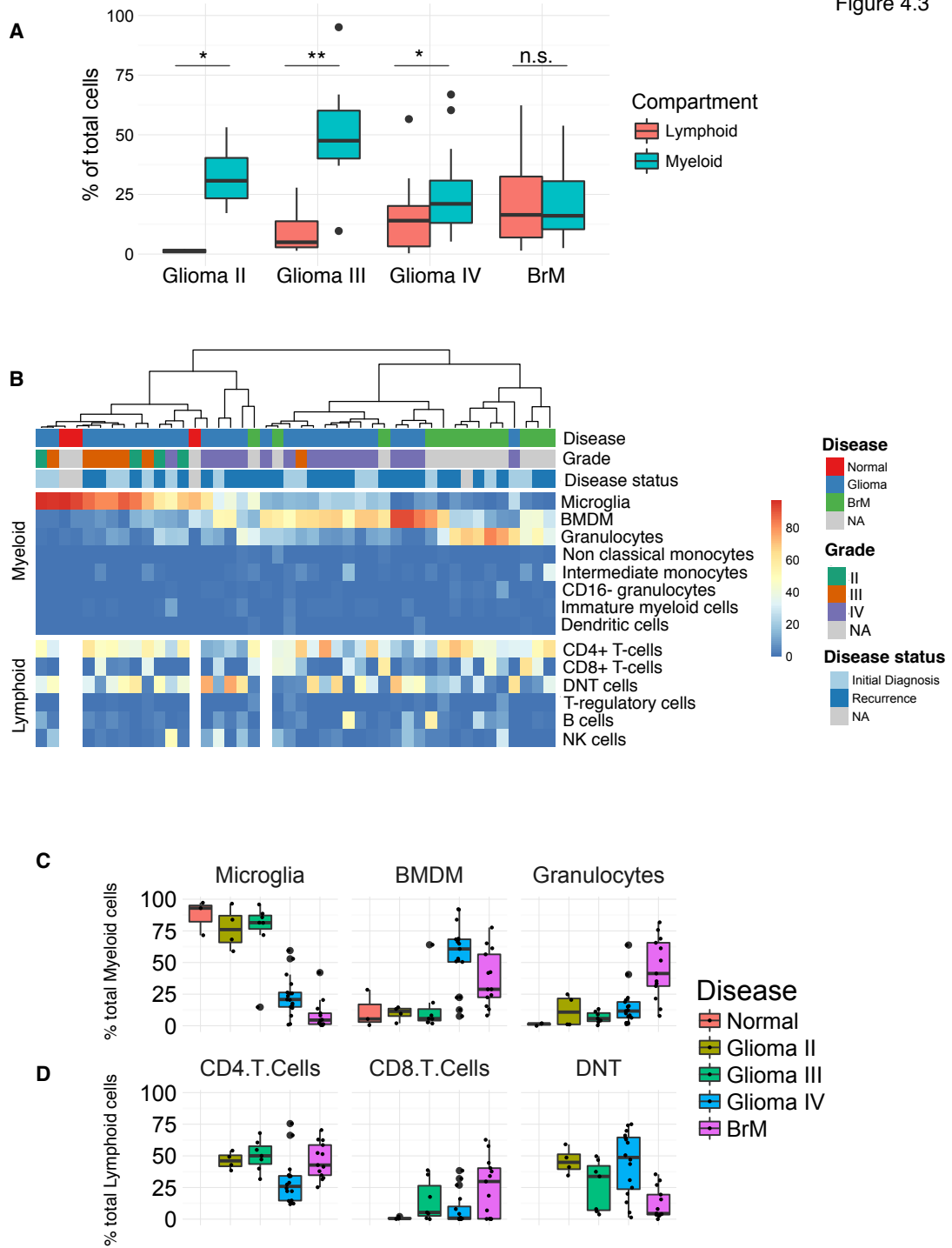
Figure 4.3: Composition of the immune cell contexture across varying brain malignancies
(A) Total lymphoid (left) and myeloid (right) cell content as a percentage of total live cells across grade II, grade III, and grade IV glioma as well as BrMs. **(B)** Heatmap depicting abundances of cellular constituents (rows) within the myeloid (top) and lymphoid (bottom) cell compartments for each tumor sample (column). Blue to red (low to high) gradient indicates abundance of cells within the myeloid or lymphoid compartment. Tumor samples are clustered based on abundances within the myeloid compartment. Disease, grade, and recurrence status are shown for each sample as indicated. Normal brain samples were either fresh autopsy specimens or non-malignant, non-adjacent, brain samples from tumor-bearing patients. **(C)** Boxplots of cellular abundances as shown in (B) grouped by disease type for microglia, BMDM, and granulocytes. **(D)** Boxplots of cellular abundances as shown in (B) grouped by disease type for CD4 T cells, CD8 T Cells, and DNTs.

Interrogation of macrophage and microglia abundance in publically available datasets

We aimed to verify these findings in multiple publicly available gene expression datasets for large patient cohorts containing both low-grade and high-grade glioma samples including both the TCGA (Brennan et al., 2013; Cancer Genome Atlas Research, 2008; Cancer Genome Atlas Research et al., 2015) and Rembrandt (Madhavan et al., 2009) databases (only TCGA data shown here). We focused on markers that distinguish microglia and macrophages, given the striking change in microglia to macrophage ratio with tumor grade. Here we found in all datasets that *ITGA4/CD49D* expression increased with tumor grade (Figure 4.4A), whereas *P2RY12*, an established microglia-enriched gene (Butovsky et al., 2014; Gautier et al., 2012), decreased with tumor grade (Figure 4.4B). These findings were in line with our observation of an accumulation in macrophages relative to microglia as tumor grade increased (Figure 4.3C). Furthermore, within grade IV GBM patients, *ITGA4* expression was highest in the Mesenchymal subtype (Figure 4.4C), a group known for enrichment of stromal cell infiltration (Cancer Genome Atlas Research, 2008; Engler et al., 2012); while no such enrichment was found for *P2RY12*, suggesting that this stromal enrichment may be restricted to peripheral infiltration (Figure 4.4C).

We next assessed whether these markers were associated with any survival difference across the patient cohorts. As expected from the correlations with grade, high *ITGA4* expression was associated with worse prognosis among all patients without grade stratification. Likewise, high *P2RY12* expression was associated with better prognosis (Figure 4.4D). Among grade IV GBM patients, *ITGA4* showed no association with overall survival, either as a whole cohort, or stratified by molecular subtype (Figure 4.4D, data not shown for subtype analysis).

Figure 4.4
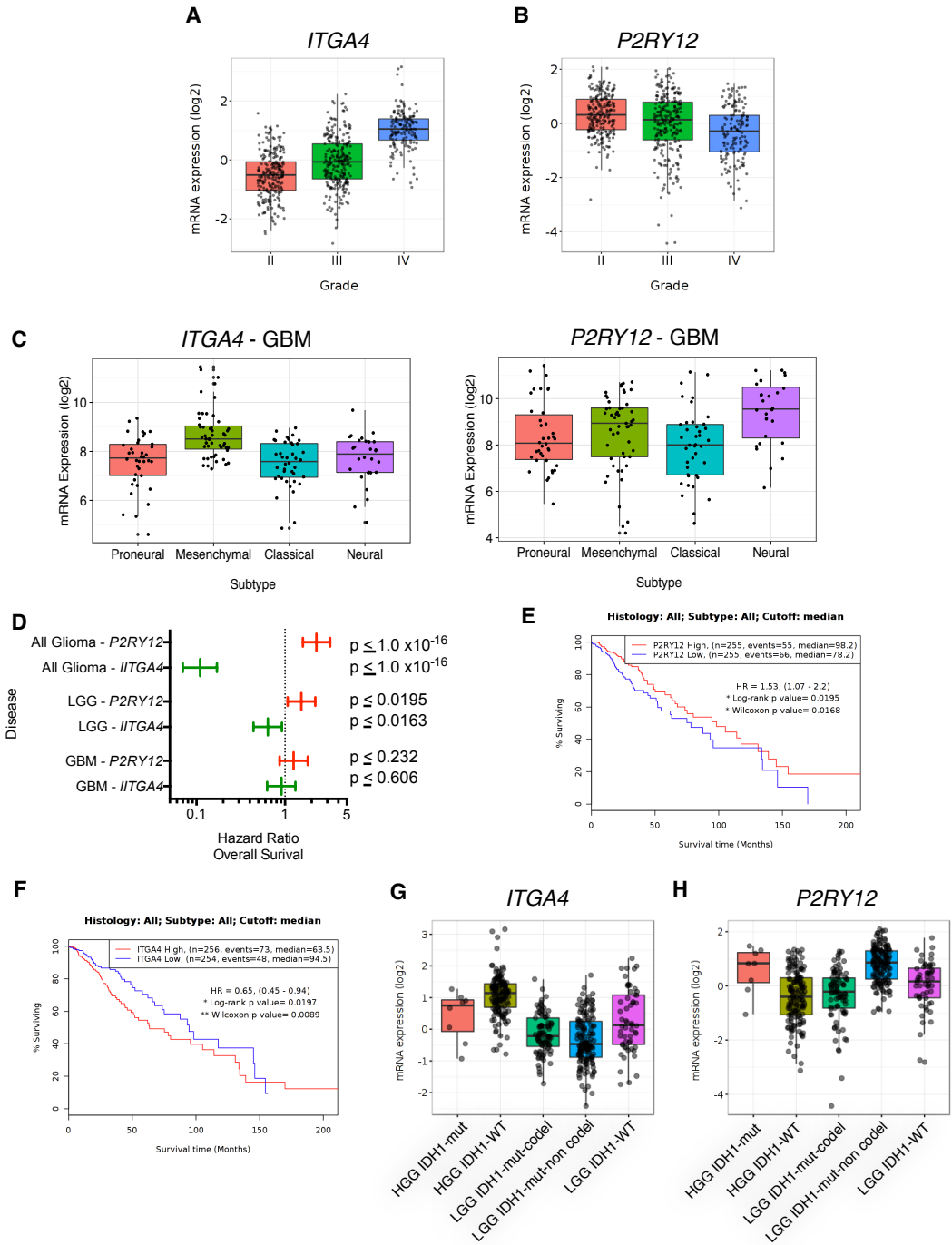
Figure 4.4: Macrophages accumulate with grade in human disease and is associated with good prognosis in low-grade glioma

(A)   Mean centered log2 RNA-seq gene expression of ITGA4 across grade in glioma (TCGA). **(B)** Mean centered log2 RNA-seq gene expression of P2RY12 across grade in glioma (TCGA).

 (C) Log2 RNA-seq gene expression data of ITGA4 in grade IV GBM patients stratified by molecular subtype (TCGA). **(D)** Hazard ratio and 96% confidence interval for cox proportional hazard analysis for ITGA4 (green) and P2RY12 (red) in all glioma patients, or subdivided into LGG or grade IV GBM. P values listed are from wald's test, and 95% CI's that do not cross 1 are significant. **(E)** Kaplan-Meier plots for LGG patients divided into two groups by median expression of ITGA4. **(F)** Kaplan-Meier plots for LGG patients divided into two groups by median expression of P2RY12. **(G)** Mean centered log2 RNA-seq gene expression of ITGA4 across IDH1 mutation and 1p19q deletion status in GBM and low-grade glioma (LGG; grade II+grade III). **(H)** Mean centered log2 RNA-seq gene expression of P2RY12 across IDH1 mutation and 1p19q deletion status in GBM and low-grade glioma (LGG; grade II+grade III).

However, among low-grade glioma patients (grade II and grade III), high *ITGA4* expression was associated with worse prognosis, while high *P2RY12* expression was associated with better prognosis (Figure 4.4D-F). Furthermore, we found that *ITGA4* expression was enriched in IDH1-wild type, 1p19q intact patients, whereas *P2RY12* was more highly expressed among *IDH1* mutant 1p19q deleted patients, consistent with their respective prognostic associations (Cancer Genome Atlas Research et al., 2015) (Figure 4.4G-H). These results further reinforce the utility of *ITGA4/CD49D* as a discriminatory marker between microglia and macrophages, and as a prognostic marker in low-grade glioma patients.

RNA sequencing verifies cell-sorting fidelity

We next utilized RNA-sequencing to begin to understand the contribution of each of these cell types to various categories of brain malignancy. We isolated RNA from sorted macrophages, microglia, granulocytes, CD4+ T cells, and CD45 negative (CD45N) cells for RNA-sequencing from a subset of the tumors that underwent immune cell profiling. In sum, we sequenced samples from 13 glioma patients, 7 brain metastasis patients, and 1 sample from adjacent non-malignant brain matched to that of a BrM patient (Figure 4.1A). In addition, we performed RNA-sequencing on CD4+ T cells, granulocytes, and classical monocytes from whole blood of healthy donors. Lastly, we performed gene expression profiling on *in vitro* differentiated monocyte-derived macrophages (MDMs). With these samples in hand, we aimed to identify 1) cell type-specific gene expression patterns, 2) gene expression programs that varied across brain malignancies between glioma and brain metastases and 3) gene expression changes in low-grade and high-grade glioma.

We first verified cell-sorting fidelity of the different cell populations by expression of marker genes associated with each specific cell type. As expected we found that CD4+ T cells were enriched for *CD3E,* granulocytes were enriched for *CEACAM8* (CD66B), *FCGR3A* (CD16) and *CXCR2* (Figure 4.5A), and all myeloid cells were enriched for *ITGAM* (CD11B). Meanwhile microglia and macrophages were enriched for *CD14, CD68,* and *CSF1R.* As expected, macrophages displayed higher expression of *ITGA4* (CD49D) compared to microglia and granulocytes (Figure 4.5A). Conversely, microglia displayed increased expression of *P2RY12*, *TMEM119,* and *MEF2C* compared to macrophages (Figure 4.5A), verifying that CD49D negative TAMs are indeed enriched for microglia. We further found that *EGFR, GFAP*, and *OLIG2* were enriched in CD45N cells, while *PTPRC* (CD45) was decreased in CD45N cells compared to the four immune cell populations (Figure 4.5A). We found that the epithelial markers *CDH1, EPCAM,* and *MUC1* were enriched in BrM CD45N cells, while *OLIG2* and *GFAP* showed restricted expression to CD45N cells in glioma samples (Figure 4.5B). In a subset of glioma samples, we were able to identify the IDH1-R132H mutation with variant alleles specifically enriched in CD45N cells with no mutant transcripts present in BMDM (Figure 4.5C). Similarly, in two lung BrMs we found *KRAS* G12D and G12A mutations enriched in CD45N cells compared with minimal mutant transcripts found in BMDM (Figure 4.5C). Meanwhile, NRAS Q61K mutant transcript enrichment was found in CD45N cells from a melanoma BrM sample, however >20% of *NRAS* transcripts in BMDM also contained the mutant allele, suggesting some contamination of tumor cells in this instance into the BMDM gate (Figure 4.5C). Given the mutation frequency in 'BMDMs' and the broad expression of the melanocyte specific transcript, *PMEL*, across multiple immune cell populations (Figure 4.5B), we excluded this particular melanoma BrM sample from further analyses.

Figure 4.5
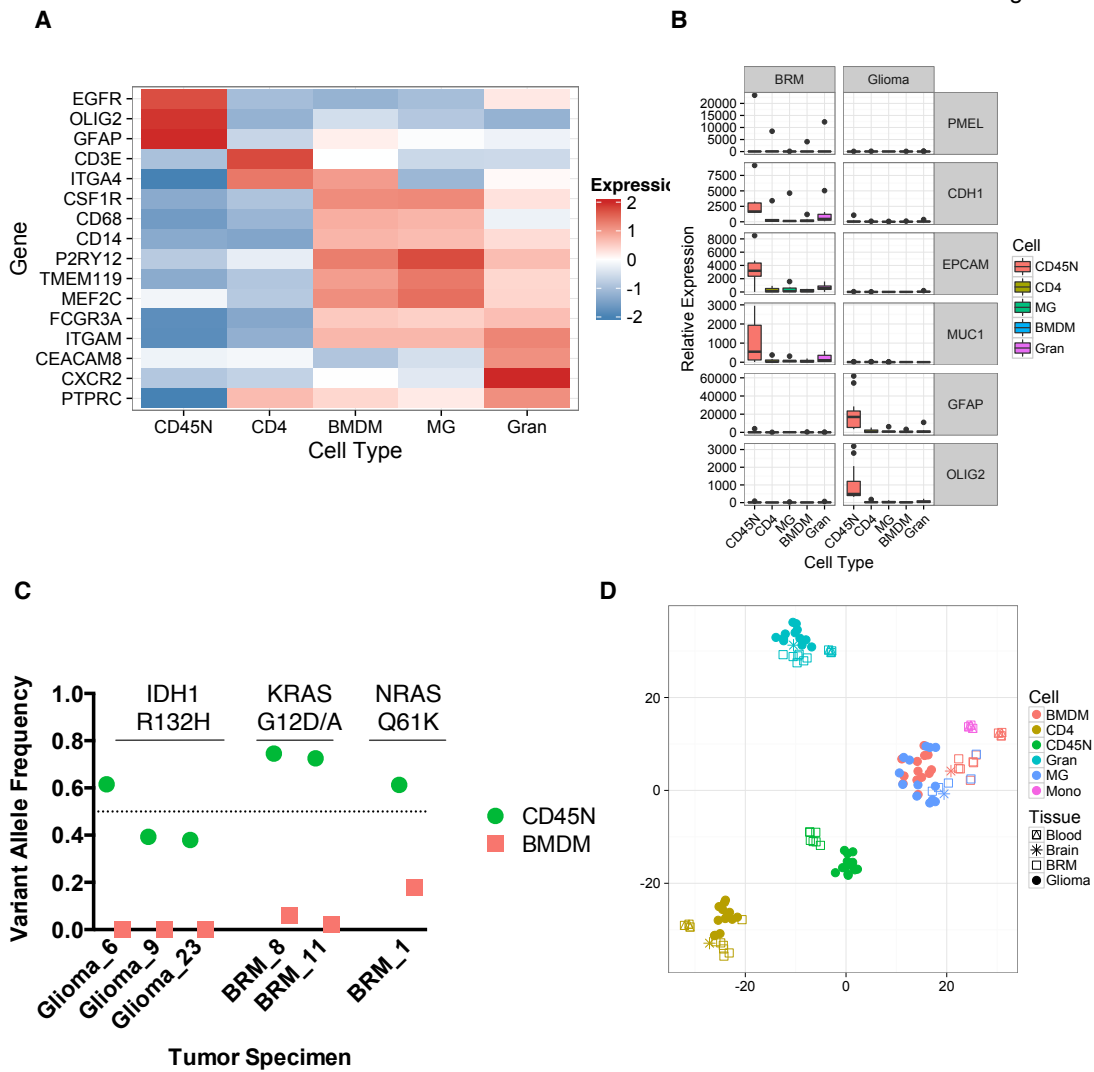
Figure 4.5: RNA-sequencing identifies cell type-specific gene expression patterns
(A) Heatmap of averaged log2 gene expression values for the indicated cell types (columns) for the indicated genes (rows). Red indicates high expression and blue indicates low expression. **(B)** Boxplots of normalized read counts from RNA-sequencing data for the indicated genes across sorted CD45N cells, CD4+ T cells, granulocytes, microglia and macrophages. **(C)** Variant allele frequencies in CD45N cells and BMDMs for IDH1 R132 mutations in three glioma patients, KRAS G12D and G12A mutations in two lung BrMs, and NRAS Q61K mutations in one melanoma BrM sample. **(D)** t-SNE visualization of global gene expression patterns from CD45N cells, CD4+ T cells, granulocytes, microglia, macrophages, and classical monocytes across blood, adjacent brain, glioma and brain metastasis samples.

We next utilized a t-distributed stochastic neighbor embedding (t-SNE) distribution to visualize global gene expression patterns (Figure 4.5D). This distribution recovered clusters of each cell type, with granulocytes, CD4+ T cells and CD45N cells each forming distinct clusters. Interestingly, within each cluster, there appeared to be separate clustering of BrM (squares) and glioma samples (filled circles). This was most clear in the CD45N cell cluster, where there was a clear divide between BrM cells and glioma cells. As expected, microglia and macrophages were a part of the same cluster, highlighting the overall similarity of these cells compared to other cell types (Figure 4.5D). Classical monocytes (pink triangles) and MDMs (red triangles) were found proximal to this cluster, again reinforcing the similarity of these cells. Hierarchical clustering revealed that microglia were more similar to the macrophages within the same tumor than with microglia in other tumors, suggesting greater intra-tumoral similarity in TAMs than cell-specific similarity across tumors (Figure 4.6A). Indeed the mean spearman correlation coefficients for matched microglia and macrophage pairs were greater than that of the mean correlation among all microglia or macrophages (Figure 4.6B). Microglia and macrophages are the only cell types to show this intra-tumoral similarity, as every other cell pair displayed greater cell-specific similarity than tumor-specific similarity.

Given this substantial similarity, we next sought to verify that the CD49D enrichment in BMDM relative to MG indeed captured these distinct populations in human samples. We implemented a generalized linear model accounting for patient-to-patient variability as a block factor to identify differentially expressed genes between BMDM and MG in both glioma and BrM samples. Using a false discovery rate (FDR) cutoff of 5% and a fold change cutoff of +/-2, these analyses identified 135 genes enriched in BMDM compared to MG in both glioma and BrM samples (Figure 4.6C, green), and 90 genes enriched in

MG (Figure 4.6C, red). As expected, *ITGA4* (CD49D) was enriched in BMDM samples in both BrM and glioma samples. Furthermore, other BMDM-enriched genes we identified in mouse were also enriched in human BMDM samples including *VDR, THSB1, IRF4, CD44, CXCL1,* and *CXCL2* (Figure 4.6D, Figure 3.5C, Figure 3.6D). Conversely, microglia were enriched for markers such as *P2RY12, TMEM119,* and the brain specific transcription factor *SALL1* (Figure 4.6D). We next assessed the pairwise comparisons of these BMDM- and MG-specific genes in TCGA-GBM RNA-sequencing samples (Brennan et al., 2013). These analyses revealed that BMDM-enriched genes showed greater correlation with *ITGA4* than *P2RY12*, while the MG-enriched genes showed the opposite trend (Figure 4.6E). These analyses verify that CD49D is indeed capable of separately identifying BMDM and MG in human specimens, and strengthen the utility of *ITGA4* and *P2RY12* expression in bulk tumor samples as surrogate markers for BMDM and MG abundance respectively.

Figure 4.6
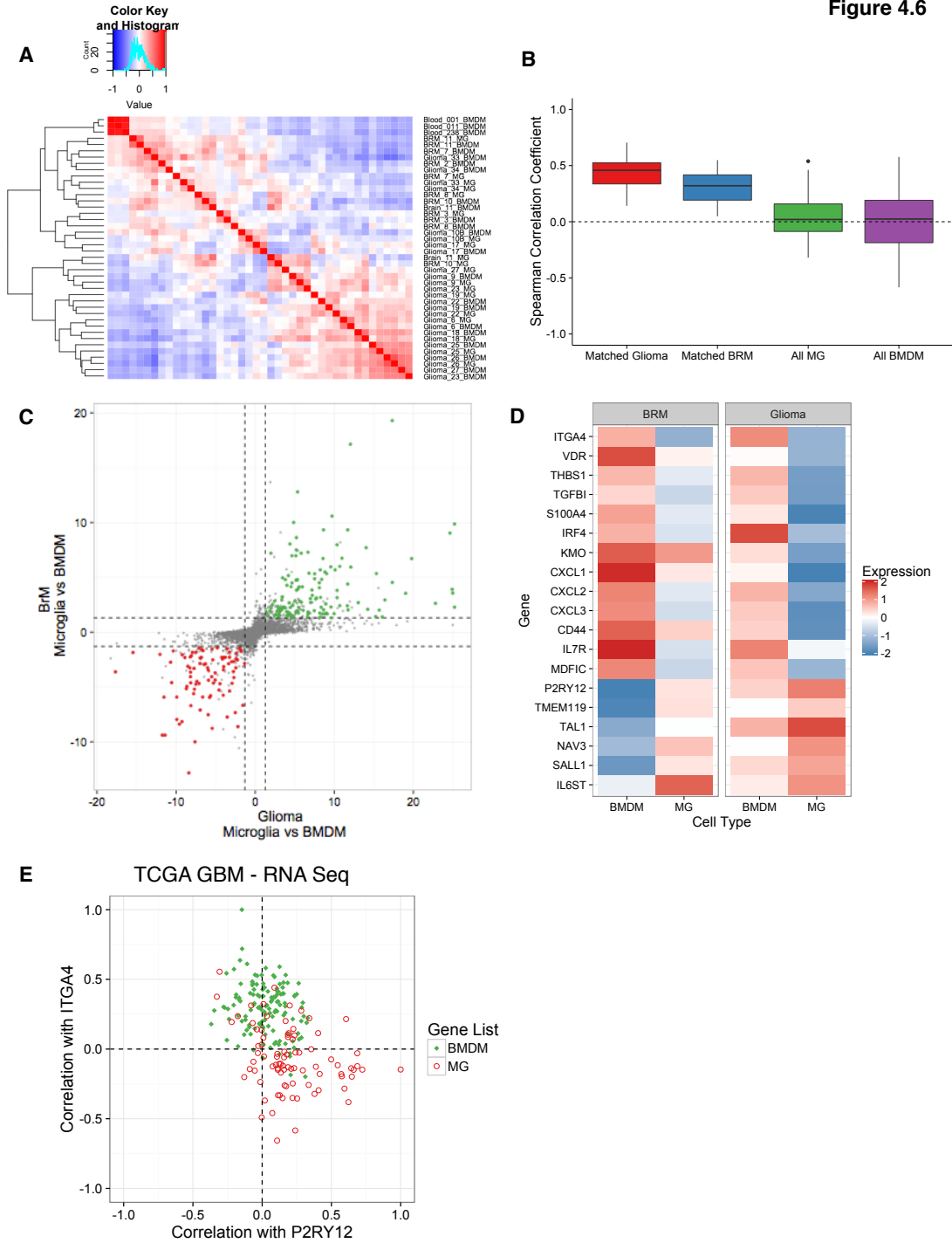
Figure 4.6: RNA-sequencing verifies CD49D-based enrichment of microglia and macrophages

(A) Correlation matrix of macrophage and microglia samples. **(B)** Boxplots of spearman correlation coefficients for matched microglia and macrophage samples from the same tumor for glioma samples (red) and brain metastasis samples (blue). The next boxplots represents the distribution of mean spearman correlation coefficients for each microglia sample compared to all other microglia samples (green) and macrophages compared to all other macrophages (purple).**(C)** Scatter plot comparing bone marrow-derived macrophages (BMDM) and microglia (MG) in glioma (X axis) and BrM samples (Y axis). Each dot represents the -log10(p value)*sign(fold change) of a given gene. Dashed lines indicate FDR cutoffs of 5%. Green dots indicate genes enriched in BMDM compared to MG in both glioma and BrM samples, while red dots indicate genes enriched in MG compared to BMDM.**(D)** Heatmap of select BMDM- and MG-specific genes from (A) in BrM and glioma samples. Each box represents the average log2 normalized expression for the indicated gene and sample grouping.
(E) Scatterplot depicting spearman correlation coefficients between the BMDM genes (green) and MG genes (red) in (A) with either ITGA4 (y axis) or P2RY12 (x-axis).

<u>Identification of BrM and glioma enriched gene expression patterns</u>

While we observed enrichment of brain-specific transcripts in microglia compared to BMDM, this enrichment appeared less robust in glioma samples compared to brain metastasis samples (Figure 4.6D). Such tissue-dependent transcriptional affects on macrophages have been reported previously (Figure 3.3E) (Gosselin et al., 2014; Lavin et al., 2014). We explored this further by comparing BMDM from BrM and glioma samples directly. Differential gene expression analysis revealed 369 genes enriched in BrM-BMDM and 401 genes enriched in glioma-BMDM (Figure 4.7B). Several of the glioma-BMDM enriched genes were well-established microglia markers including *P2RY12, CX3CR1,* and *TMEM119* in addition to the brain-enriched factors such as *SALL1, NAV3, SLC2A5* and *JAM2* (Butovsky et al., 2014) (Figure 4.7B). This suggests that the glioma TME may be a more conducive environment for BMDM brain assimilation than the BrM TME. While these genes were enriched in glioma-BMDM compared to BrM-BMDM, in most cases they were still most highly expressed in glioma-MG (Figure 4.7B). Interestingly, glioma-MG possessed higher expression of these brain-specific transcripts compared to BrM-MG, suggesting that the BrM TME may have a disruptive impact on the identity of MG.

In addition to the changes described above, in glioma-BMDM compared to BrM-BMDM we also identified enrichment of *GFAP* and *EGFR,* genes predominantly expressed in glioma-CD45N cells (Figure 4.7B, Figure 4.5B). Meanwhile, we found the epithelial markers *EPCAM* and *MUC1* were enriched in BrM-BMDM compared to glioma-BMDM (Figure 4.7B). These findings suggest that perhaps BMDM undergo similar regulatory patterns as their cognate tumor cells, a hypothesis supported by recent findings that tumor cells exchange extracellular vesicles containing miRNA and mRNA to TAMs in glioma (van der Vos et al., 2016). Another possible reason for these changes is minute

contamination of CD45N cells into the BMDM gate during sorting. Our variant allele analysis suggests that this contamination, if present, is rare (Figure 4.5C). We reasoned that genes differentially expressed by only TME cells, or CD45N cells might be least affected by potential contamination, thus we sought to identify differentially expressed genes that were "private" to the TME, showing differential expression in either granulocytes, CD4+ T cells, MG or BMDM, but not between CD45N cells in BrM and glioma samples (Figure 4.7C). Compared to genes differentially expressed in both CD45N cells and the TME, genes that were differentially expressed in the TME only were more likely to be differentially expressed in only one of the four TME cell types (Figure 4.7D, intersect vs. TME only). Not surprisingly, genes that were differentially expressed in more than one cell type were likely to be shared by MG and BMDM, highlighting the similarity of the cells (Figure 4.7E). This was true for both BrM and glioma enriched genes (Figure 4.7E). There remained three genes that were differentially expressed between BrM and glioma samples for every TME cell type assayed; the glioma-enriched *MEF2C* and *SLC2A14* and the BrM-enriched *PRODH* (Figures 4.7E). *MEF2C* is of particular interest, given its role in neural stem and progenitor differentiation (H. Li et al., 2008), as well as its association with microglia enhancer selection (Gosselin et al., 2014; Lavin et al., 2014). In addition to these changes we identified a series of chemokines: *CXCL1, CXCL2, CXCL3, CCL7, CCL8, CCL13, CCL17, CCL23* and *CCL24*, all of which were enriched in BrM-BMDM compared to glioma-BMDM (Figure 4.7F). Three of these factors, *CXCL1*, *CXCL2* and *CXCL3* also showed enrichment in BrM-CD45N cells compared to glioma-CD45N cells (Figure 4.7F). CXCL2 and CXCL3 have been shown to signal through CXCR2, a chemokine receptor found exclusively on granulocytes (Figure 4.5A). Collectively, these cytokines may contribute to the increased granulocyte content we observed in our flow cytometry analyses.

Figure 4.7
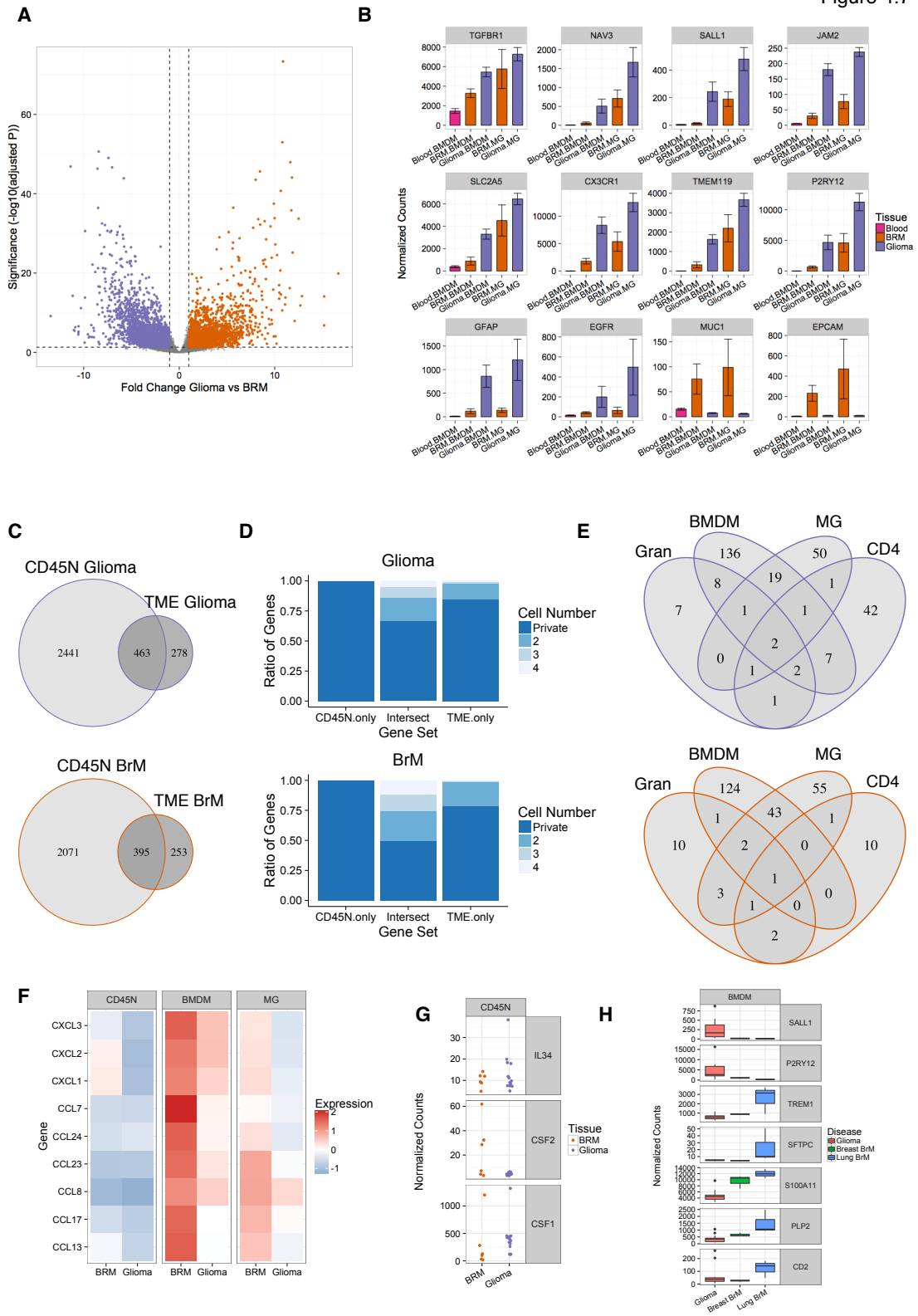
Figure 4.7: BMDM acquire microglia-like transcripts in gliomas but not BrM

(A) Volcano plot depicting BMDM gene expression in BrM samples and in glioma samples, with fold change on the x-axis and -log10(adjusted p value) on the y-axis. Purple dots indicate genes significantly enriched in glioma samples, while orange dots indicate genes significantly enriched in BrM samples. **(B)** Barplots depicting normalized gene counts in BMDM and MG samples from either monocyte-derived, in vitro differentiated, macrophages (blood; MDM), glioma, or BrM samples. **(C)** Venn diagram identifying overlapping differentially expressed genes identified in CD45N cells and any immune cell for glioma enriched genes (top) and BrM enriched genes (bottom).**(D)** Barplot depicting the number of genes that are differentially expressed in only 1 cell type for the 3 classes of genes identified in the Venn diagrams in (D). **(E)** Venn diagram of differentially expressed genes between glioma (left) and BrM (right) samples for each immune cell type listed. These genes were sub-setted for those differentially only in the TME, and not CD45N cells as described in (D). **(F)** Heatmap of chemokines and cytokines across CD45N cells, MG and BMDM in BrM and glioma samples. **(G)** Stripchart of IL34, CSF1 and CSF2 expression in CD45N cells in glioma and BrM samples. **(H)** Boxplots of gene in expression of SALL1, P2RY12, TREM1, SFTPC, S100A11, PLP2, and CD2 in BMDM from glioma, Breast-BrM and Lung-BrM samples.

We next assessed canonical macrophage-related growth factor expression to determine if there was any association with differences in BMDM and microglia abundance between BrM and glioma samples. In glioma-CD45N cells we found enrichment for CSF-1, while the alternative CSF-1R ligand, IL-34, showed little differential expression between BrM-CD45N and glioma-CD45N cells (Figure 4.7G). Interestingly, we found that a set of BrM-CD45N samples originating from lung primary tumors were enriched for *CSF2*, a cytokine necessary for alveolar lung macrophage development (Becher et al., 2014) (Figure 4.7G). When we compared Lung BrM and Breast BrM-BMDM samples directly, we found that several markers of alveolar macrophages (Gautier et al., 2012) were enriched in BMDM including *TREM1*, *SFTPC, S100A11, PLP2* and *CD2* (Figure 4.7H). From these analyses it seems likely that tissue of origin-specific, tumor cell-derived, factors are capable of eliciting changes in BMDM such that they resemble the microenvironment of the primary tissue. These results further highlight the plasticity of BMDM.

Identification of grade dependent hierarchical recruitment cascade

We next sought to interrogate gene expression patterns associated with tumor grade amongst glioma patients. This cohort contained specimens from 13 glioma patients representing distinct histological, clinical, and molecular classes. Given the differences in immune cell composition (Figure 4.3C), and the even distribution of patients between the groups, we focused on the differences between low-grade glioma (LGG grade II+III) vs. high-grade glioma (HGG, grade IV),

As in the glioma vs. BrM analysis, we identified genes that were differentially expressed between HGG and LGG uniquely within each cell population (Figure 4.8A). We identified 107 genes upregulated in LGG-CD45N cells, which showed no differential expression

among components of the microenvironment (Figure 4.8A). Meanwhile we found 172 genes enriched in HGG-CD45N cells while showing no differential expression in the TME (Figure 4.8A). Amongst these gene sets we sought to identify cytokines and chemokines that might contribute to the alterations in the immune cell composition identified in our flow cytometry analyses (Figure 4.3C). One particular factor that stood out was *POSTN,* which was abundantly expressed in granulocytes and enriched in HGG-CD45N cells compared to LGG-CD45N cells (Figure 4.8B). Interestingly, *POSTN* has been previously shown to mediate accumulation of CD163+ TAMs in glioma (Zhou et al., 2015), which our data suggests are likely macrophages as opposed to microglia (Figure 4.8B).

We next looked at stage specific expression within BMDMs. Amongst the 120 genes enriched specifically in HGG-BMDM, we identified increases in the hypoxia responsive gene *ADM,* the granulocyte chemo attractants *CXCL2* and *CXCL3*, and the cytokine *CCL18* (Figure 4.8C), a factor known to not only promote alternative macrophage activation but also recruit atypical regulatory T cells capable of producing the immunosuppressive cytokine IL-10 (Schraufstatter, Zhao, Khaldoyanidi, & Discipio, 2012). In support of this finding, we found that HGG-CD4+ T cells expressed higher levels of IL10 than LGG-CD4+ T cells (Figure 4.8D). Interestingly, CD4+ T cells in LGG samples expressed higher levels of the naïve T cell marker CD62L (*SELL*), while HGG samples expressed higher levels of *IL2RB,* the CD25 beta chain (Figure 4.8D). HGG CD4+ T cells also expressed high levels of 4-1BB ligand and receptor (*TNFSF9* and *TNFRSF9*) as well as CD103 (*ITGAE*). These findings suggest that these cells are in differential activation states in low-grade and high-grade disease, with LGG CD4+ T cells perhaps presenting with a naïve phenotype, while HGG CD4+ T cells appear to have adopted an immunosuppressive phenotype.

These differential gene expression analyses suggest a hierarchical cascade of immune cell recruitment in glioma (Figure 4.8E). In likely addition to other factors including hypoxia and *CXCL12, POSTN* expressing tumor cells mediate the accumulation of BMDM. In turn these cells are capable of producing a number of cytokines and growth factors, including the constitutively expressed of *EREG* and the grade-dependent production *CCL18, CXCL2,* and *CXCL3.* The latter cytokines bind CXCR2, which is abundantly expressed in granulocytes. Meanwhile, CCL18 has been shown to bind CCR8 (Islam, Ling, Leung, Shreffler, & Luster, 2013) and offer chemotactic properties to Th2 T cells. In addition, granulocytes constitutively express *CXCL16,* a known chemo attractant for the T cell enriched *CXCR6* (Matloubian, David, Engel, Ryan, & Cyster, 2000). While there are many more likely interactions amongst these cells, the genes identified here reveal a simple, potential heterotypic signaling loop reflective of the cell abundance differences found between low-grade and high-grade glioma.
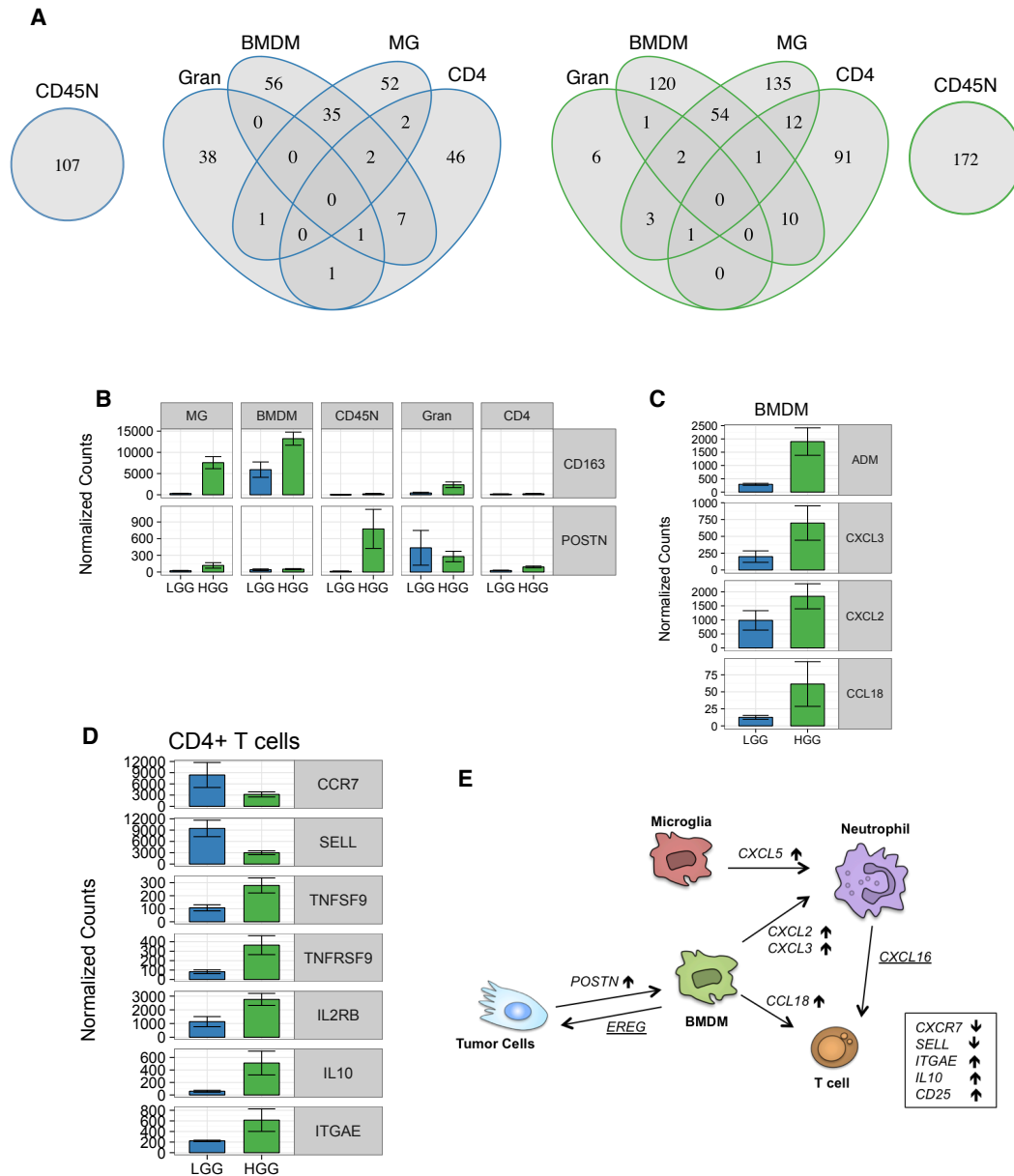
Figure 4.8

Figure 4.8: Identification of hierarchical chemotactic cascades in low-grade (LGG) and high-grade glioma (HGG)
(A) Venn diagram of differentially expressed genes between LGG (left) and HGG (right) samples for each immune cell listed. The circle for CD45N cells indicate how many genes are enriched in CD45N cells only, with no change in TME cells. **(B)** Barplot of CD163 and POSTN expression across cell types in LGG and HGG. **(C)** Barplot of ADM, CXCL3, CXCL2, and CCL18 expression in BMDM and MG in LGG and HGG. **(D)** Barplot of CCR7, SELL, TNFSF9, TNFRSF9, IL2RB, IL10 and ITGAE expression in CD4+ T cells in LGG and HGG.. **(E)** Schematic demonstrating heterotypic signaling between CD45N and immune cells within the low-grade and high-grade glioma TME. Increased expression in HGG samples relative to LGG is denoted by ⊠ while increased expression in LGG to HGG samples is denoted by ⊠.   Underlined gene (EREG and CXCL16 are constitutively expressed by BMDM and Granulocytes respectively, regardless of grade

Discussion

Herein, we have constructed a comprehensive map of the immune cell contexture in human brain malignancy. This study has identified microglia, macrophages, and granulocytes as the predominant source of myeloid cells whereas CD4+ T cells, DNT cells, and CD8+ T cells are the most abundant lymphoid cells. These populations show grade- and disease-specific enrichments, with microglia enriched in low-grade glioma, BMDM enriched in grade IV GBM, and granulocytes enriched in brain metastases. Subsequent RNA-sequencing verified that our CD49D-based enrichment strategy indeed separately identified BMDM and microglia. These cells, as well as CD4+ T cells and granulocytes, underwent grade-specific gene expression changes in glioma as well as disease-specific gene expression changes between brain metastases and glioma samples. Additional cell-specific gene expression analyses highlight heterotypic signaling loops that may influence the composition of the brain TME in a stage-dependent manner. In sum, these analyses provide a cellular and molecular atlas of immune infiltration in human glioma and brain metastasis

While our study aimed to catalogue the abundance of all immune cell components within the brain TME, there remain several cell types that have not been exhaustively described to date. Foremost the identity and function of the DNT cells, abundantly found in glioma samples, remains uncertain. While we were able to rule out simple enzymatic or mechanical cleavage of CD4 and CD8 from the surface of these cells (data not shown), we cannot formally exclude the possibility that either of these molecules were downregulated. We were able to determine that these DNT cells did not express TCR-γ/δ, likely excluding these cells as the major source of DNT cells in our patient cohort. Further RNA-sequencing in progress may provide insights into the function and origin of these cells. Additionally, while we posit that the CD45+CD11B+CD66B-

CD14+CD16-CD49D+ TAM compartment is composed of differentiated macrophages and microglia, we cannot formally exclude the presence of some classical monocytes. RNA-sequencing analysis demonstrates that this compartment is enriched for differentiation-related genes compared to classical monocytes from peripheral blood. CCR2 and MHC-II staining in a subset of patients demonstrated that this compartment is largely enriched for mature TAMs, with few CCR2$^+$MHC-II^{low} cells.

In addition to these immune cells, non-immune stromal cells including astrocytes and endothelial cells have been shown to play important roles in brain malignancy, adopting tumor-specific phenotypes (Charles, Holland, Gilbertson, Glass, & Kettenmann, 2012). Comparison of these stromal and immune cells with their non-tumor bearing counterparts will provide a more comprehensive understanding of the pathways involved in tumor education and a more comprehensive map of the brain TME. Sample collection for a subset of the immune cells from peripheral blood has been completed, however acquisition of brain-derived immune cells from non-pathologic sources, including microglia, remains a challenge.

Amongst the differences in cells analyzed, one of the most striking phenomena was the near absence of microglia in brain metastasis samples. However, it remains unclear why there are so few microglia in BrM lesions. We found that grade IV GBM patients contained significantly more BMDM than microglia, perhaps indicating that the differences seen in BrM samples are a reflection of the aggressiveness of the lesion. Contrary to what we observed here in patients, in xenograft models of brain metastases, the TAM compartment appears to be largely composed of resident microglia (Figure 3.11G). It possible that this discrepancy is related to the tissue purity, where the surgical specimens interrogated here are often derived from the tumor core,

while xenograft metastases may retain contaminating normal cortex that is rich in microglia and which cannot be macrodissected away. Ongoing immunohistochemical analyses will provide insight into the spatial distribution of microglia and macrophages in brain metastases, offering a solution to this discrepancy. In addition to the differences in abundance, both BMDM and microglia in BrM lesions compared to glioma lesions possessed lower expression of brain-specific transcripts including *P2RY12*, *CX3CR1* and *MEF2C*. These findings suggest that the brain-resident microglia identity is significantly perturbed in brain metastases, where there are potentially both brain-specific signals and tissue-specific signals from the primary site. It may be that this imbalance in tissue-derived signals is directly associated with the relative dearth of microglia, whereby microglia might be incapable of surviving in metastatic lesions lacking growth factors important for their homeostasis. An additional explanation might be that microglia are in fact capable of upregulating CD49D, and thus fall into our macrophage gate. Lineage tracing strategies employed in Chapter 3 will prove useful to test this hypothesis.

Our current immuno-profiling and RNA-sequencing cohorts contained sufficient patient numbers to assess composition and transcriptional differences in brain metastases and gliomas, as well as between low-grade glioma (grade II+III) and grade IV GBM. These analyses revealed interesting findings, however, our current cohort leaves several important questions underpowered, including understanding the associations of specific genetic alterations with TME composition and function. For instance, it remains to be seen how *IDH1* mutation status may affect the tumor microenvironment, a particularly relevant avenue of inquiry given the near demarcating association with low-grade and high-grade disease. In our flow cytometry cohort, the BMDM to microglia ratio was highest in grade IV GBM, with reduced BMDM content in grade II and III

glioma. However, in the patients we analyzed here, there was no apparent difference in macrophage content between *IDH1* mutant and *IDH1*-WT low-grade glioma samples. These findings suggest that histological grade is a more dominant predictor of TME composition than mutation status. Increased sample and immune profiling of *IDH1*-mutant grade IV glioblastoma patients will provide an interesting setting to test this hypothesis.

Further understanding of genomic association with BMDM abundance within grade IV GBM will also be of interest. Here we demonstrate that *ITGA4* is most highly expressed in the Mesenchymal subtype of grade IV GBM patients, suggestive of increased BMDM content (Figure 4.4). Given the association of *NF1* and *TP53* mutations with this subtype, it will be of interest to determine if these genomic alterations play a causative role in BMDM abundance or even an influential role in their activation (Verhaak et al., 2010). Comparison of gene expression analyses in newly diagnosed and recurrent grade IV GBM is of great interest, however the RNA-sequencing cohort collected here remains underpowered and clinically immature for such extensive analysis. Indeed, the number of interesting clinical covariates and vast heterogeneity among tumor specimens presents a problem for thorough hypothesis testing. Utilization of computational methodology for interrogation of gene expression data in large patient cohorts provides a means to test hypotheses when sample collection is limiting, especially for a rare disease such as glioma (Gentles et al., 2015).

While the analyses presented here focus on immune cell profiling and RNA-sequencing, we have also collected samples for histological analysis. Immunohistochemical analyses will not only complement the immune cell abundances assessed by flow cytometry, but will also provide critical insight towards the spatial localization of these

111

cells. Comprehensive immunohistochemical analyses have demonstrated diverse, stage specific, spatial patterning for a variety of innate and adaptive immune cells in colorectal cancer (Bindea et al., 2013). Potential spatial motifs will be of importance in the setting of recurrence, where the niche for emergent disease is a remnant of invasive edges not captured by surgical resection. In addition to histology, snap-frozen tissues were collected for molecular analyses, where ELISA based quantitation of cytokine and growth factor expression will prove useful for translating the cell specific gene expression predictions into quantifiable whole tumor analyses. Implementation of these analyses, through ELISA and immunohistochemistry, will provide a means to translate the prognostic factors identified here into clinically actionable tools.

CHAPTER 5

DISCUSSION

Conclusions

Through my thesis I have aimed to understand the composition, and interrogate the function of, the brain tumor microenvironment. This started with dissecting the ontogeny of tumor-associated macrophages and expanded to profiling the abundances of all major immune constituents in the brain tumor microenvironment. With the information gathered in these studies, and others performed concurrently during my thesis research, we have achieved a better understanding of how the local environment dictates cellular function and eventually develop therapeutic options for disease.

CD49D distinguishes ontogenetically and transcriptionally distinct microglia and macrophages in brain malignancy

I first utilized multiple mouse models of glioma with genetic lineage tracing strategies to demonstrate that the tumor-associated macrophage compartment in brain malignancy is composed of the ontogenetically distinct brain-resident microglia and peripherally-derived macrophages. RNA-sequencing demonstrated that these cells possess opposed activation states; while microglia expressed pro-inflammatory molecules, macrophages expressed anti-inflammatory cytokines and engaged a wound healing phenotype. Computational analyses indicated that these activation states were reflective of epigenetic and transcriptional programs underlying the cells' distinct developmental origins. I next integrated gene expression and epigenetic data to identify cell surface markers capable of distinguishing microglia and macrophages. CD49D was one of these markers, showing specific repression in microglia. This finding provides a

tool that, for the first time, is capable of distinguishing microglia and macrophages in murine models of brain malignancy and in human disease.

An atlas of the immune contexture in brain malignancy

We next used the CD49D marker in a comprehensive flow cytometry panel to catalogue to abundance of various immune components across glioma grade and treatment status in patients, as well as across a panel of brain metastases arising from different primary sites. These analyses revealed that microglia were the predominant myeloid population in low-grade glioma (grade II+III), macrophages were most abundant in grade IV gliomas, and brain metastasis samples were largely composed of both macrophages and neutrophils. The lymphoid cell compartment was predominantly composed of CD4+ T cells in addition to less abundant CD8+ T cells and double-negative CD4- CD8- T cells. Further RNA-sequencing identified cell- and stage-specific gene expression patterns, elucidating pathways of immune cell education in brain malignancy.

Perspectives and clinical implications

Brain macrophage identity and ontogeny

How developmental origins affect macrophage function has been the central question in the first part of my thesis. Like all tissue-resident macrophages, microglia are at least partially a product of their environment, where local TGFβ and IL-34 are necessary for their development (Butovsky et al., 2014; Greter et al., 2012; Y. Wang et al., 2012). Only under select inflammatory conditions can peripherally-derived macrophages enter into the brain parenchyma, whereupon these cells are also exposed to the brain environment (Bruttger et al., 2015; Mildner et al., 2007). Our data here suggest that peripherally derived macrophages can acquire microglia-like transcript expression including *Cx3cr1, P2ry1*2, and *Mef2c* expression. This phenomenon of assimilation to

the local environment (Gosselin et al., 2014; Lavin et al., 2014), and the high similarity between microglia and macrophages, has stymied the field in understanding the differences between the cells. Our studies here utilize genetic lineage tracing systems to circumvent these issues, and offer new tools to distinguish these cells. What remains is the fundamental question of how these cells engage in distinct transcriptional programs, despite being exposed to the same environmental cues. Our data support the hypothesis that the distinct ontogeny of microglia and peripherally-derived macrophages influences their downstream function in homeostasis and inflammation. While well supported by epigenetic data, and consistent with the idea of hierarchical transcriptional control of macrophage identity, other hypotheses remain (Glass & Natoli, 2015; Lawrence & Natoli, 2011).

In addition to differential ontogenies, microglia and macrophages differ in their capacity for self-renewal and radiation resistance (Sedgwick et al., 1991). Where microglia show robust capacity for these faculties, peripherally derived macrophages have been shown to not contribute to the long-term brain resident macrophage pool (Ajami et al., 2007). Recent work has shown that *Maf* and *Mafb* act as repressors of genes related to self-renewal in some tissue-resident macrophage populations (Soucie et al., 2016). Indeed, *Maf* is expressed at lower levels in adult microglia compared to fetal microglia, suggesting derepressed chromatin in adult microglia and enhanced self-renewal (Kierdorf, Erny, et al., 2013). Meanwhile, our data show that monocytes express little if any *Maf* and *Mafb* (data not shown). In addition, our transcription factor activity modeling suggests that MAF-mediated gene repression is strongest in TAM BMDM with significantly less repression in microglia (data not shown). It is conceivable that the MAF-mediated self-renewal programs in tissue-resident macrophages coincide with significantly different effector functions in peripherally-derived macrophages.

Previous research suggests that self-renewal and long-term contribution to the microglia pool is unique to resident microglia compared to peripherally-derived macrophages in homeostasis and inflammation. However, recent work by Bruttger and colleagues demonstrated that irradiation treatment, in combination with microglia depletion, can lead to long-term accumulation of peripherally-derived macrophages in the brain parenchyma (Bruttger et al., 2015). In this experimental setting, it will be of great importance to determine if the peripheral macrophages that constitute the new brain macrophage pool are irradiation sensitive. In other words, is the irradiation resistance of microglia a feature of their developmental origins or rather of the brain environment? Recent work in the developmentally related Langerhans cells of the skin has elucidated the molecular mechanisms governing irradiation resistance, where CDKN1A expression mediates rapid DNA repair and irradiation resistance (Price et al., 2015); perhaps similar mechanisms are at play in microglia irradiation resistance. This is of particular importance in the therapeutic setting, where ionizing radiation is standard therapy in glioma and also used in brain metastases (Stupp et al., 2005). How therapeutic irradiation affects the remaining microglia and macrophage pool at the tumor site may have profound impacts on the mechanisms of recurrence. In addition, if peripheral macrophages are capable of maintaining the brain-macrophage pool, can upregulate microglia specific transcripts, and display irradiation resistance, then few differences remain between microglia and macrophages except for their developmental origins and the consequent epigenetic patterning imprinted upon them.

Discovery of tumor-associated macrophage subpopulations

While our research has focused on subdividing TAMs into developmentally distinct subsets, there likely remain further subpopulations within the microglia and macrophage compartments. Blood vessels, necrosis, and invasive edges are potential sources of

spatial heterogeneity and likely elicit different activation programs in neighboring cells (Charles et al., 2012). Indeed, previous reports have found that macrophages at these locations in other tumor microenvironments (such as the breast) execute distinct functions (Casazza et al., 2013; Ojalvo, Whittaker, Condeelis, & Pollard, 2010). Future intra-vital imaging approaches may prove particularly informative in understanding spatial plasticity of cells within these niches, a technique that has already been used to identify intercellular communication between TAMs and tumor cells in glioma (van der Vos et al., 2016). In addition to spatial heterogeneity, the length of time spent within the tumor may also have profound effects on macrophage activation; currently, the kinetics of TAM recruitment to brain malignancy remain to be determined. The *Cx3cr1*:CreER lineage tracing system employed herein may be a useful tool in a pulse-chase system to interrogate TAM residency time and kinetics of recruitment.

In addition to these sources of heterogeneity, technical advances in single cell technology now offer substantial opportunities for unbiased subpopulation discovery. Single cell RNA-seq has been successful in exploring the heterogeneity of tumor cells within glioma patients (Patel et al., 2014) as well as identifying rare cell populations in mouse retina (Macosko et al., 2015). Similar technology can be adapted to identify transcriptionally distinct clusters of TAMs in the brain TME. In addition, advances in mass cytometry may offer great potential to identify functionally distinct TAM subpopulations by integrating diverse cell surface marker sets with cytokine and phosphorylation specific flow cytometry for broad pathway interrogation (Becher et al., 2014). Combining these methodologies with models of phagocytosis and antigen presentation should prove fruitful for identifying functionally distinct TAM subsets (Broz et al., 2014).

Spatially distinct TAMs possess high cathepsin activity mediated by IL-4 and IL-6

In addition to phagocytosis and antigen presentation, tumor-associated macrophages have emerged as prominent accessory cells in promoting extracellular matrix remodeling, invasion, angiogenesis, and metastasis. Cysteine cathepsin proteases, produced by macrophages and cancer cells, are known to regulate these processes, but at the beginning of my thesis research it was unclear how these typically lysosomal enzymes were regulated and secreted within the tumor microenvironment. In a collaborative study in the lab (with Hao-Wei Wang and Dongyao Yan) we identified a novel synergy between the STAT3 and STAT6 signaling pathways that potently upregulated cathepsin secretion by macrophages (Yan et al, manuscript in revision). Systematic whole genome expression analyses revealed that the T_H2 cytokine IL-4 synergized with IL-6 or IL-10 to activate an unfolded protein response (UPR) pathway via STAT3 and STAT6. Pharmacological inhibition of the UPR effector IRE1α blocked cathepsin secretion by macrophages and blunted macrophage-mediated invasion of cancer cells. We also demonstrated that genetic ablation of STAT3 and STAT6 signaling components impaired tumor development and invasion *in vivo*. Together, these findings demonstrated that cytokine-activated STAT3 and STAT6 cooperated in macrophages to promote a professional secretory phenotype capable of enhancing tumor progression in a cathepsin-dependent manner. In addition, these studies highlight how transcriptional profiling and pathway interrogation can provide novel functional insights into TAM activity.

Depletion strategies for functional evaluation of TAM MG and TAM BMDM in brain malignancy

This thesis has been successful in identifying markers capable of distinguishing microglia and macrophages, however the functional faculties of these cells, and the

effects of their respective depletion or re-education, remains to be determined. Genetic tools to deplete microglia can be readily integrated into the experimental systems described here. Previous work has shown that the *Cx3cr1*:CreER lineage tracing system employed here can be used to deplete microglia when combined with a Rosa26:lsl-DTR (diphtheria toxin receptor) allele (Bruttger et al., 2015; Parkhurst et al., 2013). This allows for specific depletion of microglia upon the administration of diphtheria toxin (following a tamoxifen pulse to recombine the DTR allele in microglia). We have previously employed a CD11b:DTR line in efforts to deplete TAMs in glioma, however there was no evident depletion in tumors (Pyonteck et al., 2013). This discrepancy in efficacy between the models may be due to promoter strength of the CD11b promoter compared to that of the Rosa26 locus. In addition, CD11b:DTR line likely targets both microglia, macrophages and peripheral myeloid cells, which will likely have pleiotropic effects on homeostasis and tumor progression. Perhaps the inefficacy of the CD11b:DTR mouse results from targeting combinations of these populations, highlighting the need for more specific targeting strategies. Despite the prior lack of success with DTR-based strategies, this currently remains the most promising approach for microglia-specific depletion.

Macrophage-specific targeting presents a more complicated goal. In addition to the CD11b-DTR strategy described above, previous attempts in our lab have utilized a CCR2:CFP-DTR strategy and clodronate loaded liposomes (Pyonteck et al., 2013). Neither of these approaches led to appreciable difference in TAM abundance. However, both of these strategies were employed in the *Ink4a/Arf*-deficient PDGFB model described in this thesis, where microglia compose >90% of the TAM content (as shown by CD49D staining). It is likely that the skewing of microglia to macrophage ratio makes it difficult to identify decreases in TAM BMDM content. Moreover, the gene expression

data shown here suggests that CCR2 is downregulated in TAM BMDM upon differentiation, further complicating any expected efficacy with the CCR2-DTR model. One interesting genetic approach has combined the myeloid enriched LysM:Cre line with a Csf1r: lsl-DTR allele to restrict expression of the DTR allele to monocytes and macrophages (Schreiber et al., 2013). A similar approach could be employed to restrict DTR expression to macrophages by combining the Flt3:Cre lineage tracing system here with the Csf1r:lsl-DTR allele. While this may have pleiotropic effects by peripheral depletion of monocytes and dendritic cells, it would restrict diphtheria toxin from targeting microglia. Similar strategies could be used to re-engineer the commonly used MAFIA mouse model (Burnett et al., 2004) to be dependent upon either Flt3:Cre recombination for macrophages or Cx3cr1:CreER recombination for microglia.

CD49D blockade as a macrophage depletion tool and therapeutic strategy

In addition to these diphtheria toxin-based strategies, CD49D blockade may also be a useful tool to prevent the recruitment of TAM BMDM in tumors. This approach is not without potential pleiotropic effects however, as CD49D blockade has been shown to block T cell and NK cell influx in mouse models of experimental autoimmune encephalitis (Gan, Liu, Wu, Bomprezzi, & Shi, 2012; Mindur, Ito, Dhib-Jalbut, & Ito, 2014). Despite this potential effect, preliminary data shows that TAM BMDM recruitment can indeed be blocked with an anti-CD49D antibody in the context of tumor recurrence following ionizing radiation (IR) (data not shown; in collaboration with Dr. Leila Akkari). This BMDM blockade was associated with increased survival following IR treatment, reminiscent of previous CXCR4 blockade with AMD-3100 following IR (Kioi et al., 2010; S. C. Liu et al., 2014).

A humanized monoclonal antibody targeting CD49D, Natalizumab, is an FDA approved therapy for multiple sclerosis patients (Miller et al., 2003), and might represent an interesting clinical approach in glioma patients. Rigorous inclusion criteria would be necessary in testing Natalizumab, as treatment in MS patients has led to the development of lethal progressive multifocal leukoencephalopathy (PML), a manifestation of JC-virus infection (Langer-Gould, Atlas, Green, Bollen, & Pelletier, 2005). Thus screening patients for seroconversion of JC-virus would be necessary to prevent the development of this lethal side effect. Given that CD49D blockade will likely affect T cell influx, it's possible that immune checkpoint blockade and CD49D blockade may be incongruent. Thus biomarker development for immune checkpoint blockade efficacy would also be critical in patient selection. Other factors including MGMT promoter methylation and hypermutation status should also be taken into account (Hunter et al., 2006; Stupp et al., 2005).

<u>CSF-1R inhibition as a therapeutic option</u>

Concurrent with the work presented here, I performed collaborative studies within the Joyce lab with the goal of investigating the efficacy of targeting tumor-associated microglia and macrophages in glioblastoma (with Stephanie Pyonteck, Leila Akkari, Alberto J. Schuhmacher and Daniela Quail). In addition to strategies discussed above, the most widely used approach to targeting TAMs has been through inhibition of the CSF-1 receptor. In a study from the Segall lab using the GL261 glioma model, CSF-1R inhibition with PLX3997 was capable of significantly decreasing TAM content in a prevention trial, leading to reduced proliferation and tumor invasion (Coniglio et al., 2012). However, it remains unclear if CSF-1R inhibition skewed the ratio of microglia to macrophages or if there was a concomitant decrease in both populations. We have previously demonstrated that CSF-1R blockade with the small molecule BLZ945 (as well

as PLX3997, unpublished results), blocked glioma progression in a prevention trial, and led to regression of established grade IV gliomas in an intervention trial (Pyonteck et al., 2013). Despite efficient depletion in peripheral tissues and normal brain, we were surprised to find that BLZ945 did not deplete TAMs. Instead, we identified glioma-derived survival factors capable of protecting TAMs from BLZ945 mediated killing, and surviving TAMs showed reduced expression of M2/alternative activation markers. With these two models and additional models generated in our lab, we suggest that there are both "protective" and "non-protective" gliomas, which display different magnitudes of response to CSF-1R inhibition.

These studies suggest that rather than depleting TAMs, "re-education" strategies may prove more fruitful (Bowman & Joyce, 2014). Yet, the mechanisms underlying this efficacy and "re-education" remain unclear. Gene expression profiling of bulk TAMs from BLZ945-treated gliomas revealed down-regulation of a set of markers associated with M2 macrophage polarization including *Cd163*, *Mrc1*, *Arg1*, *Hmox1*, *Stab1*, *Il1r2*, *Cdh1*, *Adm*, and *F13a1* (Pyonteck et al., 2013). While histological analyses on bone marrow-transplanted mice revealed no significant alteration in BMDM and MG numbers in this earlier study (Pyonteck et al., 2013), work in this thesis shows that most of these genes are more predominantly expressed in BMDM as opposed to MG. These data thus suggest that CSF-1R inhibition likely has asymmetric effects on BMDM and MG. Current studies are in progress to understand how acute and chronic CSF-1R inhibition differentially affect BMDM and MG function and abundance. Such efforts, combined with the comprehensive transcriptional profiling performed here, have the potential to identify therapeutic targets that may synergize with CSF-1R inhibition.

Indeed, a collaborative study in the lab with Dr. Daniela Quail revealed that chronic treatment with BLZ945 promoted long-term, stable regression in murine models of glioma. However, a subset of mice eventually developed microenvironment-mediated resistance. Transcriptional profiling of bulk TAMs isolated from resistant tumors revealed a specific upregulation of *Igf1*, and concomitant upregulation of *Igf1r* and PI3K signaling in tumor cells. Therapeutic intervention demonstrated that CSF-1R inhibitor resistant tumors possessed a unique sensitivity to either PI3K or IGF1R inhibition. Transcriptional profiling also revealed STAT6-NFAT-mediated alternative macrophage activation underlying TAM reprogramming and IGF1 production. In sum, these analyses reveal that long-term inhibition of CSF-1R may present a viable clinical option in glioma. In addition, acquired, or potentially *de novo*, resistance to such inhibition may present with microenvironment-mediated engagement of alternative signaling pathways (Quail et al., 2016)

Biomarkers for TAM-targeted therapy

Like most therapies, potential toxicity has been an important concern in the development of TAM-targeted therapy. Previous studies have shown that CSF-1R inhibition with either small molecules or antibodies is associated with increased serum ALT and AST levels in monkeys and rodents, suggestive of liver damage (Radi et al., 2011; T. Wang et al., 2011). However, caution should be taken in the interpretation of these results as multiple models of Kupffer cell depletion also lead to serum enzyme levels increases in the absence of liver pathology (Radi et al., 2011). Similar results were seen in *Csf1*-deficient mice (Radi et al., 2011), suggesting that serum enzyme elevation is a frequent result of targeting CSF-1R or macrophages. Thus, under CSF-1R inhibition, increased ALT and AST may be a consequence of altered enzyme recycling from the blood in the absence of Kupffer cells, given there is no histological evidence of occult liver damage in

long-term experiments. In our own studies, mice treated daily, over the course of 5 months with BLZ945 showed no microscopic or overt signs of liver disease. Further investigation into TAM targeted therapy and liver function will be necessary to understand the utility of serum enzyme levels for detecting liver toxicity.

Pharmacological studies to assess dosing schemes for TAM-targeted therapies will be necessary to maximize clinical efficacy. While most phase I trials aim to identify the maximum tolerated dose (MTD) of a therapeutic agent, efforts to re-educate TAMs may require a new paradigm. In the case of CSF-1R blockade, excessive dosing may lead to TAM depletion, where lower doses, or more infrequent doses, may lead to TAM re-education. Thorough preclinical studies identifying biomarkers of response will be necessary to facilitate clinical action. Work during my thesis research identified a 5-gene signature of response to BLZ945 treatment in mice, which also provided prognostic value in proneural GBM patients (Pyonteck et al., 2013). Two of these gene products, F13a1 and Adm, are present in serum and may thus serve as a useful tool for measuring responsiveness to CSF-1R blockade.

Immune contexture in prognosis and therapeutic response

In addition to the biomarkers for TAM-targeted therapy described above, we posit that the TME itself can also provide a source of biomarkers for either tumor cell-targeted therapy or immunotherapy. We have shown here that transcript abundance of the BMDM marker *ITGA4* and the microglia marker *P2RY12* offer prognostic power in low-grade glioma. While our current cohort is underpowered for extensive survival analyses, It will be interesting in future studies to see if these predictions can be verified using a clinically relevant immunohistochemistry assay. This will be of particular interest for *P2RY12*, as the prognostic value demonstrated with increased expression could indicate

124

that either 1) greater microglia content is a positive prognostic finding or 2) acquisition of microglia markers by macrophages is a good prognostic outcome. If either of these scenarios proves to be important for disease progression, it would lead to fundamentally different approaches in targeting. Efforts to block peripheral macrophage accumulation would be ideal in the first instance, while influencing their tissue residency assimilation might be more ideal in the second setting. In either case, the profiling and bioinformatics analyses performed here provide an expansive resource to probe the pathways controlling recruitment and differentiation.

In addition to the microglia to macrophage ratio, other components of the TME may prove useful as biomarkers of therapeutic response. Several clinical trials are currently investigating the utility of immunotherapy in glioma and brain metastases. We demonstrate here that a large percentage of the lymphoid cell compartment of the TME is composed of CD4- CD8- double negative T (DNT) cells. In a select few patients we have demonstrated that this compartment is not composed of γ/δ T cells, however further insights into their identity and function are required. One report demonstrated in mouse that CD8+ T cells down-regulate *Cd8a* expression and lose effector function when tumor cells do not express MHC-I (Prins et al., 2004). Others have found these DNT cells to exert their immunosuppressive capacity through suppression of IL-2 signaling (Hamad et al., 2003). These data provide a potential clue as to the identity of the DNT cells and further RNA-sequencing of this population will provide greater insight into their function. In our cohort we have identified several patients that show increased CD8+ T cell counts compared to DNTs. One attractive hypothesis is that these patients might possess distinctive clinical or genomic characteristics that may be more permissive to immune checkpoint blockade, however our current cohort is underpowered to draw any firm conclusions. If these DNT cells are indeed cytotoxic T cells that have

downregulated CD8, then understanding the mechanisms of this repression, the subsequent function of the DNT cells, and relevance in the setting of checkpoint blockade will be critical to the development of these therapies.

Summary

In sum, my thesis has conclusively addressed the ontogenetic composition of TAMs in brain malignancy. These studies have offered further insights into how developmental origins influence cellular response to inflammatory stimuli. We have identified distinct transcriptional programs and cell surface markers in microglia and macrophages in multiple brain malignancies in patients and in mouse models. These results, combined with the immune profiling on human tumor specimens, lay the foundation to identify TME-centric therapeutic avenues and markers of clinical response.

Aside from the work presented here, collaborative studies during my thesis evaluated stage-dependent tumor-stroma interactions in breast metastasis to the brain, bone and lung. In this study we found mechanistic and prognostic significance for tumor and stroma-derived cathepsin S in mediating breast to brain metastasis (Sevenich et al, 2014). Additional collaborative studies aimed at probing similar tumor-stroma interactions in the brain TME through therapeutic intervention with small molecule inhibitors of the macrophage-specific receptor CSF-1R. These studies identified mechanisms underlying efficacy, and eventual resistance to, CSF-1R inhibition, uncovering a novel therapeutic option in GBM (Pyonteck et al, 2013; Quail et al, 2016). Lastly, concurrent work aimed to uncover mechanistic insights into how T_H2 cytokines mediated cathepsin secretion in tumor-associated macrophages. Here focused top-down pathway interrogation identified a novel cooption of the unfolded protein response in regulating macrophage activation and cathepsin secretion (Yan et al, 2016).

Collectively, these studies have provided fundamental insights into the processes regulating tumor-stroma interactions in multiple disease sites, and offer mechanistic insight for specific functions in the metastatic cascade. In sum, my thesis research has provided a broad understanding of tumor-associated macrophage ontogeny, education, and capacity for therapeutic intervention within the tumor microenvironment.

BIBLIOGRAPHY

Adams, S., Braidy, N., Bessede, A., Brew, B. J., Grant, R., Teo, C., & Guillemin, G. J. (2012). The kynurenine pathway in brain tumor pathogenesis. *Cancer Res, 72*(22), 5649-5657. doi: 10.1158/0008-5472.CAN-12-0549

Adams, S., Teo, C., McDonald, K. L., Zinger, A., Bustamante, S., Lim, C. K., . . . Guillemin, G. J. (2014). Involvement of the kynurenine pathway in human glioma pathophysiology. *PLoS One, 9*(11), e112945. doi: 10.1371/journal.pone.0112945

Aderem, A., & Underhill, D. M. (1999). Mechanisms of phagocytosis in macrophages. *Annu Rev Immunol, 17*, 593-623. doi: 10.1146/annurev.immunol.17.1.593

Ahmed, K. A., Stallworth, D. G., Kim, Y., Johnstone, P. A., Harrison, L. B., Caudell, J. J., . . . Gibney, G. T. (2015). Clinical outcomes of melanoma brain metastases treated with stereotactic radiation and anti-PD-1 therapy. *Ann Oncol*. doi: 10.1093/annonc/mdv622

Ajami, B., Bennett, J. L., Krieger, C., McNagny, K. M., & Rossi, F. M. (2011). Infiltrating monocytes trigger EAE progression, but do not contribute to the resident microglia pool. *Nat Neurosci, 14*(9), 1142-1149. doi: 10.1038/nn.2887

Ajami, B., Bennett, J. L., Krieger, C., Tetzlaff, W., & Rossi, F. M. (2007). Local self-renewal can sustain CNS microglia maintenance and function throughout adult life. *Nat Neurosci, 10*(12), 1538-1543. doi: 10.1038/nn2014

Alder, J. K., Georgantas, R. W., 3rd, Hildreth, R. L., Kaplan, I. M., Morisot, S., Yu, X., . . . Civin, C. I. (2008). Kruppel-like factor 4 is essential for inflammatory monocyte differentiation in vivo. *J Immunol, 180*(8), 5645-5652.

Alliot, F., Godin, I., & Pessac, B. (1999). Microglia derive from progenitors, originating from the yolk sac, and which proliferate in the brain. *Brain Res Dev Brain Res, 117*(2), 145-152.

Amit, I., Winter, D. R., & Jung, S. (2015). The role of the local environment and epigenetics in shaping macrophage identity and their effect on tissue homeostasis. *Nat Immunol, 17*(1), 18-25. doi: 10.1038/ni.3325

Bain, C. C., Bravo-Blas, A., Scott, C. L., Gomez Perdiguero, E., Geissmann, F., Henri, S., . . . Mowat, A. M. (2014). Constant replenishment from circulating monocytes maintains the macrophage pool in the intestine of adult mice. *Nat Immunol, 15*(10), 929-937. doi: 10.1038/ni.2967

Balwierz, P. J., Pachkov, M., Arnold, P., Gruber, A. J., Zavolan, M., & van Nimwegen, E. (2014). ISMARA: automated modeling of genomic signals as a democracy of regulatory motifs. *Genome Res, 24*(5), 869-884. doi: 10.1101/gr.169508.113

Barker, C. F., & Billingham, R. E. (1977). Immunologically privileged sites. *Adv Immunol, 25*, 1-54.

Becher, B., Schlitzer, A., Chen, J., Mair, F., Sumatoh, H. R., Teng, K. W., . . . Newell, E. W. (2014). High-dimensional analysis of the murine myeloid cell system. *Nat Immunol, 15*(12), 1181-1189. doi: 10.1038/ni.3006

Bell, J. K., Mullen, G. E., Leifer, C. A., Mazzoni, A., Davies, D. R., & Segal, D. M. (2003). Leucine-rich repeats and pathogen recognition in Toll-like receptors. *Trends Immunol, 24*(10), 528-533.

Bennett, G. D., & Kay, M. M. (1981). Homeostatic removal of senescent murine erythrocytes by splenic macrophages. *Exp Hematol, 9*(3), 297-307.

Benz, C., Martins, V. C., Radtke, F., & Bleul, C. C. (2008). The stream of precursors that colonizes the thymus proceeds selectively through the early T lineage precursor stage of T cell development. *J Exp Med, 205*(5), 1187-1199. doi: 10.1084/jem.20072168

Berens, M. E., & Giese, A. (1999). "...those left behind." Biology and oncology of invasive glioma cells. *Neoplasia, 1*(3), 208-219.

Bindea, G., Mlecnik, B., Tosolini, M., Kirilovsky, A., Waldner, M., Obenauf, A. C., . . . Galon, J. (2013). Spatiotemporal dynamics of intratumoral immune cells reveal the immune landscape in human cancer. *Immunity, 39*(4), 782-795. doi: 10.1016/j.immuni.2013.10.003

Biswas, S. K., Gangi, L., Paul, S., Schioppa, T., Saccani, A., Sironi, M., . . . Sica, A. (2006). A distinct and unique transcriptional program expressed by tumor-associated macrophages (defective NF-kappaB and enhanced IRF-3/STAT1 activation). *Blood, 107*(5), 2112-2122. doi: 10.1182/blood-2005-01-0428

Biswas, S. K., & Mantovani, A. (2010). Macrophage plasticity and interaction with lymphocyte subsets: cancer as a paradigm. *Nat Immunol, 11*(10), 889-896. doi: 10.1038/ni.1937

Boehm, U., Klamp, T., Groot, M., & Howard, J. C. (1997). Cellular responses to interferon-gamma. *Annu Rev Immunol, 15*, 749-795. doi: 10.1146/annurev.immunol.15.1.749

Borghaei, H., Paz-Ares, L., Horn, L., Spigel, D. R., Steins, M., Ready, N. E., . . . Brahmer, J. R. (2015). Nivolumab versus Docetaxel in Advanced Nonsquamous Non-Small-Cell Lung Cancer. *N Engl J Med, 373*(17), 1627-1639. doi: 10.1056/NEJMoa1507643

Bos, P. D., Zhang, X. H., Nadal, C., Shu, W., Gomis, R. R., Nguyen, D. X., . . . Massague, J. (2009). Genes that mediate breast cancer metastasis to the brain. *Nature, 459*(7249), 1005-1009. doi: 10.1038/nature08021

Boss, J. M. (1997). Regulation of transcription of MHC class II genes. *Curr Opin Immunol, 9*(1), 107-113.

Bowman, R. L., & Joyce, J. A. (2014). Therapeutic targeting of tumor-associated macrophages and microglia in glioblastoma. *Immunotherapy, 6*(6), 663-666. doi: 10.2217/imt.14.48

Boyer, S. W., Schroeder, A. V., Smith-Berdan, S., & Forsberg, E. C. (2011). All hematopoietic cells develop from hematopoietic stem cells through Flk2/Flt3-positive progenitor cells. *Cell Stem Cell, 9*(1), 64-73. doi: 10.1016/j.stem.2011.04.021

Brastianos, P. K., Carter, S. L., Santagata, S., Cahill, D. P., Taylor-Weiner, A., Jones, R. T., . . . Hahn, W. C. (2015). Genomic Characterization of Brain Metastases Reveals Branched Evolution and Potential Therapeutic Targets. *Cancer Discov, 5*(11), 1164-1177. doi: 10.1158/2159-8290.CD-15-0369

Brastianos, P. K., Curry, W. T., & Oh, K. S. (2013). Clinical discussion and review of the management of brain metastases. *J Natl Compr Canc Netw, 11*(9), 1153-1164.

Brennan, C. W., Verhaak, R. G., McKenna, A., Campos, B., Noushmehr, H., Salama, S. R., . . . Network, T. R. (2013). The somatic genomic landscape of glioblastoma. *Cell, 155*(2), 462-477. doi: 10.1016/j.cell.2013.09.034

Brooks, W. H., Markesbery, W. R., Gupta, G. D., & Roszman, T. L. (1978). Relationship of lymphocyte invasion and survival of brain tumor patients. *Ann Neurol, 4*(3), 219-224. doi: 10.1002/ana.410040305

Broz, M. L., Binnewies, M., Boldajipour, B., Nelson, A. E., Pollack, J. L., Erle, D. J., . . . Krummel, M. F. (2014). Dissecting the tumor myeloid compartment reveals rare activating antigen-presenting cells critical for T cell immunity. *Cancer Cell, 26*(5), 638-652. doi: 10.1016/j.ccell.2014.09.007

Bruttger, J., Karram, K., Wortge, S., Regen, T., Marini, F., Hoppmann, N., . . . Waisman, A. (2015). Genetic Cell Ablation Reveals Clusters of Local Self-Renewing

Microglia in the Mammalian Central Nervous System. *Immunity, 43*(1), 92-106. doi: 10.1016/j.immuni.2015.06.012

Burnett, S. H., Kershen, E. J., Zhang, J., Zeng, L., Straley, S. C., Kaplan, A. M., & Cohen, D. A. (2004). Conditional macrophage ablation in transgenic mice expressing a Fas-based suicide gene. *J Leukoc Biol, 75*(4), 612-623. doi: 10.1189/jlb.0903442

Bussmann, L. H., Schubert, A., Vu Manh, T. P., De Andres, L., Desbordes, S. C., Parra, M., . . . Graf, T. (2009). A robust and highly efficient immune cell reprogramming system. *Cell Stem Cell, 5*(5), 554-566. doi: 10.1016/j.stem.2009.10.004

Butovsky, O., Jedrychowski, M. P., Moore, C. S., Cialic, R., Lanser, A. J., Gabriely, G., . . . Weiner, H. L. (2014). Identification of a unique TGF-beta-dependent molecular and functional signature in microglia. *Nat Neurosci, 17*(1), 131-143. doi: 10.1038/nn.3599

Buza-Vidas, N., Woll, P., Hultquist, A., Duarte, S., Lutteropp, M., Bouriez-Jones, T., . . . Jacobsen, S. E. (2011). FLT3 expression initiates in fully multipotent mouse hematopoietic progenitor cells. *Blood, 118*(6), 1544-1548. doi: 10.1182/blood-2010-10-316232

Cancer Genome Atlas Research, N. (2008). Comprehensive genomic characterization defines human glioblastoma genes and core pathways. *Nature, 455*(7216), 1061-1068. doi: 10.1038/nature07385

Cancer Genome Atlas Research, N., Brat, D. J., Verhaak, R. G., Aldape, K. D., Yung, W. K., Salama, S. R., . . . Zhang, J. (2015). Comprehensive, Integrative Genomic Analysis of Diffuse Lower-Grade Gliomas. *N Engl J Med, 372*(26), 2481-2498. doi: 10.1056/NEJMoa1402121

Cancer Genome Atlas Research, N., Weinstein, J. N., Collisson, E. A., Mills, G. B., Shaw, K. R., Ozenberger, B. A., . . . Stuart, J. M. (2013). The Cancer Genome Atlas Pan-Cancer analysis project. *Nat Genet, 45*(10), 1113-1120. doi: 10.1038/ng.2764

Capotondo, A., Milazzo, R., Politi, L. S., Quattrini, A., Palini, A., Plati, T., . . . Biffi, A. (2012). Brain conditioning is instrumental for successful microglia reconstitution following hematopoietic stem cell transplantation. *Proc Natl Acad Sci U S A, 109*(37), 15018-15023. doi: 10.1073/pnas.1205858109

Carson, M. J., Doose, J. M., Melchior, B., Schmid, C. D., & Ploix, C. C. (2006). CNS immune privilege: hiding in plain sight. *Immunol Rev, 213*, 48-65. doi: 10.1111/j.1600-065X.2006.00441.x

Casazza, A., Laoui, D., Wenes, M., Rizzolio, S., Bassani, N., Mambretti, M., . . . Mazzone, M. (2013). Impeding macrophage entry into hypoxic tumor areas by Sema3A/Nrp1 signaling blockade inhibits angiogenesis and restores antitumor immunity. *Cancer Cell, 24*(6), 695-709. doi: 10.1016/j.ccr.2013.11.007

Caux, C., Massacrier, C., Vanbervliet, B., Barthelemy, C., Liu, Y. J., & Banchereau, J. (1994). Interleukin 10 inhibits T cell alloreaction induced by human dendritic cells. *Int Immunol, 6*(8), 1177-1185.

Ceccarelli, M., Barthel, F. P., Malta, T. M., Sabedot, T. S., Salama, S. R., Murray, B. A., . . . Verhaak, R. G. (2016). Molecular Profiling Reveals Biologically Discrete Subsets and Pathways of Progression in Diffuse Glioma. *Cell, 164*(3), 550-563. doi: 10.1016/j.cell.2015.12.028

Cecchini, M. G., Dominguez, M. G., Mocci, S., Wetterwald, A., Felix, R., Fleisch, H., . . . Stanley, E. R. (1994). Role of colony stimulating factor-1 in the establishment and regulation of tissue macrophages during postnatal development of the mouse. *Development, 120*(6), 1357-1372.

Chalaris, A., Garbers, C., Rabe, B., Rose-John, S., & Scheller, J. (2011). The soluble Interleukin 6 receptor: generation and role in inflammation and cancer. *Eur J Cell Biol, 90*(6-7), 484-494. doi: 10.1016/j.ejcb.2010.10.007

Chang, E. L., Wefel, J. S., Hess, K. R., Allen, P. K., Lang, F. F., Kornguth, D. G., . . . Meyers, C. A. (2009). Neurocognition in patients with brain metastases treated with radiosurgery or radiosurgery plus whole-brain irradiation: a randomised controlled trial. *Lancet Oncol, 10*(11), 1037-1044. doi: 10.1016/S1470-2045(09)70263-3

Charles, N. A., Holland, E. C., Gilbertson, R., Glass, R., & Kettenmann, H. (2011). The brain tumor microenvironment. *Glia, 59*(8), 1169-1180. doi: 10.1002/glia.21136

Charles, N. A., Holland, E. C., Gilbertson, R., Glass, R., & Kettenmann, H. (2012). The brain tumor microenvironment. *Glia, 60*(3), 502-514.

Chen, H. (2015). VennDiagram: Generate High-Resolution Venn and Euler Plots. from http://CRAN.R-project.org/package=VennDiagram

Chitu, V., & Stanley, E. R. (2006). Colony-stimulating factor-1 in immunity and inflammation. *Curr Opin Immunol, 18*(1), 39-48. doi: 10.1016/j.coi.2005.11.006

Chomarat, P., Banchereau, J., Davoust, J., & Palucka, A. K. (2000). IL-6 switches the differentiation of monocytes from dendritic cells to macrophages. *Nat Immunol, 1*(6), 510-514. doi: 10.1038/82763

Choukrallah, M. A., & Matthias, P. (2014). The Interplay between Chromatin and Transcription Factor Networks during B Cell Development: Who Pulls the Trigger First? *Front Immunol, 5*, 156. doi: 10.3389/fimmu.2014.00156

Clausen, B. E., Burkhardt, C., Reith, W., Renkawitz, R., & Forster, I. (1999). Conditional gene targeting in macrophages and granulocytes using LysMcre mice. *Transgenic Res, 8*(4), 265-277.

Coniglio, S. J., Eugenin, E., Dobrenis, K., Stanley, E. R., West, B. L., Symons, M. H., & Segall, J. E. (2012). Microglial stimulation of glioblastoma invasion involves epidermal growth factor receptor (EGFR) and colony stimulating factor 1 receptor (CSF-1R) signaling. *Mol Med, 18*, 519-527. doi: 10.2119/molmed.2011.00217

Consortium, F., Suzuki, H., Forrest, A. R., van Nimwegen, E., Daub, C. O., Balwierz, P. J., . . . Hayashizaki, Y. (2009). The transcriptional network that controls growth arrest and differentiation in a human myeloid leukemia cell line. *Nat Genet, 41*(5), 553-562. doi: 10.1038/ng.375

Couzin-Frankel, J. (2013). Breakthrough of the year 2013. Cancer immunotherapy. *Science, 342*(6165), 1432-1433. doi: 10.1126/science.342.6165.1432

Crowther, M., Brown, N. J., Bishop, E. T., & Lewis, C. E. (2001). Microenvironmental influence on macrophage regulation of angiogenesis in wounds and malignant tumors. *J Leukoc Biol, 70*(4), 478-490.

Dai, X. M., Ryan, G. R., Hapel, A. J., Dominguez, M. G., Russell, R. G., Kapp, S., . . . Stanley, E. R. (2002). Targeted disruption of the mouse colony-stimulating factor 1 receptor gene results in osteopetrosis, mononuclear phagocyte deficiency, increased primitive progenitor cell frequencies, and reproductive defects. *Blood, 99*(1), 111-120.

DeKoter, R. P., & Singh, H. (2000). Regulation of B lymphocyte and macrophage development by graded expression of PU.1. *Science, 288*(5470), 1439-1441.

Dennis, G., Jr., Sherman, B. T., Hosack, D. A., Yang, J., Gao, W., Lane, H. C., & Lempicki, R. A. (2003). DAVID: Database for Annotation, Visualization, and Integrated Discovery. *Genome Biol, 4*(5), P3.

Diaz, M. O., Pomykala, H. M., Bohlander, S. K., Maltepe, E., Malik, K., Brownstein, B., & Olopade, O. I. (1994). Structure of the human type-I interferon gene cluster

determined from a YAC clone contig. *Genomics, 22*(3), 540-552. doi: 10.1006/geno.1994.1427

Diehl, S., & Rincon, M. (2002). The two faces of IL-6 on Th1/Th2 differentiation. *Mol Immunol, 39*(9), 531-536.

Dobin, A., Davis, C. A., Schlesinger, F., Drenkow, J., Zaleski, C., Jha, S., . . . Gingeras, T. R. (2013). STAR: ultrafast universal RNA-seq aligner. *Bioinformatics, 29*(1), 15-21. doi: 10.1093/bioinformatics/bts635

Du, R., Lu, K. V., Petritsch, C., Liu, P., Ganss, R., Passegue, E., . . . Bergers, G. (2008). HIF1alpha induces the recruitment of bone marrow-derived vascular modulatory cells to regulate tumor angiogenesis and invasion. *Cancer Cell, 13*(3), 206-220. doi: 10.1016/j.ccr.2008.01.034

Eckel-Passow, J. E., Lachance, D. H., Molinaro, A. M., Walsh, K. M., Decker, P. A., Sicotte, H., . . . Jenkins, R. B. (2015). Glioma Groups Based on 1p/19q, IDH, and TERT Promoter Mutations in Tumors. *N Engl J Med, 372*(26), 2499-2508. doi: 10.1056/NEJMoa1407279

El Andaloussi, A., & Lesniak, M. S. (2006). An increase in CD4+CD25+FOXP3+ regulatory T cells in tumor-infiltrating lymphocytes of human glioblastoma multiforme. *Neuro Oncol, 8*(3), 234-243. doi: 10.1215/15228517-2006-006

Engler, J. R., Robinson, A. E., Smirnov, I., Hodgson, J. G., Berger, M. S., Gupta, N., . . . Phillips, J. J. (2012). Increased microglia/macrophage gene expression in a subset of adult and pediatric astrocytomas. *PLoS One, 7*(8), e43339. doi: 10.1371/journal.pone.0043339

Feinberg, M. W., Wara, A. K., Cao, Z., Lebedeva, M. A., Rosenbauer, F., Iwasaki, H., . . . Jain, M. K. (2007). The Kruppel-like factor KLF4 is a critical regulator of monocyte differentiation. *EMBO J, 26*(18), 4138-4148. doi: 10.1038/sj.emboj.7601824

Feng, R., Desbordes, S. C., Xie, H., Tillo, E. S., Pixley, F., Stanley, E. R., & Graf, T. (2008). PU.1 and C/EBPalpha/beta convert fibroblasts into macrophage-like cells. *Proc Natl Acad Sci U S A, 105*(16), 6057-6062. doi: 10.1073/pnas.0711961105

Fogg, D. K., Sibon, C., Miled, C., Jung, S., Aucouturier, P., Littman, D. R., . . . Geissmann, F. (2006). A clonogenic bone marrow progenitor specific for macrophages and dendritic cells. *Science, 311*(5757), 83-87. doi: 10.1126/science.1117729

Friedman, J., Hastie, T., & Tibshirani, R. (2010). Regularization Paths for Generalized Linear Models via Coordinate Descent. *J Stat Softw, 33*(1), 1-22.

Fujita, M., Kohanbash, G., Fellows-Mayle, W., Hamilton, R. L., Komohara, Y., Decker, S. A., . . . Okada, H. (2011). COX-2 blockade suppresses gliomagenesis by inhibiting myeloid-derived suppressor cells. *Cancer Res, 71*(7), 2664-2674. doi: 10.1158/0008-5472.CAN-10-3055

Gabrusiewicz, K., Ellert-Miklaszewska, A., Lipko, M., Sielska, M., Frankowska, M., & Kaminska, B. (2011). Characteristics of the alternative phenotype of microglia/macrophages and its modulation in experimental gliomas. *PLoS One, 6*(8), e23902. doi: 10.1371/journal.pone.0023902

Gan, Y., Liu, R., Wu, W., Bomprezzi, R., & Shi, F. D. (2012). Antibody to alpha4 integrin suppresses natural killer cells infiltration in central nervous system in experimental autoimmune encephalomyelitis. *J Neuroimmunol, 247*(1-2), 9-15. doi: 10.1016/j.jneuroim.2012.03.011

Gautier, E. L., Shay, T., Miller, J., Greter, M., Jakubzick, C., Ivanov, S., . . . Immunological Genome, C. (2012). Gene-expression profiles and transcriptional

regulatory pathways that underlie the identity and diversity of mouse tissue macrophages. *Nat Immunol, 13*(11), 1118-1128. doi: 10.1038/ni.2419

Gavrilovic, I. T., & Posner, J. B. (2005). Brain metastases: epidemiology and pathophysiology. *J Neurooncol, 75*(1), 5-14. doi: 10.1007/s11060-004-8093-6

Gentles, A. J., Newman, A. M., Liu, C. L., Bratman, S. V., Feng, W., Kim, D., . . . Alizadeh, A. A. (2015). The prognostic landscape of genes and infiltrating immune cells across human cancers. *Nat Med, 21*(8), 938-945. doi: 10.1038/nm.3909

Gilbert, M. R., Dignam, J. J., Armstrong, T. S., Wefel, J. S., Blumenthal, D. T., Vogelbaum, M. A., . . . Mehta, M. P. (2014). A randomized trial of bevacizumab for newly diagnosed glioblastoma. *N Engl J Med, 370*(8), 699-708. doi: 10.1056/NEJMoa1308573

Ginhoux, F., Greter, M., Leboeuf, M., Nandi, S., See, P., Gokhan, S., . . . Merad, M. (2010). Fate mapping analysis reveals that adult microglia derive from primitive macrophages. *Science, 330*(6005), 841-845. doi: 10.1126/science.1194637

Glass, C. K., & Natoli, G. (2015). Molecular control of activation and priming in macrophages. *Nat Immunol, 17*(1), 26-33. doi: 10.1038/ni.3306

Gomez Perdiguero, E., Klapproth, K., Schulz, C., Busch, K., Azzoni, E., Crozet, L., . . . Rodewald, H. R. (2015). Tissue-resident macrophages originate from yolk-sac-derived erythro-myeloid progenitors. *Nature, 518*(7540), 547-551. doi: 10.1038/nature13989

Gomez Perdiguero, E., Klapproth, K., Schulz, C., Busch, K., de Bruijn, M., Rodewald, H. R., & Geissmann, F. (2015). The Origin of Tissue-Resident Macrophages: When an Erythro-myeloid Progenitor Is an Erythro-myeloid Progenitor. *Immunity, 43*(6), 1023-1024. doi: 10.1016/j.immuni.2015.11.022

Gordon, S., & Taylor, P. R. (2005). Monocyte and macrophage heterogeneity. *Nat Rev Immunol, 5*(12), 953-964. doi: 10.1038/nri1733

Gosselin, D., Link, V. M., Romanoski, C. E., Fonseca, G. J., Eichenfield, D. Z., Spann, N. J., . . . Glass, C. K. (2014). Environment drives selection and function of enhancers controlling tissue-specific macrophage identities. *Cell, 159*(6), 1327-1340. doi: 10.1016/j.cell.2014.11.023

Greter, M., Lelios, I., Pelczar, P., Hoeffel, G., Price, J., Leboeuf, M., . . . Becher, B. (2012). Stroma-derived interleukin-34 controls the development and maintenance of langerhans cells and the maintenance of microglia. *Immunity, 37*(6), 1050-1060. doi: 10.1016/j.immuni.2012.11.001

Gupta, S., Jiang, M., Anthony, A., & Pernis, A. B. (1999). Lineage-specific modulation of interleukin 4 signaling by interferon regulatory factor 4. *J Exp Med, 190*(12), 1837-1848.

Hacker, H., Mischak, H., Miethke, T., Liptay, S., Schmid, R., Sparwasser, T., . . . Wagner, H. (1998). CpG-DNA-specific activation of antigen-presenting cells requires stress kinase activity and is preceded by non-specific endocytosis and endosomal maturation. *EMBO J, 17*(21), 6230-6240. doi: 10.1093/emboj/17.21.6230

Hakyemez, B., Erdogan, C., Ercan, I., Ergin, N., Uysal, S., & Atahan, S. (2005). High-grade and low-grade gliomas: differentiation by using perfusion MR imaging. *Clin Radiol, 60*(4), 493-502. doi: 10.1016/j.crad.2004.09.009

Haldar, M., Kohyama, M., So, A. Y., Kc, W., Wu, X., Briseno, C. G., . . . Murphy, K. M. (2014). Heme-mediated SPI-C induction promotes monocyte differentiation into iron-recycling macrophages. *Cell, 156*(6), 1223-1234. doi: 10.1016/j.cell.2014.01.069

Hamad, A. R., Mohamood, A. S., Trujillo, C. J., Huang, C. T., Yuan, E., & Schneck, J. P. (2003). B220+ double-negative T cells suppress polyclonal T cell activation by a Fas-independent mechanism that involves inhibition of IL-2 production. *J Immunol, 171*(5), 2421-2426.

Hambardzumyan, D., Gutmann, D. H., & Kettenmann, H. (2015). The role of microglia and macrophages in glioma maintenance and progression. *Nat Neurosci, 19*(1), 20-27. doi: 10.1038/nn.4185

Hamilton, J. A. (2008). Colony-stimulating factors in inflammation and autoimmunity. *Nat Rev Immunol, 8*(7), 533-544. doi: 10.1038/nri2356

Hashimoto, D., Chow, A., Noizat, C., Teo, P., Beasley, M. B., Leboeuf, M., . . . Merad, M. (2013). Tissue-resident macrophages self-maintain locally throughout adult life with minimal contribution from circulating monocytes. *Immunity, 38*(4), 792-804. doi: 10.1016/j.immuni.2013.04.004

Hayashi, F., Smith, K. D., Ozinsky, A., Hawn, T. R., Yi, E. C., Goodlett, D. R., . . . Aderem, A. (2001). The innate immune response to bacterial flagellin is mediated by Toll-like receptor 5. *Nature, 410*(6832), 1099-1103. doi: 10.1038/35074106

Hebenstreit, D., Wirnsberger, G., Horejs-Hoeck, J., & Duschl, A. (2006). Signaling mechanisms, interaction partners, and target genes of STAT6. *Cytokine Growth Factor Rev, 17*(3), 173-188. doi: 10.1016/j.cytogfr.2006.01.004

Hegi, M. E., Diserens, A. C., Gorlia, T., Hamou, M. F., de Tribolet, N., Weller, M., . . . Stupp, R. (2005). MGMT gene silencing and benefit from temozolomide in glioblastoma. *N Engl J Med, 352*(10), 997-1003. doi: 10.1056/NEJMoa043331

Heinz, S., Benner, C., Spann, N., Bertolino, E., Lin, Y. C., Laslo, P., . . . Glass, C. K. (2010). Simple combinations of lineage-determining transcription factors prime cis-regulatory elements required for macrophage and B cell identities. *Mol Cell, 38*(4), 576-589. doi: 10.1016/j.molcel.2010.05.004

Hemmi, H., Takeuchi, O., Kawai, T., Kaisho, T., Sato, S., Sanjo, H., . . . Akira, S. (2000). A Toll-like receptor recognizes bacterial DNA. *Nature, 408*(6813), 740-745. doi: 10.1038/35047123

Henkel, G. W., McKercher, S. R., Yamamoto, H., Anderson, K. L., Oshima, R. G., & Maki, R. A. (1996). PU.1 but not ets-2 is essential for macrophage development from embryonic stem cells. *Blood, 88*(8), 2917-2926.

Hoeffel, G., Chen, J., Lavin, Y., Low, D., Almeida, F. F., See, P., . . . Ginhoux, F. (2015). C-Myb(+) erythro-myeloid progenitor-derived fetal monocytes give rise to adult tissue-resident macrophages. *Immunity, 42*(4), 665-678. doi: 10.1016/j.immuni.2015.03.011

Hohl, T. M., Rivera, A., Lipuma, L., Gallegos, A., Shi, C., Mack, M., & Pamer, E. G. (2009). Inflammatory monocytes facilitate adaptive CD4 T cell responses during respiratory fungal infection. *Cell Host Microbe, 6*(5), 470-481. doi: 10.1016/j.chom.2009.10.007

Holland, E. C., Hively, W. P., DePinho, R. A., & Varmus, H. E. (1998). A constitutively active epidermal growth factor receptor cooperates with disruption of G1 cell-cycle arrest pathways to induce glioma-like lesions in mice. *Genes Dev, 12*(23), 3675-3685.

Howlader, N., Noone, A., Krapcho, M., Garshell, J., DMiller, Altekruse, S., . . . Cronin, K. (1975-2011). SEER Cancer Statistics Review, National Cancer Institute. Bethesda, MD,. Retrieved February, 8th, 2016, from http://seer.cancer.gov/csr/1975_2011/

Huang, Y., Hoffman, C., Rajappa, P., Kim, J. H., Hu, W., Huse, J., . . . Greenfield, J. P. (2014). Oligodendrocyte progenitor cells promote neovascularization in glioma by

disrupting the blood-brain barrier. *Cancer Res, 74*(4), 1011-1021. doi: 10.1158/0008-5472.CAN-13-1072

Huber, S., Hoffmann, R., Muskens, F., & Voehringer, D. (2010). Alternatively activated macrophages inhibit T-cell proliferation by Stat6-dependent expression of PD-L2. *Blood, 116*(17), 3311-3320. doi: 10.1182/blood-2010-02-271981

Hunter, C., Smith, R., Cahill, D. P., Stephens, P., Stevens, C., Teague, J., . . . Wooster, R. (2006). A hypermutation phenotype and somatic MSH6 mutations in recurrent human malignant gliomas after alkylator chemotherapy. *Cancer Res, 66*(8), 3987-3991. doi: 10.1158/0008-5472.CAN-06-0127

Hurst, S. M., Wilkinson, T. S., McLoughlin, R. M., Jones, S., Horiuchi, S., Yamamoto, N., . . . Jones, S. A. (2001). Il-6 and its soluble receptor orchestrate a temporal switch in the pattern of leukocyte recruitment seen during acute inflammation. *Immunity, 14*(6), 705-714.

Hussain, S. F., Yang, D., Suki, D., Aldape, K., Grimm, E., & Heimberger, A. B. (2006). The role of human glioma-infiltrating microglia/macrophages in mediating antitumor immune responses. *Neuro Oncol, 8*(3), 261-279. doi: 10.1215/15228517-2006-008

Hutchins, A. P., Takahashi, Y., & Miranda-Saavedra, D. (2015). Genomic analysis of LPS-stimulated myeloid cells identifies a common pro-inflammatory response but divergent IL-10 anti-inflammatory responses. *Sci Rep, 5*, 9100. doi: 10.1038/srep09100

Isaacs, A., & Lindenmann, J. (1957). Virus interference. I. The interferon. *Proc R Soc Lond B Biol Sci, 147*(927), 258-267.

Islam, S. A., Ling, M. F., Leung, J., Shreffler, W. G., & Luster, A. D. (2013). Identification of human CCR8 as a CCL18 receptor. *J Exp Med, 210*(10), 1889-1898. doi: 10.1084/jem.20130240

Ivashkiv, L. B., & Donlin, L. T. (2014). Regulation of type I interferon responses. *Nat Rev Immunol, 14*(1), 36-49. doi: 10.1038/nri3581

Iwasaki, A., & Medzhitov, R. (2010). Regulation of adaptive immunity by the innate immune system. *Science, 327*(5963), 291-295. doi: 10.1126/science.1183021

Jackson, C., Ruzevick, J., Brem, H., & Lim, M. (2013). Vaccine strategies for glioblastoma: progress and future directions. *Immunotherapy, 5*(2), 155-167. doi: 10.2217/imt.12.155

Jenkins, R. B., Blair, H., Ballman, K. V., Giannini, C., Arusell, R. M., Law, M., . . . Buckner, J. C. (2006). A t(1;19)(q10;p10) mediates the combined deletions of 1p and 19q and predicts a better prognosis of patients with oligodendroglioma. *Cancer Res, 66*(20), 9852-9861. doi: 10.1158/0008-5472.CAN-06-1796

Jha, A. K., Huang, S. C., Sergushichev, A., Lampropoulou, V., Ivanova, Y., Loginicheva, E., . . . Artyomov, M. N. (2015). Network integration of parallel metabolic and transcriptional data reveals metabolic modules that regulate macrophage polarization. *Immunity, 42*(3), 419-430. doi: 10.1016/j.immuni.2015.02.005

Jiang, Z., Mak, T. W., Sen, G., & Li, X. (2004). Toll-like receptor 3-mediated activation of NF-kappaB and IRF3 diverges at Toll-IL-1 receptor domain-containing adapter inducing IFN-beta. *Proc Natl Acad Sci U S A, 101*(10), 3533-3538. doi: 10.1073/pnas.0308496101

Johnson, L. A., Scholler, J., Ohkuri, T., Kosaka, A., Patel, P. R., McGettigan, S. E., . . . Maus, M. V. (2015). Rational development and characterization of humanized anti-EGFR variant III chimeric antigen receptor T cells for glioblastoma. *Sci Transl Med, 7*(275), 275ra222. doi: 10.1126/scitranslmed.aaa4963

Joyce, J. A. (2005). Therapeutic targeting of the tumor microenvironment. *Cancer Cell, 7*(6), 513-520. doi: 10.1016/j.ccr.2005.05.024

Joyce, J. A., & Fearon, D. T. (2015). T cell exclusion, immune privilege, and the tumor microenvironment. *Science, 348*(6230), 74-80. doi: 10.1126/science.aaa6204

Kato, J. Y., Roussel, M. F., Ashmun, R. A., & Sherr, C. J. (1989). Transduction of human colony-stimulating factor-1 (CSF-1) receptor into interleukin-3-dependent mouse myeloid cells induces both CSF-1-dependent and factor-independent growth. *Mol Cell Biol, 9*(9), 4069-4073.

Kelley, K. A., & Pitha, P. M. (1985). Characterization of a mouse interferon gene locus I. Isolation of a cluster of four alpha interferon genes. *Nucleic Acids Res, 13*(3), 805-823.

Kennedy, D. W., & Abkowitz, J. L. (1997). Kinetics of central nervous system microglial and macrophage engraftment: analysis using a transgenic bone marrow transplantation model. *Blood, 90*(3), 986-993.

Kierdorf, K., Erny, D., Goldmann, T., Sander, V., Schulz, C., Perdiguero, E. G., . . . Prinz, M. (2013). Microglia emerge from erythromyeloid precursors via Pu.1- and Irf8-dependent pathways. *Nat Neurosci, 16*(3), 273-280. doi: 10.1038/nn.3318

Kierdorf, K., Katzmarski, N., Haas, C. A., & Prinz, M. (2013). Bone marrow cell recruitment to the brain in the absence of irradiation or parabiosis bias. *PLoS One, 8*(3), e58544. doi: 10.1371/journal.pone.0058544

Killela, P. J., Reitman, Z. J., Jiao, Y., Bettegowda, C., Agrawal, N., Diaz, L. A., Jr., . . . Yan, H. (2013). TERT promoter mutations occur frequently in gliomas and a subset of tumors derived from cells with low rates of self-renewal. *Proc Natl Acad Sci U S A, 110*(15), 6021-6026. doi: 10.1073/pnas.1303607110

Kioi, M., Vogel, H., Schultz, G., Hoffman, R. M., Harsh, G. R., & Brown, J. M. (2010). Inhibition of vasculogenesis, but not angiogenesis, prevents the recurrence of glioblastoma after irradiation in mice. *J Clin Invest, 120*(3), 694-705. doi: 10.1172/JCI40283

Kmiecik, J., Poli, A., Brons, N. H., Waha, A., Eide, G. E., Enger, P. O., . . . Chekenya, M. (2013). Elevated CD3+ and CD8+ tumor-infiltrating immune cells correlate with prolonged survival in glioblastoma patients despite integrated immunosuppressive mechanisms in the tumor microenvironment and at the systemic level. *J Neuroimmunol, 264*(1-2), 71-83. doi: 10.1016/j.jneuroim.2013.08.013

Kodandapani, R., Pio, F., Ni, C. Z., Piccialli, G., Klemsz, M., McKercher, S., . . . Ely, K. R. (1996). A new pattern for helix-turn-helix recognition revealed by the PU.1 ETS-domain-DNA complex. *Nature, 380*(6573), 456-460. doi: 10.1038/380456a0

Kohyama, M., Ise, W., Edelson, B. T., Wilker, P. R., Hildner, K., Mejia, C., . . . Murphy, K. M. (2009). Role for Spi-C in the development of red pulp macrophages and splenic iron homeostasis. *Nature, 457*(7227), 318-321. doi: 10.1038/nature07472

Kolde, R. (2015). pheatmap: Pretty Heatmaps. from http://CRAN.R-project.org/package=pheatmap

Komohara, Y., Ohnishi, K., Kuratsu, J., & Takeya, M. (2008). Possible involvement of the M2 anti-inflammatory macrophage phenotype in growth of human gliomas. *J Pathol, 216*(1), 15-24. doi: 10.1002/path.2370

Kreutz, M., Andreesen, R., Krause, S. W., Szabo, A., Ritz, E., & Reichel, H. (1993). 1,25-dihydroxyvitamin D3 production and vitamin D3 receptor expression are developmentally regulated during differentiation of human monocytes into macrophages. *Blood, 82*(4), 1300-1307.

Lai, C. F., Ripperger, J., Morella, K. K., Jurlander, J., Hawley, T. S., Carson, W. E., . . . Baumann, H. (1996). Receptors for interleukin (IL)-10 and IL-6-type cytokines use similar signaling mechanisms for inducing transcription through IL-6 response elements. *J Biol Chem, 271*(24), 13968-13975.

Langer-Gould, A., Atlas, S. W., Green, A. J., Bollen, A. W., & Pelletier, D. (2005). Progressive multifocal leukoencephalopathy in a patient treated with natalizumab. *N Engl J Med, 353*(4), 375-381. doi: 10.1056/NEJMoa051847

Larkin, J., Chiarion-Sileni, V., Gonzalez, R., Grob, J. J., Cowey, C. L., Lao, C. D., . . . Wolchok, J. D. (2015). Combined Nivolumab and Ipilimumab or Monotherapy in Untreated Melanoma. *N Engl J Med, 373*(1), 23-34. doi: 10.1056/NEJMoa1504030

Lavin, Y., Winter, D., Blecher-Gonen, R., David, E., Keren-Shaul, H., Merad, M., . . . Amit, I. (2014). Tissue-resident macrophage enhancer landscapes are shaped by the local microenvironment. *Cell, 159*(6), 1312-1326. doi: 10.1016/j.cell.2014.11.018

Lawrence, T., & Natoli, G. (2011). Transcriptional regulation of macrophage polarization: enabling diversity with identity. *Nat Rev Immunol, 11*(11), 750-761. doi: 10.1038/nri3088

Lewis, N. D., Hill, J. D., Juchem, K. W., Stefanopoulos, D. E., & Modis, L. K. (2014). RNA sequencing of microglia and monocyte-derived macrophages from mice with experimental autoimmune encephalomyelitis illustrates a changing phenotype with disease course. *J Neuroimmunol, 277*(1-2), 26-38. doi: 10.1016/j.jneuroim.2014.09.014

Li, H., Radford, J. C., Ragusa, M. J., Shea, K. L., McKercher, S. R., Zaremba, J. D., . . . Lipton, S. A. (2008). Transcription factor MEF2C influences neural stem/progenitor cell differentiation and maturation in vivo. *Proc Natl Acad Sci U S A, 105*(27), 9397-9402. doi: 10.1073/pnas.0802876105

Li, Y., Du, X. F., Liu, C. S., Wen, Z. L., & Du, J. L. (2012). Reciprocal regulation between resting microglial dynamics and neuronal activity in vivo. *Dev Cell, 23*(6), 1189-1202. doi: 10.1016/j.devcel.2012.10.027

Liao, X., Sharma, N., Kapadia, F., Zhou, G., Lu, Y., Hong, H., . . . Jain, M. K. (2011). Kruppel-like factor 4 regulates macrophage polarization. *J Clin Invest, 121*(7), 2736-2749. doi: 10.1172/JCI45444

Link, V. M., Gosselin, D., & Glass, C. K. (2015). Mechanisms Underlying the Selection and Function of Macrophage-Specific Enhancers. *Cold Spring Harb Symp Quant Biol*. doi: 10.1101/sqb.2015.80.027367

Liu, S. C., Alomran, R., Chernikova, S. B., Lartey, F., Stafford, J., Jang, T., . . . Brown, J. M. (2014). Blockade of SDF-1 after irradiation inhibits tumor recurrences of autochthonous brain tumors in rats. *Neuro Oncol, 16*(1), 21-28. doi: 10.1093/neuonc/not149

Liu, W. Y., Wang, Z. B., Zhang, L. C., Wei, X., & Li, L. (2012). Tight junction in blood-brain barrier: an overview of structure, regulation, and regulator substances. *CNS Neurosci Ther, 18*(8), 609-615. doi: 10.1111/j.1755-5949.2012.00340.x

Locatelli, G., Wortge, S., Buch, T., Ingold, B., Frommer, F., Sobottka, B., . . . Becher, B. (2012). Primary oligodendrocyte death does not elicit anti-CNS immunity. *Nat Neurosci, 15*(4), 543-550. doi: 10.1038/nn.3062

Long, J. Z., Lackan, C. S., & Hadjantonakis, A. K. (2005). Genetic and spectrally distinct in vivo imaging: embryonic stem cells and mice with widespread expression of a monomeric red fluorescent protein. *BMC Biotechnol, 5*, 20. doi: 10.1186/1472-6750-5-20

Louis, D. N., Ohgaki, H., Wiestler, O. D., Cavenee, W. K., Burger, P. C., Jouvet, A., . . . Kleihues, P. (2007). The 2007 WHO classification of tumours of the central nervous system. *Acta Neuropathol, 114*(2), 97-109. doi: 10.1007/s00401-007-0243-4

Louveau, A., Harris, T. H., & Kipnis, J. (2015). Revisiting the Mechanisms of CNS Immune Privilege. *Trends Immunol, 36*(10), 569-577. doi: 10.1016/j.it.2015.08.006

Louveau, A., Smirnov, I., Keyes, T. J., Eccles, J. D., Rouhani, S. J., Peske, J. D., . . . Kipnis, J. (2015). Structural and functional features of central nervous system lymphatic vessels. *Nature, 523*(7560), 337-341. doi: 10.1038/nature14432

Love, M. I., Huber, W., & Anders, S. (2014). Moderated estimation of fold change and dispersion for RNA-seq data with DESeq2. *Genome Biol, 15*(12), 550. doi: 10.1186/s13059-014-0550-8

Maaten, L. J. P. v. d., & Hinton, G. E. (2008). Visualizing High-Dimensional Data Using t-SNE. *Journal of Machine Learning Research*(9), 2579-2605.

MacMicking, J., Xie, Q. W., & Nathan, C. (1997). Nitric oxide and macrophage function. *Annu Rev Immunol, 15*, 323-350. doi: 10.1146/annurev.immunol.15.1.323

Macosko, E. Z., Basu, A., Satija, R., Nemesh, J., Shekhar, K., Goldman, M., . . . McCarroll, S. A. (2015). Highly Parallel Genome-wide Expression Profiling of Individual Cells Using Nanoliter Droplets. *Cell, 161*(5), 1202-1214. doi: 10.1016/j.cell.2015.05.002

Madhavan, S., Zenklusen, J. C., Kotliarov, Y., Sahni, H., Fine, H. A., & Buetow, K. (2009). Rembrandt: helping personalized medicine become a reality through integrative translational research. *Mol Cancer Res, 7*(2), 157-167. doi: 10.1158/1541-7786.MCR-08-0435

Madisen, L., Zwingman, T. A., Sunkin, S. M., Oh, S. W., Zariwala, H. A., Gu, H., . . . Zeng, H. (2010). A robust and high-throughput Cre reporting and characterization system for the whole mouse brain. *Nat Neurosci, 13*(1), 133-140. doi: 10.1038/nn.2467

Maecker, H. T., McCoy, J. P., & Nussenblatt, R. (2012). Standardizing immunophenotyping for the Human Immunology Project. *Nat Rev Immunol, 12*(3), 191-200. doi: 10.1038/nri3158

Maes, W., Verschuere, T., Van Hoylandt, A., Boon, L., & Van Gool, S. (2013). Depletion of regulatory T cells in a mouse experimental glioma model through anti-CD25 treatment results in the infiltration of non-immunosuppressive myeloid cells in the brain. *Clin Dev Immunol, 2013*, 952469. doi: 10.1155/2013/952469

Mak, K. S., Funnell, A. P., Pearson, R. C., & Crossley, M. (2011). PU.1 and Haematopoietic Cell Fate: Dosage Matters. *Int J Cell Biol, 2011*, 808524. doi: 10.1155/2011/808524

Martinez, F. O., Helming, L., & Gordon, S. (2009). Alternative activation of macrophages: an immunologic functional perspective. *Annu Rev Immunol, 27*, 451-483. doi: 10.1146/annurev.immunol.021908.132532

Martinez, F. O., Helming, L., Milde, R., Varin, A., Melgert, B. N., Draijer, C., . . . Gordon, S. (2013). Genetic programs expressed in resting and IL-4 alternatively activated mouse and human macrophages: similarities and differences. *Blood, 121*(9), e57-69. doi: 10.1182/blood-2012-06-436212

Matloubian, M., David, A., Engel, S., Ryan, J. E., & Cyster, J. G. (2000). A transmembrane CXC chemokine is a ligand for HIV-coreceptor Bonzo. *Nat Immunol, 1*(4), 298-304. doi: 10.1038/79738

Mauer, J., Chaurasia, B., Goldau, J., Vogt, M. C., Ruud, J., Nguyen, K. D., . . . Bruning, J. C. (2014). Signaling by IL-6 promotes alternative activation of macrophages to limit endotoxemia and obesity-associated resistance to insulin. *Nat Immunol, 15*(5), 423-430. doi: 10.1038/ni.2865

Merad, M., Manz, M. G., Karsunky, H., Wagers, A., Peters, W., Charo, I., . . . Engleman, E. G. (2002). Langerhans cells renew in the skin throughout life under steady-state conditions. *Nat Immunol, 3*(12), 1135-1141. doi: 10.1038/ni852

Mildner, A., Schmidt, H., Nitsche, M., Merkler, D., Hanisch, U. K., Mack, M., . . . Prinz, M. (2007). Microglia in the adult brain arise from Ly-6ChiCCR2+ monocytes only under defined host conditions. *Nat Neurosci, 10*(12), 1544-1553. doi: 10.1038/nn2015

Miller, D. H., Khan, O. A., Sheremata, W. A., Blumhardt, L. D., Rice, G. P., Libonati, M. A., . . . International Natalizumab Multiple Sclerosis Trial, G. (2003). A controlled trial of natalizumab for relapsing multiple sclerosis. *N Engl J Med, 348*(1), 15-23. doi: 10.1056/NEJMoa020696

Mills, C. D. (2012). M1 and M2 Macrophages: Oracles of Health and Disease. *Crit Rev Immunol, 32*(6), 463-488.

Mills, C. D., Kincaid, K., Alt, J. M., Heilman, M. J., & Hill, A. M. (2000). M-1/M-2 macrophages and the Th1/Th2 paradigm. *J Immunol, 164*(12), 6166-6173.

Mindur, J. E., Ito, N., Dhib-Jalbut, S., & Ito, K. (2014). Early treatment with anti-VLA-4 mAb can prevent the infiltration and/or development of pathogenic CD11b+CD4+ T cells in the CNS during progressive EAE. *PLoS One, 9*(6), e99068. doi: 10.1371/journal.pone.0099068

Mosser, D. M., & Edwards, J. P. (2008). Exploring the full spectrum of macrophage activation. *Nat Rev Immunol, 8*(12), 958-969. doi: 10.1038/nri2448

Mullen, A. C., Orlando, D. A., Newman, J. J., Loven, J., Kumar, R. M., Bilodeau, S., . . . Young, R. A. (2011). Master transcription factors determine cell-type-specific responses to TGF-beta signaling. *Cell, 147*(3), 565-576. doi: 10.1016/j.cell.2011.08.050

Muller, A., Brandenburg, S., Turkowski, K., Muller, S., & Vajkoczy, P. (2015). Resident microglia, and not peripheral macrophages, are the main source of brain tumor mononuclear cells. *Int J Cancer, 137*(2), 278-288. doi: 10.1002/ijc.29379

Murray, P. J. (2005). The primary mechanism of the IL-10-regulated antiinflammatory response is to selectively inhibit transcription. *Proc Natl Acad Sci U S A, 102*(24), 8686-8691. doi: 10.1073/pnas.0500419102

Murray, P. J., Allen, J. E., Biswas, S. K., Fisher, E. A., Gilroy, D. W., Goerdt, S., . . . Wynn, T. A. (2014). Macrophage activation and polarization: nomenclature and experimental guidelines. *Immunity, 41*(1), 14-20. doi: 10.1016/j.immuni.2014.06.008

Muzumdar, M. D., Tasic, B., Miyamichi, K., Li, L., & Luo, L. (2007). A global double-fluorescent Cre reporter mouse. *Genesis, 45*(9), 593-605. doi: 10.1002/dvg.20335

Newton, K., & Dixit, V. M. (2012). Signaling in innate immunity and inflammation. *Cold Spring Harb Perspect Biol, 4*(3). doi: 10.1101/cshperspect.a006049

Niwinska, A., Tacikowska, M., & Murawska, M. (2010). The effect of early detection of occult brain metastases in HER2-positive breast cancer patients on survival and cause of death. *Int J Radiat Oncol Biol Phys, 77*(4), 1134-1139. doi: 10.1016/j.ijrobp.2009.06.030

Noushmehr, H., Weisenberger, D. J., Diefes, K., Phillips, H. S., Pujara, K., Berman, B. P., . . . Cancer Genome Atlas Research, N. (2010). Identification of a CpG island methylator phenotype that defines a distinct subgroup of glioma. *Cancer Cell, 17*(5), 510-522. doi: 10.1016/j.ccr.2010.03.017

O'Farrell, A. M., Liu, Y., Moore, K. W., & Mui, A. L. (1998). IL-10 inhibits macrophage activation and proliferation by distinct signaling mechanisms: evidence for Stat3-

dependent and -independent pathways. *EMBO J, 17*(4), 1006-1018. doi: 10.1093/emboj/17.4.1006

Ohmori, Y., & Hamilton, T. A. (1997). IL-4-induced STAT6 suppresses IFN-gamma-stimulated STAT1-dependent transcription in mouse macrophages. *J Immunol, 159*(11), 5474-5482.

Ojalvo, L. S., Whittaker, C. A., Condeelis, J. S., & Pollard, J. W. (2010). Gene expression analysis of macrophages that facilitate tumor invasion supports a role for Wnt-signaling in mediating their activity in primary mammary tumors. *J Immunol, 184*(2), 702-712. doi: 10.4049/jimmunol.0902360

Okabe, M., Ikawa, M., Kominami, K., Nakanishi, T., & Nishimune, Y. (1997). 'Green mice' as a source of ubiquitous green cells. *FEBS Lett, 407*(3), 313-319.

Okabe, Y., & Medzhitov, R. (2015). Tissue biology perspective on macrophages. *Nat Immunol, 17*(1), 9-17. doi: 10.1038/ni.3320

Opitz, C. A., Litzenburger, U. M., Sahm, F., Ott, M., Tritschler, I., Trump, S., . . . Platten, M. (2011). An endogenous tumour-promoting ligand of the human aryl hydrocarbon receptor. *Nature, 478*(7368), 197-203. doi: 10.1038/nature10491

Ostuni, R., & Natoli, G. (2011). Transcriptional control of macrophage diversity and specialization. *Eur J Immunol, 41*(9), 2486-2490. doi: 10.1002/eji.201141706

Ostuni, R., Piccolo, V., Barozzi, I., Polletti, S., Termanini, A., Bonifacio, S., . . . Natoli, G. (2013). Latent enhancers activated by stimulation in differentiated cells. *Cell, 152*(1-2), 157-171. doi: 10.1016/j.cell.2012.12.018

Ozawa, T., Riester, M., Cheng, Y. K., Huse, J. T., Squatrito, M., Helmy, K., . . . Holland, E. C. (2014). Most human non-GCIMP glioblastoma subtypes evolve from a common proneural-like precursor glioma. *Cancer Cell, 26*(2), 288-300. doi: 10.1016/j.ccr.2014.06.005

Palmieri, D., Chambers, A. F., Felding-Habermann, B., Huang, S., & Steeg, P. S. (2007). The biology of metastasis to a sanctuary site. *Clin Cancer Res, 13*(6), 1656-1662. doi: 10.1158/1078-0432.CCR-06-2659

Paolicelli, R. C., Bolasco, G., Pagani, F., Maggi, L., Scianni, M., Panzanelli, P., . . . Gross, C. T. (2011). Synaptic pruning by microglia is necessary for normal brain development. *Science, 333*(6048), 1456-1458. doi: 10.1126/science.1202529

Parkhurst, C. N., Yang, G., Ninan, I., Savas, J. N., Yates, J. R., 3rd, Lafaille, J. J., . . . Gan, W. B. (2013). Microglia promote learning-dependent synapse formation through brain-derived neurotrophic factor. *Cell, 155*(7), 1596-1609. doi: 10.1016/j.cell.2013.11.030

Parkin, J., & Cohen, B. (2001). An overview of the immune system. *Lancet, 357*(9270), 1777-1789. doi: 10.1016/S0140-6736(00)04904-7

Parney, I. F., Waldron, J. S., & Parsa, A. T. (2009). Flow cytometry and in vitro analysis of human glioma-associated macrophages. Laboratory investigation. *J Neurosurg, 110*(3), 572-582. doi: 10.3171/2008.7.JNS08475

Patchell, R. A., Tibbs, P. A., Walsh, J. W., Dempsey, R. J., Maruyama, Y., Kryscio, R. J., . . . Young, B. (1990). A randomized trial of surgery in the treatment of single metastases to the brain. *N Engl J Med, 322*(8), 494-500. doi: 10.1056/NEJM199002223220802

Patel, A. P., Tirosh, I., Trombetta, J. J., Shalek, A. K., Gillespie, S. M., Wakimoto, H., . . . Bernstein, B. E. (2014). Single-cell RNA-seq highlights intratumoral heterogeneity in primary glioblastoma. *Science, 344*(6190), 1396-1401. doi: 10.1126/science.1254257

Pauleau, A. L., Rutschman, R., Lang, R., Pernis, A., Watowich, S. S., & Murray, P. J. (2004). Enhancer-mediated control of macrophage-specific arginase I expression. *J Immunol, 172*(12), 7565-7573.

Pixley, F. J., & Stanley, E. R. (2004). CSF-1 regulation of the wandering macrophage: complexity in action. *Trends Cell Biol, 14*(11), 628-638. doi: 10.1016/j.tcb.2004.09.016

Platanias, L. C. (2005). Mechanisms of type-I- and type-II-interferon-mediated signalling. *Nat Rev Immunol, 5*(5), 375-386. doi: 10.1038/nri1604

Pollard, J. W. (2009). Trophic macrophages in development and disease. *Nat Rev Immunol, 9*(4), 259-270. doi: 10.1038/nri2528

Poltorak, A., He, X., Smirnova, I., Liu, M. Y., Van Huffel, C., Du, X., . . . Beutler, B. (1998). Defective LPS signaling in C3H/HeJ and C57BL/10ScCr mice: mutations in Tlr4 gene. *Science, 282*(5396), 2085-2088.

Pong, W. W., Walker, J., Wylie, T., Magrini, V., Luo, J., Emnett, R. J., . . . Gutmann, D. H. (2013). F11R is a novel monocyte prognostic biomarker for malignant glioma. *PLoS One, 8*(10), e77571. doi: 10.1371/journal.pone.0077571

Ponomarev, V., Doubrovin, M., Serganova, I., Vider, J., Shavrin, A., Beresten, T., . . . Gelovani Tjuvajev, J. (2004). A novel triple-modality reporter gene for whole-body fluorescent, bioluminescent, and nuclear noninvasive imaging. *Eur J Nucl Med Mol Imaging, 31*(5), 740-751. doi: 10.1007/s00259-003-1441-5

Preusser, M., Lim, M., Hafler, D. A., Reardon, D. A., & Sampson, J. H. (2015). Prospects of immune checkpoint modulators in the treatment of glioblastoma. *Nat Rev Neurol, 11*(9), 504-514. doi: 10.1038/nrneurol.2015.139

Price, J. G., Idoyaga, J., Salmon, H., Hogstad, B., Bigarella, C. L., Ghaffari, S., . . . Merad, M. (2015). CDKN1A regulates Langerhans cell survival and promotes Treg cell generation upon exposure to ionizing irradiation. *Nat Immunol, 16*(10), 1060-1068. doi: 10.1038/ni.3270

Prins, R. M., Incardona, F., Lau, R., Lee, P., Claus, S., Zhang, W., . . . Wheeler, C. J. (2004). Characterization of defective CD4-CD8- T cells in murine tumors generated independent of antigen specificity. *J Immunol, 172*(3), 1602-1611.

Pyonteck, S. M., Akkari, L., Schuhmacher, A. J., Bowman, R. L., Sevenich, L., Quail, D. F., . . . Joyce, J. A. (2013). CSF-1R inhibition alters macrophage polarization and blocks glioma progression. *Nat Med, 19*(10), 1264-1272. doi: 10.1038/nm.3337

Quail, D. F., Bowman, R. L., Akkari, L., Quick, M. L., Schuhmacher, A. J., Huse, J., . . . Joyce, J. A. (2016). The tumor microenvironment underlies acquired resistance to CSF1R inhibition in gliomas. *Science*.

Quail, D. F., & Joyce, J. A. (2013). Microenvironmental regulation of tumor progression and metastasis. *Nat Med, 19*(11), 1423-1437. doi: 10.1038/nm.3394

Radi, Z. A., Koza-Taylor, P. H., Bell, R. R., Obert, L. A., Runnels, H. A., Beebe, J. S., . . . Sadis, S. (2011). Increased serum enzyme levels associated with kupffer cell reduction with no signs of hepatic or skeletal muscle injury. *Am J Pathol, 179*(1), 240-247. doi: 10.1016/j.ajpath.2011.03.029

Ramirez, F., Dundar, F., Diehl, S., Gruning, B. A., & Manke, T. (2014). deepTools: a flexible platform for exploring deep-sequencing data. *Nucleic Acids Res, 42*(Web Server issue), W187-191. doi: 10.1093/nar/gku365

Raychaudhuri, B., Rayman, P., Huang, P., Grabowski, M., Hambardzumyan, D., Finke, J. H., & Vogelbaum, M. A. (2015). Myeloid derived suppressor cell infiltration of murine and human gliomas is associated with reduction of tumor infiltrating lymphocytes. *J Neurooncol, 122*(2), 293-301. doi: 10.1007/s11060-015-1720-6

Reith, W., LeibundGut-Landmann, S., & Waldburger, J. M. (2005). Regulation of MHC class II gene expression by the class II transactivator. *Nat Rev Immunol, 5*(10), 793-806. doi: 10.1038/nri1708

Ridley, A., & Cavanagh, J. B. (1971). Lymphocytic infiltration in gliomas: evidence of possible host resistance. *Brain, 94*(1), 117-124.

Ritchie, M. E., Phipson, B., Wu, D., Hu, Y., Law, C. W., Shi, W., & Smyth, G. K. (2015). limma powers differential expression analyses for RNA-sequencing and microarray studies. *Nucleic Acids Res, 43*(7), e47. doi: 10.1093/nar/gkv007

Rong, Y., Durden, D. L., Van Meir, E. G., & Brat, D. J. (2006). 'Pseudopalisading' necrosis in glioblastoma: a familiar morphologic feature that links vascular pathology, hypoxia, and angiogenesis. *J Neuropathol Exp Neurol, 65*(6), 529-539.

Ruffell, B., Chang-Strachan, D., Chan, V., Rosenbusch, A., Ho, C. M., Pryer, N., . . . Coussens, L. M. (2014). Macrophage IL-10 blocks CD8+ T cell-dependent responses to chemotherapy by suppressing IL-12 expression in intratumoral dendritic cells. *Cancer Cell, 26*(5), 623-637. doi: 10.1016/j.ccell.2014.09.006

Sahm, F., Oezen, I., Opitz, C. A., Radlwimmer, B., von Deimling, A., Ahrendt, T., . . . Platten, M. (2013). The endogenous tryptophan metabolite and NAD+ precursor quinolinic acid confers resistance of gliomas to oxidative stress. *Cancer Res, 73*(11), 3225-3234. doi: 10.1158/0008-5472.CAN-12-3831

Salhia, B., Kiefer, J., Ross, J. T., Metapally, R., Martinez, R. A., Johnson, K. N., . . . Tran, N. L. (2014). Integrated genomic and epigenomic analysis of breast cancer brain metastasis. *PLoS One, 9*(1), e85448. doi: 10.1371/journal.pone.0085448

Sanai, N., Chang, S., & Berger, M. S. (2011). Low-grade gliomas in adults. *J Neurosurg, 115*(5), 948-965. doi: 10.3171/2011.7.JNS101238

Sanborn, J. Z., Salama, S. R., Grifford, M., Brennan, C. W., Mikkelsen, T., Jhanwar, S., . . . Haussler, D. (2013). Double minute chromosomes in glioblastoma multiforme are revealed by precise reconstruction of oncogenic amplicons. *Cancer Res, 73*(19), 6036-6045. doi: 10.1158/0008-5472.CAN-13-0186

Satoh, T., Takeuchi, O., Vandenbon, A., Yasuda, K., Tanaka, Y., Kumagai, Y., . . . Akira, S. (2010). The Jmjd3-Irf4 axis regulates M2 macrophage polarization and host responses against helminth infection. *Nat Immunol, 11*(10), 936-944. doi: 10.1038/ni.1920

Sawyers, C. (2004). Targeted cancer therapy. *Nature, 432*(7015), 294-297. doi: 10.1038/nature03095

Scheller, J., Chalaris, A., Schmidt-Arras, D., & Rose-John, S. (2011). The pro- and anti-inflammatory properties of the cytokine interleukin-6. *Biochim Biophys Acta, 1813*(5), 878-888. doi: 10.1016/j.bbamcr.2011.01.034

Schneider, C., & Kopf, M. (2015). tEMPting Fate MaYBe the Solution. *Immunity, 42*(4), 597-599. doi: 10.1016/j.immuni.2015.04.001

Schneider, C., Nobs, S. P., Kurrer, M., Rehrauer, H., Thiele, C., & Kopf, M. (2014). Induction of the nuclear receptor PPAR-gamma by the cytokine GM-CSF is critical for the differentiation of fetal monocytes into alveolar macrophages. *Nat Immunol, 15*(11), 1026-1037. doi: 10.1038/ni.3005

Schraufstatter, I. U., Zhao, M., Khaldoyanidi, S. K., & Discipio, R. G. (2012). The chemokine CCL18 causes maturation of cultured monocytes to macrophages in the M2 spectrum. *Immunology, 135*(4), 287-298. doi: 10.1111/j.1365-2567.2011.03541.x

Schreiber, H. A., Loschko, J., Karssemeijer, R. A., Escolano, A., Meredith, M. M., Mucida, D., . . . Nussenzweig, M. C. (2013). Intestinal monocytes and macrophages are required for T cell polarization in response to Citrobacter rodentium. *J Exp Med, 210*(10), 2025-2039. doi: 10.1084/jem.20130903

Schroder, K., Hertzog, P. J., Ravasi, T., & Hume, D. A. (2004). Interferon-gamma: an overview of signals, mechanisms and functions. *J Leukoc Biol, 75*(2), 163-189. doi: 10.1189/jlb.0603252

Scott, E. W., Simon, M. C., Anastasi, J., & Singh, H. (1994). Requirement of transcription factor PU.1 in the development of multiple hematopoietic lineages. *Science, 265*(5178), 1573-1577.

Sedgwick, J. D., Schwender, S., Imrich, H., Dorries, R., Butcher, G. W., & ter Meulen, V. (1991). Isolation and direct characterization of resident microglial cells from the normal and inflamed central nervous system. *Proc Natl Acad Sci U S A, 88*(16), 7438-7442.

Setty, M., Helmy, K., Khan, A. A., Silber, J., Arvey, A., Neezen, F., . . . Leslie, C. S. (2012). Inferring transcriptional and microRNA-mediated regulatory programs in glioblastoma. *Mol Syst Biol, 8*, 605. doi: 10.1038/msb.2012.37

Sevenich, L., Bowman, R. L., Mason, S. D., Quail, D. F., Rapaport, F., Elie, B. T., . . . Joyce, J. A. (2014). Analysis of tumour- and stroma-supplied proteolytic networks reveals a brain-metastasis-promoting role for cathepsin S. *Nat Cell Biol, 16*(9), 876-888. doi: 10.1038/ncb3011

Shepard, J. L., & Zon, L. I. (2000). Developmental derivation of embryonic and adult macrophages. *Curr Opin Hematol, 7*(1), 3-8.

Solga, A. C., Pong, W. W., Kim, K. Y., Cimino, P. J., Toonen, J. A., Walker, J., . . . Gutmann, D. H. (2015). RNA Sequencing of Tumor-Associated Microglia Reveals Ccl5 as a Stromal Chemokine Critical for Neurofibromatosis-1 Glioma Growth. *Neoplasia, 17*(10), 776-788. doi: 10.1016/j.neo.2015.10.002

Sottoriva, A., Spiteri, I., Piccirillo, S. G., Touloumis, A., Collins, V. P., Marioni, J. C., . . . Tavare, S. (2013). Intratumor heterogeneity in human glioblastoma reflects cancer evolutionary dynamics. *Proc Natl Acad Sci U S A, 110*(10), 4009-4014. doi: 10.1073/pnas.1219747110

Soucie, E. L., Weng, Z., Geirsdottir, L., Molawi, K., Maurizio, J., Fenouil, R., . . . Sieweke, M. H. (2016). Lineage-specific enhancers activate self-renewal genes in macrophages and embryonic stem cells. *Science*. doi: 10.1126/science.aad5510

Spooner, C. J., Cheng, J. X., Pujadas, E., Laslo, P., & Singh, H. (2009). A recurrent network involving the transcription factors PU.1 and Gfi1 orchestrates innate and adaptive immune cell fates. *Immunity, 31*(4), 576-586. doi: 10.1016/j.immuni.2009.07.011

Stein, M., Keshav, S., Harris, N., & Gordon, S. (1992). Interleukin 4 potently enhances murine macrophage mannose receptor activity: a marker of alternative immunologic macrophage activation. *J Exp Med, 176*(1), 287-292.

Stephan, A. H., Barres, B. A., & Stevens, B. (2012). The complement system: an unexpected role in synaptic pruning during development and disease. *Annu Rev Neurosci, 35*, 369-389. doi: 10.1146/annurev-neuro-061010-113810

Stupp, R., Mason, W. P., van den Bent, M. J., Weller, M., Fisher, B., Taphoorn, M. J., . . . National Cancer Institute of Canada Clinical Trials, G. (2005). Radiotherapy plus concomitant and adjuvant temozolomide for glioblastoma. *N Engl J Med, 352*(10), 987-996. doi: 10.1056/NEJMoa043330

Sun, J. C., Beilke, J. N., & Lanier, L. L. (2009). Adaptive immune features of natural killer cells. *Nature, 457*(7229), 557-561. doi: 10.1038/nature07665

Swartz, A. M., Li, Q. J., & Sampson, J. H. (2014). Rindopepimut: a promising immunotherapeutic for the treatment of glioblastoma multiforme. *Immunotherapy, 6*(6), 679-690. doi: 10.2217/imt.14.21

Swinton, J. Vennerable: Venn and Euler area-proportional diagrams.

Szulzewsky, F., Pelz, A., Feng, X., Synowitz, M., Markovic, D., Langmann, T., . . . Kettenmann, H. (2015). Glioma-associated microglia/macrophages display an expression profile different from M1 and M2 polarization and highly express

Gpnmb and Spp1. *PLoS One, 10*(2), e0116644. doi: 10.1371/journal.pone.0116644

Takeda, K., & Akira, S. (2005). Toll-like receptors in innate immunity. *Int Immunol, 17*(1), 1-14. doi: 10.1093/intimm/dxh186

Takeuchi, O., Takeda, K., Hoshino, K., Adachi, O., Ogawa, T., & Akira, S. (2000). Cellular responses to bacterial cell wall components are mediated through MyD88-dependent signaling cascades. *Int Immunol, 12*(1), 113-117.

Tauber, A. I. (2003). Metchnikoff and the phagocytosis theory. *Nat Rev Mol Cell Biol, 4*(11), 897-901. doi: 10.1038/nrm1244

Teitelbaum, S. L. (2000). Bone resorption by osteoclasts. *Science, 289*(5484), 1504-1508.

Teles, R. M., Graeber, T. G., Krutzik, S. R., Montoya, D., Schenk, M., Lee, D. J., . . . Modlin, R. L. (2013). Type I interferon suppresses type II interferon-triggered human anti-mycobacterial responses. *Science, 339*(6126), 1448-1453. doi: 10.1126/science.1233665

Trinchieri, G. (2010). Type I interferon: friend or foe? *J Exp Med, 207*(10), 2053-2063. doi: 10.1084/jem.20101664

Trombetta, E. S., & Mellman, I. (2005). Cell biology of antigen processing in vitro and in vivo. *Annu Rev Immunol, 23*, 975-1028. doi: 10.1146/annurev.immunol.22.012703.104538

Trotman, L. C., Niki, M., Dotan, Z. A., Koutcher, J. A., Di Cristofano, A., Xiao, A., . . . Pandolfi, P. P. (2003). Pten dose dictates cancer progression in the prostate. *PLoS Biol, 1*(3), E59. doi: 10.1371/journal.pbio.0000059

Umemura, N., Saio, M., Suwa, T., Kitoh, Y., Bai, J., Nonaka, K., . . . Takami, T. (2008). Tumor-infiltrating myeloid-derived suppressor cells are pleiotropic-inflamed monocytes/macrophages that bear M1- and M2-type characteristics. *J Leukoc Biol, 83*(5), 1136-1144. doi: 10.1189/jlb.0907611

van der Vos, K. E., Abels, E. R., Zhang, X., Lai, C., Carrizosa, E., Oakley, D., . . . Breakefield, X. O. (2016). Directly visualized glioblastoma-derived extracellular vesicles transfer RNA to microglia/macrophages in the brain. *Neuro Oncol, 18*(1), 58-69. doi: 10.1093/neuonc/nov244

Verhaak, R. G., Hoadley, K. A., Purdom, E., Wang, V., Qi, Y., Wilkerson, M. D., . . . Cancer Genome Atlas Research, N. (2010). Integrated genomic analysis identifies clinically relevant subtypes of glioblastoma characterized by abnormalities in PDGFRA, IDH1, EGFR, and NF1. *Cancer Cell, 17*(1), 98-110. doi: 10.1016/j.ccr.2009.12.020

Villagra, A., Cheng, F., Wang, H. W., Suarez, I., Glozak, M., Maurin, M., . . . Sotomayor, E. M. (2009). The histone deacetylase HDAC11 regulates the expression of interleukin 10 and immune tolerance. *Nat Immunol, 10*(1), 92-100. doi: 10.1038/ni.1673

Vom Berg, J., Vrohlings, M., Haller, S., Haimovici, A., Kulig, P., Sledzinska, A., . . . Becher, B. (2013). Intratumoral IL-12 combined with CTLA-4 blockade elicits T cell-mediated glioma rejection. *J Exp Med, 210*(13), 2803-2811. doi: 10.1084/jem.20130678

Wainwright, D. A., Chang, A. L., Dey, M., Balyasnikova, I. V., Kim, C. K., Tobias, A., . . . Lesniak, M. S. (2014). Durable therapeutic efficacy utilizing combinatorial blockade against IDO, CTLA-4, and PD-L1 in mice with brain tumors. *Clin Cancer Res, 20*(20), 5290-5301. doi: 10.1158/1078-0432.CCR-14-0514

Wang, H., Xu, T., Jiang, Y., Xu, H., Yan, Y., Fu, D., & Chen, J. (2015). The challenges and the promise of molecular targeted therapy in malignant gliomas. *Neoplasia, 17*(3), 239-255. doi: 10.1016/j.neo.2015.02.002

Wang, H. W., & Joyce, J. A. (2010). Alternative activation of tumor-associated macrophages by IL-4: priming for protumoral functions. *Cell Cycle, 9*(24), 4824-4835.

Wang, S. I., Puc, J., Li, J., Bruce, J. N., Cairns, P., Sidransky, D., & Parsons, R. (1997). Somatic mutations of PTEN in glioblastoma multiforme. *Cancer Res, 57*(19), 4183-4186.

Wang, T., Papoutsi, M., Wiesmann, M., DeCristofaro, M., Keselica, M. C., Skuba, E., . . . Kluwe, W. (2011). Investigation of correlation among safety biomarkers in serum, histopathological examination, and toxicogenomics. *Int J Toxicol, 30*(3), 300-312. doi: 10.1177/1091581811401920

Wang, Y., Szretter, K. J., Vermi, W., Gilfillan, S., Rossini, C., Cella, M., . . . Colonna, M. (2012). IL-34 is a tissue-restricted ligand of CSF1R required for the development of Langerhans cells and microglia. *Nat Immunol, 13*(8), 753-760. doi: 10.1038/ni.2360

Warnes, G. R., Bolker, B., Bonebakker, L., Gentleman, R., Huber, W., Liaw, A., . . . Venables, B. (2015). gplots: Various R Programming Tools for Plotting Data. from http://CRAN.R-project.org/package=gplots

Waziri, A., Killory, B., Ogden, A. T., 3rd, Canoll, P., Anderson, R. C., Kent, S. C., . . . Bruce, J. N. (2008). Preferential in situ CD4+CD56+ T cell activation and expansion within human glioblastoma. *J Immunol, 180*(11), 7673-7680.

Wickham, H. (2009). *ggplot2: Elegant Graphics for Data Analysis*.

Will, B., Vogler, T. O., Narayanagari, S., Bartholdy, B., Todorova, T. I., da Silva Ferreira, M., . . . Steidl, U. (2015). Minimal PU.1 reduction induces a preleukemic state and promotes development of acute myeloid leukemia. *Nat Med, 21*(10), 1172-1181. doi: 10.1038/nm.3936

Xue, J., Schmidt, S. V., Sander, J., Draffehn, A., Krebs, W., Quester, I., . . . Schultze, J. L. (2014). Transcriptome-based network analysis reveals a spectrum model of human macrophage activation. *Immunity, 40*(2), 274-288. doi: 10.1016/j.immuni.2014.01.006

Yan D, Wang H-W, Bowman RL, and Joyce JA. STAT3 and STAT6 signaling pathways synergize to promote cathepsin secretion from macrophages via IRE1α activation. (Manuscript in revision).

Yau, T., Swanton, C., Chua, S., Sue, A., Walsh, G., Rostom, A., . . . Smith, I. E. (2006). Incidence, pattern and timing of brain metastases among patients with advanced breast cancer treated with trastuzumab. *Acta Oncol, 45*(2), 196-201. doi: 10.1080/02841860500486630

Ye, X. Z., Xu, S. L., Xin, Y. H., Yu, S. C., Ping, Y. F., Chen, L., . . . Bian, X. W. (2012). Tumor-associated microglia/macrophages enhance the invasion of glioma stem-like cells via TGF-beta1 signaling pathway. *J Immunol, 189*(1), 444-453. doi: 10.4049/jimmunol.1103248

Yona, S., Kim, K. W., Wolf, Y., Mildner, A., Varol, D., Breker, M., . . . Jung, S. (2013). Fate mapping reveals origins and dynamics of monocytes and tissue macrophages under homeostasis. *Immunity, 38*(1), 79-91. doi: 10.1016/j.immuni.2012.12.001

Yoshida, A., Koide, Y., Uchijima, M., & Yoshida, T. O. (1994). IFN-gamma induces IL-12 mRNA expression by a murine macrophage cell line, J774. *Biochem Biophys Res Commun, 198*(3), 857-861. doi: 10.1006/bbrc.1994.1122

Zarnegar, M. A., & Rothenberg, E. V. (2012). Ikaros represses and activates PU.1 cell-type-specifically through the multifunctional Sfpi1 URE and a myeloid specific enhancer. *Oncogene, 31*(43), 4647-4654. doi: 10.1038/onc.2011.597

Zhou, W., Ke, S. Q., Huang, Z., Flavahan, W., Fang, X., Paul, J., . . . Bao, S. (2015). Periostin secreted by glioblastoma stem cells recruits M2 tumour-associated macrophages and promotes malignant growth. *Nat Cell Biol, 17*(2), 170-182. doi: 10.1038/ncb3090